THE UNIVERSITY
of EDINBURGH

Trichome morphology and development in the genus *Antirrhinum*

Ying Tan

Doctor of Philosophy

Institute of Molecular Plant Sciences

School of Biological Sciences

The University of Edinburgh

2018

Declaration

I declare that this thesis has been composed solely by myself and that it has not been submitted, in whole or in part, in any previous application for a degree. Except where stated otherwise by reference or acknowledgment, the work presented is entirely my own.

_____ _____

Ying Tan Date

Acknowledgments

Many people helped and supported me during my study. First, I would like to express my deepest gratitude to my supervisor, Professor Andrew Hudson. He has supported me since my PhD application and always provides his valuable direction and advice. Other members of Prof. Hudson's research group, especially Erica de Leau and Matthew Barnbrook, taught me lots of experiment skills. They gave me extra assistance during my pregnancy. I would also like to thank Yvette Wilson who collected *Antirrhinum* samples for my study.

Pablo Vargas supplied me collections of the Antirrhineae species and allow me to access the specimen of the Antirrhineae in the Real Jardín Botánico Herbarium. Attila Molnar and his group members taught me how to conduct VIGS. Patricia Watson, William Adams and Sophie Haupt taught me skills to grow *Antirrhinum* plants and helped me take care of my plants.

I would also like to thank my colleagues in the Rutherford 'big lab' for their help and friendship, especially Yen-ting Lu who made agarose gels containing ethidium bromide and ran a gel electrophoresis for me when I was pregnant. I would like to thank Xin Tian and Yuan Li who helped me adapt to life in Edinburgh and gave advice for my experiments.

I would like to express my sincere thanks to the Darwin Trust of Edinburgh for the financial support during my PhD study and the SYNTHESYS Project financed by European Community Research Infrastructure Action under the FP7 Integrating Activities Programme which sponsored my trip to Madrid.

At the end, a special thank to my parents and husband for their love and support.

Abbreviations

µg	Microgram
µl	Microlitre
AD	Activation Domain
BCIP	5-Bromo-4-Chloro-3-Indolyl Phosphate
BD	Binding Domain
BLAST	Basic Local Alignment Search Tool
BSA	Bovine Serum Albumin
CR	Coding Region
CTAB	Cetrimonium Bromide
DEPC	Diethyl Pyrocarbonate
DMF	Dimethylformamide
DTT	Dithiothreitol
DNA:	Deoxyribonucleic acid
E. coli	*Escherichia coli*
EDTA	Ethylenediaminetetraacetic acid
GRX	Glutaredoxin
LB	Luria Bertani medium
MS	Murashige and Skoog medium
NBT	Nitrotetrazolium Blue Chloride
PCR	Polymerase Chain Reaction
RNA	Ribonucleic Acid
RNA	RNA interference
SE	Standard Error
SNP	Single Nucleotide Polymorphism
SSC	Saline-sodium citrate buffer
TE	Tris/EDTA buffer
Tris	tris(hydroxymethyl)aminomethane
UV	Ultraviolet
UTR	Untranslated Region
YMM	Yeast Minimal Media
YPDA	Yeast Peptone Dextrose Adenine media

Abstract

The distribution of epidermal hairs (trichomes) is an important taxonomic character in the genus *Antirrhinum*. Most species in subsection *Antirrhinum* produce trichomes from lower internodes and leaves, then have bald stems and leaf blades after the third node and resume trichomes production again in the inflorescence (the "bald" phenotype). All species in subsection *Kickxiella* produce trichomes throughout development (the "hairy" phenotype). Populations of some species are polymorphic for trichome distribution—both bald and hairy individuals were observed in *A. australe*, *A. graniticum*, *A. latifolium* and *A. meonanthum*.

Antirrhinum species also varied in trichome morphology. Five types were recognized according to length and the presence or absence of a secretory gland. Some types were present in all species and had similar distributions—for example short glandular trichomes were found on the adaxial midribs of all leaves in all species, and the lower leaves and internodes of all species shared longer glandular and long eglandular trichomes. However, the trichomes on leaf blades and stems at higher vegetative nodes of hairy species and in the inflorescences differed in morphology between species, suggesting that they are regulated differently from trichomes at more basal positions. Other species in the tribe Antirrhineae showed similar variation in trichome morphology and distribution to *Antirrhinum*, suggesting that the control of trichome development might be conserved within the tribe.

To understand the genetic basis for variation in trichome distribution, a near-isogenic line (NIL) was generated by introducing regions of the genome of *A. charidemi* (hairy, subsection *Kickxiella*) into the genetic background of *A. majus* subsp. *majus* (bald, subsection *Antirrhinum*). One NIL segregated bald and hairy progeny, with the same trichome distributions as the parent species, in a ratio that suggested a single locus is responsible for the differences and baldness is dominant. The locus was named as *Hairy* and assumed to act as a suppressor of trichome formation. Progeny of the NIL were used in genome resequencing of bulked phenotype pools (Pool-seq) to map *Hairy*. No recombination between *Hairy* and a candidate gene (*GRX1*) from the Glutaredoxin gene family, was detected in the mapping population. In addition, RNA-seq revealed that *GRX1* was expressed in bald parts of bald progeny, but not in the same parts of hairy progeny, and *in situ* hybridisation showed *GRX1* RNA was restricted to epidermal cells, which form trichomes in the absence of Hairy activity. A virus-induced gene silencing (VIGS) method was also developed to test *GRX1* function further. Reducing *GRX1* activity allowed ectopic trichome formation in the bald NIL. Together, this evidence strongly supported *Hairy* being *GRX1*.

To investigate evolution of *Hairy* and its relationship to variation in trichome

distribution, the NIL was crossed to other *Antirrhinum* species. These allelism tests suggested that *Hairy* underlies variation in trichome distribution throughout the genus, with the exception of *A. siculum*, which has a bald phenotype but might lack activity of *hairy* and a gene needed for trichome formation. *Hairy* sequences were obtained from representative of 24 *Antirrhinum* species and two related species in the tribe Antirrhineae. The conserved trichome-suppressing function of the sequence from one of these species (*Misopates orontium*, bald phenotype) was confirmed by VIGS. Gene phylogenies combined with RNA expression analysis suggested that the ancestral *Antirrhinum* had a bald phenotype, that a single mutation could have given rise to the *hairy* alleles in the majority of *Kickxiella* species, that these alleles were also present in polymorphic populations in the other subsections, consistent with transfer from *Kickxiella* by hybridisation, and that multiple, independent mutations had been involved in parallel evolution of the hairy phenotype in a minority of *Kickxiella* species.

Phylogenetic analysis of GRX proteins suggested that Hairy gained its trichome-repressing function relatively late in the evolutionary history of eudicots, after the Antirrhineae-Phrymoideae split, but before divergence of the lineages leading to *Antirrhinum* and *Misopates*.

A yeast two-hybrid screen identified members of the TGA and HD-Zip IV transcription factors as potential substrates of the Hairy GRX.

List of Figures

List of Tables

List of Contents

Chapter 1

1. Introduction

Antirrhinum L, commonly known as snapdragons, are widely used in horticulture. This genus was originally placed in the family Schrophulariaceae (Olmstead & Reeves, 1995), but was transferred to the Plantaginaceae according to APGIII (The Angiosperm Phylogeny Group, 2009). About 28 species are recognized in *Antirrhinum* and they have been divided into three subsections: *Antirrhinum*, *Streptosepalum* and *Kickxiella* (Webb, 1971). This taxonomic treatment is supported by the phylogenetic analysis based on nuclear genetic distances (Wilson & Hudson, 2011). However, the detailed relationships among species in subsections remain obscure.

Trichome density is a vital taxonomic character in *Antirrhinum* and usually correlated with the habitat of a species. Most species of subsection *Kickxiella* are small alpine plants and covered with very dense hairs. Species of subsections *Antirrhinum* and *Streptosepalum* are bigger and more upright plants. They are almost bald except for the inflorescence and lower nodes. Not only is the trichome density different, but the trichome type also varies. In previous studies, both foliar trichomes and fruit trichomes showed variable morphology among species (Juan et al., 1996). Doaigey and Harkiss suggested that the epidermal characters may be useful for taxonomy of *Antirrhinum* species (Doaigey & Harkiss, 1991). However, the variation pattern of trichome morphology may shed light on the evolutionary history of *Antirrhinum*.

1.1 Trichome morphology

Plant hairs or trichomes are outgrowths from the epidermis. They have highly variable shapes which are related with their functions (Uphof et al., 1962, Werker, 2000). They can be roughly classified into glandular trichomes and non-glandular trichomes. Glandular trichomes have secretory cells in their heads that secrete defense or pollinator attracting metabolites, whereas non-glandular trichomes have been proposed to act as physical barrier to UV radiation, heat stress, water loss and herbivores (Dalin et al., 2008). Both types can be unicellular or multicellular, uniseriate or multiseriate (hairs made from more than two rows of cells), and simple or branched. The shape of trichomes is usually described as stellate, T-shaped, dendritic, scaly, shaggy, spiny, hooked, rounded, flattened or spiral.

Non-glandular trichomes are commonly found in plants, especially monocotyledons. Staple cereals, such as rice and maize, are covered with simple trichomes. Trichomes of the model plant *Arabidopsis thaliana* are unicellular, non-glandular and usually have three branches. These trichomes can protect plants from being eaten or having eggs laid on them by insects. Herbivore damage is found to be negatively related to trichome density, with glabrous plants usually receiving more damage (Handley et al., 2005, Puentes & Ågren, 2013). In the Brassicaceae that *Arabidopsis* belongs to, hairs can be unbranched or branched. Phylogenetic data suggests that branched trichomes may have evolved independently several times in the family (Beilstein et al., 2006).

In most cases, glandular trichomes and non-glandular trichomes coexist in the same species and distributed on the different or the same organs. For example, cotton (*Gossypium hirsutum*) fibres, which are widely used in our daily life, are unicellular seed trichomes, however, nulticellular non-glandular hairs occur on the leaves, bracts and stems of cotton and they act as a defense strategy against herbivory (Levin, 1973,

Treacy et al., 1985, Treacy et al., 1986). Glandular trichomes and non-glandular trichomes can be observed together on the leaves of some species from the Asteraceae, Bignoniaceae, Lamiaceae, Plantaginaceae and Solanaceae (Hu et al., 2012, Nogueira et al., 2013). For example, in the antimalarial herb *Artemisia annua*, there are two kinds of foliar trichomes: biseriate glandular trichomes and T-shaped trichomes. From wild tomato (*Solanum habrochaites*), at least five types of trichomes were identified, and three of them glandular (Fig. 1.1). Among them, type VI, glandular trichomes with four head cells, is the predominant type (Tissier, 2012). Capitate trichomes of type I differs from the long simple trichomes of type II only by the presence of a single glandular cell at the tip (Luckwill, 1943). This may support the hypothesis that glandular trichomes evolved from non-glandular trichomes through the differentiation of apical cells into secretory cells (Uphof et al., 1962). However, another possibility is that glandular trichomes lost their secretory cells to form simple trichomes.

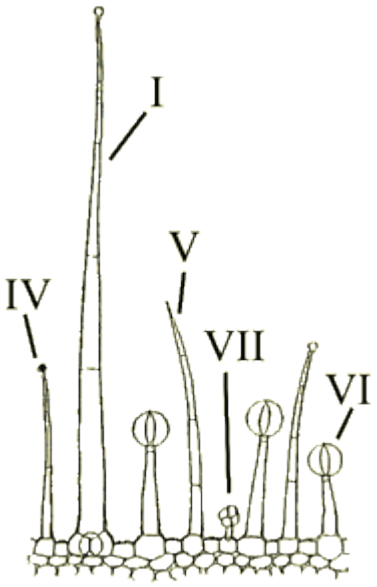

Figure 1.1 Trichome morphology of tomato (Luckwill, 1943).

Glandular trichomes are biosynthesis factories. Substances like essential oils, carbohydrates and resins are synthesized in secretory cells. Oil producing

trichomes, which occur in the flowers of species from the Liliaceae and the Orchidaceae, play critical roles in pollination by specialized bees (Buchmann, 1987). Essential oils are the most abundant substances secreted by capitate and peltate trichomes in the Lamiaceae species (Serrato-Valenti et al., 1997, Gersbach, 2002). Previous studies found the antibacterial and antifungal activities of essential oils and suggested that glandular trichomes enhanced plants' resistance to pathogens (Inouye et al., 2001, Pinto et al., 2006). Trichomes of Solanaceae species produce compounds called acyl sugars that constitute a significant proportion of leaf biomass (Schilmiller et al., 2008). Acyl sugars have an important defensive role against insects. Besides the function of defense against pathogens and insects, trichomes also can help plants against mammals, such as the stinging hairs of nettles (e.g. *Urticadiocia thunbergiana*) (Iwamoto et al., 2014). Fahn concluded that the secretions of glandular trichomes function as protection against herbivores and pathogens and attraction of pollinators, and that their protective functions precede the function of attraction (Fahn, 2002).

1.2 Regulatory networks of trichome formation

The *Arabidopsis thaliana* trichome has become an important model of cell differentiation. Trichome initiation in *Arabidopsis* is controlled by an activation complex that consists of a WD40 protein TRANSPARENT TESTA GLABRA1 (TTG1), an R2R3 MYB protein GLABRA1 (GL1) and a basic helix-loop-helix transcription factor GL3 or its homologue, ENHANCER of GL3 (EGL3) (Hülskamp et al., 1994, Payne et al., 2000, Schiefelbein, 2003, Ishida et al., 2008). Several MYB transcription factors have been determined to function in trichome development via incorporation into this complex. MYB23, another R2R3 transcription factor, has partially overlapping functions with GL1 and can interact with EGL3 (Kirik et al., 2001). MYB82 restored trichome formation in a *gl1*

mutant suggesting that MYB82 and GL1 are functionally equivalent. However, overexpression of a *MYB82* genomic sequence led to reduced trichome number because MYB82 and GL1 can both form homodimers and heterodimers suggesting that overexpression produced more MYB82 homodimers that were not functional (Liang et al., 2014). The homeodomain-leucine zipper (HD-Zip) protein GL2 acts as a transcription factor downstream from GL1 and TTG (Hülskamp et al., 1994). Unlike *GL1*, *GL2* is not only expressed in developing trichomes, but also in mature trichomes. GL2 is required early for trichome formation and later for the subsequent phases of trichome branching, cell expansion and the formation of papillae on the trichome cell wall (Szymanski et al., 1998). A set of single repeat R3 MYB factors including TRICHOMELESS1 (TCL1), TCL2, TRYPTOCHON (TRY), CAPRICE (CPC), ENHANCER OF TRY AND CPC1 (ETC1), ETC2 and ETC3, act as negative regulator of trichome development by competing with GL1 for binding GL3 or EGL3 to block the formation of the activator complex TTG1-GL3/EGL3-GL1 (Wada et al., 1997, Schnittger et al., 1998, Schnittger et al., 1999, Morohashi et al., 2007, Wang et al., 2007, Gan et al., 2011). The R3 MYB proteins are produced by future trichome cells and can move to neighbouring cells. Their interactions with the activating complex result in trichome spacing.

The development of cotton fibres and *Arabidopsis* leaf trichomes share common mechanisms at transcriptional and posttranscriptional levels. Cotton seed fibre is positive regulated by cotton R2R3 MYB transcript factor GaMYB2, which was cloned from *G. arboretum* and is a functional homologue of *AtGL1* (Wang et al., 2004). In tetraploid cotton, *G. hirsutum*, two WD-repeat transcriptions factor genes, *GhTTG1* and *GhTTG3*, are functional homologues of *AtTTG1*, which are able to restore trichome development in *Arabidopsis ttg1* mutant (Humphries et al., 2005). A MYB MIXTA-like transcription factor gene, *GhMYB25*, identified from transcriptome comparsion between wild-type and fibreless cotton mutants, plays a

key role in early cotton fibre and trichome initiation. *GhMYB25* is predominantly expressed in developing fibres and trichomes. Silencing of it resulted in the short seed fibre and a reduction of trichomes on other parts of the plant (Machado et al., 2009). Another MIXTA-like gene *GhMYB25Like* only affects seed fibre intiation. RNA interference expression of *GhMYB25Like* resulted in fibreless seeds (Walford et al., 2011). HD-Zip transcription factors also play important roles in fibre and trichome formation. *GhHD-1*, expressed in trichomes and early fibres, promotes the formation of cotton fibres and epidermal trichomes (eglandular and unicellular) (Walford et al., 2012). GhHD-1 may act in a protein complex with GhMYB25, which is essential for fibre development in cotton (Bedon et al., 2014). The function of *GbHD-1* is conserved with *G. barbadense GhHD-1*. Mutations in *GbHD-1* resulted in the hairless stem phenotype (Ding et al., 2015). A gene responsible for glandular trichomes in cotton was reported. Gossypium *PIGMENT GLAND FORMATION GENE* (*PGF*), isolated from cotton glandless mutants, encodes a basic helix-hoop-helix transcription factor. Silence of *PGF* in *G. barbadense* and *G. hirsutum* resulted in a glandless or low gland number phenotype, suggesting that *PGF* is a positive regulator of gland formation. However, silencing of *PGF* did not affect the growth of eglandular trichomes, suggesting that the development of eglandular and glandular trichomes may have different genetic machinery in cotton (Ma et al., 2016).

The HD-Zip family of transcription factors, especially HD-Zip IV, plays an important role in controlling the differentiation and maintenance of epidermal cell fate (Ariel et al., 2007). Most members of the HD-Zip IV family are preferentially expressed in the outer cell layer of plant organs (Nakamura et al., 2006) and some of them have been suggested to be functional in trichome development, such as AtGL2 in *Arabidopsis* (Szymanski et al., 1998), AhHD1 (Walford et al., 2012) and AbHD1 (Ding et al., 2015) in promoting cotton trichome initiation. In contrast, the *Outer*

Cell Layer 4 gene (*ZmOCL4*) inhibits trichome development in maize (*Zea mays*). The *ocl4* mutants or *OCL4*-RNAi transgenic plants had long eglandular trichomes (macrohairs) on the edge of leaves, whereas wild-type plants had short and prickle hairs. Expression of *ZaOCL4* in *Arabidopsis* reduced trichome numbers, suggesting *ZaOCL4* inhibits trichome development both in maize and *Arabidopsis* (Vernoud et al., 2009). A novel HD-Zip IV transcription factor, AaHD1, was identified recently from the medicinal plant *Artemisia annua*. It positively regulates both glandular and T-shaped nonglandular trichome initiation in *A. annua* (Yan et al., 2017). The expression of *AaHD1* could be positively regulated by a HD-Zip IV/MIXTA complex (AaHD8/AaMIXTA1). AaHD8 interacts with AaMIXTA1 to form a complex that positively regulates the expression of *AaHD1*, thereby promoting trichome initiation in *A. annua* (Yan et al., 2018). Both HD-Zip IV and MIXTA-like are important regulator of trichome development. The HD-Zip IV/MIXTA complex (GhHD-1/GhMYB25) promotes cotton fibre initiation and nonglandular trichome development in cotton. Recent studies showed that a class I homeodomain-leucine zipper gene *Micro-trichome* (*Mict*), which is highly expressed in trichomes, represses fruit trichome and wart formation in cucumber (*Cucumis sativus*) (Zhao et al., 2015). A cucumber WD-repeat homolog CsTTG1, localized in the nucleus and cytomembrane, interacts with Mict to promote the initiation of fruit trichomes and spines (Chen et al., 2016).

Glandular and nonglandular trichome development is regulated by different genes in cotton. The same molecular mechanism is responsible for glandular and nonglandular trichome initiation and patterning in some species. In tomato (*S. lycopersicum*), there are several morphologically distinct trichome types. The *Woolly* gene encodes a HD-Zip transcription factor that is essential specifically for the development of type I trichomes. Woolly interacts with a B-type cyclin, SlCycB2—both of them participate in type I trichome formation (Yang et al., 2011).

A recently isolated gene *SlHairless* in tomato encodes a Racl-associated protein (SlSRA1) subunit of the WAVE regulator complex, which regulate branching of actin filaments. Mutations in *SlHairless* disturb the formation of all types of trichome. The recessive *hairless* mutation produces distorted and shortened trichomes on all aerial tissue, making plants hairless visually (Kang et al., 2016). The genes that are responsible for the fundamental development of trichomes are likely able to regulate both glandular and eglandular trichome development.

It is widely accepted that trichomes of Rosids species develop through a transcriptional regulatory network that differs from those regulating trichome formation in Asterids species. In *Antirrhinum majus*, a R2R3 MYB transcription factor MIXTA regulates conical cell formation in petals. Overexpression of *AmMIXTA* promotes the formation of trichomes and conical cell on the leaves of *Antirrhinum* and tobacco implying that *AmMIXTA* gene has the potential to control multicellular trichome production in these Rosid species (Glover et al., 1998). In contrast, overexpression of *AtGL1* has no effect on trichome formation in tobacco (Payne et al., 1999). Similarly, overexpression of *MIXTA* does not complement the phenotype of *gl1* in *A. thanliana* (Payne et al., 1999). One explanation is that the GL1 network only exists in members of the Rosids. Another possibility is that regulatory network of glandular trichomes initiation is different from that of non-glandular trichomes. Little is known about the genetic network of glandular trichomes. Trichomes known to be regulated by GL1 are all unicellular and different types of trichomes may be regulated by distinct regulatory pathways.

1.3 Trichome distribution in *Antirrhinum*

Both glandular trichomes and simple trichomes were observed in the previous studies of *Antirrhinum* species. Glandular trichomes were usually found on the adaxial

epidermis of the midribs. Subspecies of *A. majus* and *A. latifolium* were almost glabrous except for the inflorescence and adaxial midrib. Eglandular trichomes with thick, warty walls were found in *A. charidemi*, *A. microphyllum*, *A. pertegasii*, *A. pulverulentum* and *A. sempervirens*. *Antirrhinum molle* and *A. mollissimum* seemed similar in morphology due to the presence of glandular and non-glandular trichomes (Doaigey & Harkiss, 1991, Juan et al., 1996). However, little is known about trichome regulation in *Antirrhinum*.

Antirrhinum species are known to differ in trichome distribution. Many members of taxonomic subsection *Antirrhinum*, including the subspecies of *A. majus*, produce leaves with few trichomes while members of subsection *Kickxiella* are densely hairy. Crosses between *A. majus* and either *A. charidemi* or *A. molle* (both from subsection *Kickxiella*) had been used to map a locus responsible for most of the parental differences in trichome density to a region of chromosome 6, close to the self-incompatibility (*S*) locus. A near-isogenic line (NIL) had been produced by back-crossing an *A. majus* × *A. charidemi* hybrid to *A. majus* subsp. *majus* eight times (Costa et al., 2012). This was heterozygous for a region of chromosome 6 from *A. charidemi* in a background that was mainly *A. majus* subsp. *majus*. According to the segregation of phenotypes of progeny, a single locus responsible for trichome density and hairy allele from *A. charidemi* is recessive. We named this gene *Hairy* and roughly mapped it to chromosome 6 and between *CYCLODIEA* (*CYC*) and the *S*-locus. This project aimed at isolating the *Hairy* gene and providing evidence for the genetic basis of trichome distribution and formation in *Antirrhinum*. *Antirrhinum* and its relatives in the tribe Antirrhineae were sampled to study the diversity of trichome morphology and distribution and evolution of the hairiness character.

Chapter 2

2. Materials and methods

2.1 Plant materials and growth conditions

All 28 recognized species or subspecies of the genus *Antirrhinum* were examined. Species used in this study, except for *A. majus* subsp. *majus*, were cultivated from seeds collected from wild populations (Table 2.1) and grown in glasshouses of the University of Edinburgh or the Real Jardín Botánico de Madrid. Some herbarium specimens were also used in this study. Seeds of near-isogenic lines (NILs) were acquired from a previous study (Costa et al., 2012). *Antirrhinum* seeds were sterilized according to the method of Manchado Rojo et al. (2012). Seeds were firstly washed in 70% ethanol for 15 minutes, then in 20% bleach plus a drop of washing up detergent for 15 minutes. They were rinsed with sterile distilled water three times for 5 minutes, then sowed on 1/2 MS plates and placed in a tissue culture room (21^{o}C, 16 h light, 8 h night) after sealing with Parafilm. Seedlings were transplanted into compost when the first leaves came out. Plants were then moved to the glasshouse (21^{o}C, 16 h light, 8 h night), or GroDome (21^{o}C, 16 h light, 8 h night). Either Levington M3 or John Innes No. 2 compost was used.

Misopates orontium, produced by several generations of inbreeding from wild-collected seeds, wild-collected *Chaenorrhinum* species and *Nicotiana benthamina* plants were sowed in compost in the GroDome. Individuals were then transplanted to single pots after germination.

2.2 Trichome morphological analysis

Phenotypes of plants were first checked by eye. Bald phenotype is defined as follows: Inflorescences are covered with dense hair; vegetative parts have decreasing trichome density from bottom to top; nodes and leaves beneath inflorescence are bald or almost bald. For hairy plants, whole plants are covered with thick hairs. To study the morphology of trichomes, whole plants or leaves were imaged with a stereo light microscope or scanning electron microscope (SEM) or leaves were cleared and stained. For seedlings, whole plants were collected when the second true leaves came out. Leaves of different development stages and sepals were taken from mature flowering plants.

Table 2.1. Information of species samples in this study

Species	Accession	Location
Subsection *Antirrhinum*		
A. australe Rothm.	L95	El Burgo, Malaga, Spain
	L83	Benamahoma, Cadiz, Spain
	L84	El Boyar, Cadiz, Spain
	L91	Gaucin, Malaga, Spain
	TM4-9	
A. barrelieri Boreau	L150	Cadiar, Granada, Spain
	MbarL167	Taineste, Morocco
	TM37	
A. graniticum Rothm.	L116	Celorica da Beira, Guarda, Portugal
	TM25	Tornavacos, Caceres, Spain
	L40	Braganca, Braganca, Portugal
	L69	Ledanca, Guadalajara, Spain
A. latifolium Miller	AC1066	St Martin d'Entraunes, Alpes-Maritimes, France
	MA63381	Serra del Cadí, Catalonia, Spain
A. majus subsp. *cirrhigerum* Filcaho	L123	Algave, Portugal
	L114	Praia de Mira, Coimbra, Portugal
	TM41	Serra do Montejunto, Estremadura, Portugal

Table 2.1. continued

Species	Accession	Location
A. majus subsp. *linkianum* Boiss & Reuter	L108	Almada, Setubal. Portugal
	L110	Pernes, Santarem, Portugal
	MA865666	Serra do Montejunto, Estremadura, Portugal
	TM23	Serra do Montejunto, Estremadura, Portugal
A. majus subsp. *litigiosum*	L3	Chesta, Valencia, Spain
A. majus subsp. *majus* L.	JI.7	from John Innes Centre
A. majus subsp. *pseudomajus*	L53	Minerve, Herault, France
A .majus subsp. *striatum*	AC1125	Alet les Bains, Aude, France
A .majus subsp. *tortuosum*	L92	Casares, Malaga, Spain
A. siculum Millar	AC1177	Taormina, Sicily, Italy
	TM35	Pedra, Sicily, Italy
Subsection *Kickxiella*		
A. boissieri Rothm.	L104	Ermita Virgen de la Sierra, Cordoba, Spain
	L18	Guadahortuna, Granada, Spain
A. charidemi Lange	E23	Cabo de Gata, Almeria, Spain
	TM33	
A. grosii Font Quer	L175	Sierra de Gredos, Toledo, Spain
A. hispanicum Chav.	L99	Almargan, Malaga, Spain
A. lopesianum Rothm.	*	Vimioso, Braganca, Portugal
A. microphyllum Rothm.	L72	Sacedon, Guadalajara, Spain
	L73	Pantano de Buendia, Guadalajara, Spain
	L74	Buendia, Guadalajara, Spain
A. molle Lange	E51	Gerri de la Sal, Lleida, Spain
A. mollisimum Rothm.	L21	Enix, Almeria, Spain
A. pertegasii Rothm.	E65	Castellon, Spain
A. pulverulentum Lazaro	L68	Pelegrina, Guadalajara, Spain
	L70	Alcorlo, Guadalajara, Spain
	L77	Poveda de la Sierra, Guadalajara, Spain
	L78	Hoz de Beteta, Cuenca, Spain
A. rupestre Rothm	L139	Capieleria, Granada Province, Spain
A. sempervirens Lapeyre.	L50	Col d'Aubisque, Hautes-Pyrenees, France
	L52	Luz, Hautes-Pyrenees, France
	TM16	Panticosa, Huesca, Spain
A. subbaeticum Guemes	E72	Albacete, Spain
A. valentinum Font Quer	AC1173	La Drova, Valencia, Spain

Table 2.1. continued

Species	Accession	Location
Subsection *Streptosepalum*		
A. braun-blanquetii Rothm.	E20	St Pietro de Villanueva, Asturias, Spain
A. meonanthum Hoffmans. & Link	L118	Poco do Inferno, Manteigas, Guarda, Portugal
	79Y80	
Related species		
Chaenorhinum origanifolium Fourr		Gijón, Asturias, Spain
C. rubrifolium Fourr		Bolarque, Guadalajara, Spain

2.2.1 Leaf clearing

To gain a clear image of the epidermis, samples were cleared with a modification of the method described by Gudesblat *et al.* (2012). First the tissues were incubated in 100% ethanol to remove chlorophyll. When tissues became completely pale, they were rinsed three times with phosphate buffered saline (PBS; 137 mM NaCl, 2.7 mM KCl, 10 mM Na_2HPO_4 and 2 mM KH_2PO_4) buffer and incubated in 0.5 M NaOH at 60°C for 60 minutes. They were then rinsed three times in PBS buffer and stained in safranin (1% in ethanol) for 2 minutes. Pictures of cleared tissues were taken using Nikon SMZ 1500 and E600 microscopes equipped with a Leica camera. Trichome characters were measured with imageJ.

2.2.2 SEM

Materials for SEM were prepared as described by Kang (Kang et al., 2010). Plant tissues were collected and immediately fixed in 2.5% formaldehyde, 2.5% glutaraldehyde in 0.15 M phosphate buffer (pH 7.4) for a week. The samples were then rinsed with PBS. Dehydration was done in an ethanol dilution series (30%, 50%, 70%, 90% ethanol, with 15 minutes in each step; followed by two 1 hour steps in 100% ethanol). Ethanol was replaced with liquid CO_2 in a critical point dryer

and CO_2 allowed to convert to gas at its critical point by reducing the pressure. Samples were affixed to specimen stubs with double-sided tape and then sputter-coated with gold. Observations were conducted using a Hitachi 4700 II cold field-emission SEM.

2.2.3 Resin sectioning

Fixation and dehydration followed the same procedures as for SEM. Tissues were embedded in JB-4 embedding kit (Sigma-Aldrich) according to the manufacturer's instructions. Briefly tissues were infiltrated with increasing concentrations of resin in ethanol (50%, 70%, 90% resin, for 1 hour at each step) followed by three one-hour steps in 100% resin. Resin was then polymerized under vacuum. Leaves were sectioned transversely into 5 μm slices using a microscope slide as a glass knife in a rotary microtome following Ruzin's instructions (Ruzin, 1999). Sections were placed in water drops on glass slides and dried on a hot plate at 42°C overnight. After that, slides were stained in 0.05% toludine blue for 1 minute, rinsed with water and dried in a flow hood. Photos of sections were taken with a Nikon E600 microscope.

2.3 Bulked segregant analysis

2.3.1 Mapping population construction

A population of near isogenetic line had been generated by crossing *A. majus* supsb. *majus* (JI.7) to *A. charidemi* and backcrossing to *A. majus* subsp. *majus* for eight generations. A locus involved in hair distribution (*Hairy, H*) had mapped to chromosome 6 and it found to be linked to the Self-incompatibility (*S*) locus. To indentify the *Hairy* gene, we needed a bald NIL individual which was heterozygous at the *Hairy* locus (H^m/h^c) and segregated bald and hairy progeny. Chromosome 6

from *A. charidemi* carries an active *S* allele (S^c) linked to the recessive *hairy* allele (h^c). A NIL that was heterozygous at *Hairy* (H^m/h^c) had also been found to be heterozygous at the *S* locus, carrying both the active inactive *A. majus* subsp. *majus* and *A. charidemi* alleles (s^m/S^c). In self-pollination, pollen carrying S^c was rejected, therefore hairy progeny (h^c/h^c) were only produced at a low frequency, by fertilization by h^cs^m pollen that carried a recombinant chromosome. To obtain a NIL that was heterozygous at *Hairy* (H^m/h^c) and homozygous at the *S* locus (s^m/s^m), a bald NIL progeny (*9) was crossed with a hairy sibling (H5), which had to carry at least one recombinant h^cs^m chromosome. To identify plants of genotype H^ms^m/h^cs^m in the F_1 population, a cleaved amplified polymorphic sequence (CAPS) marker was identified by sequencing the F-box component of the *S* alleles from *A. majus* subsp. *majus* and *A. charidemi* (see Section 2.3.2). After the heterozygous plants were identified, they were crossed with other *Antirrhinum* species to test whether the same locus was responsible for trichome density throughout the genus *Antirrhinum*. Meanwhile, an H^ms^m/h^cs^m heterozygous plant was self-pollinated to produce an F_2 population (M430) for bulked segregant analysis.

2.3.1 DNA extraction from the mapping population

Plant DNA was extracted from fresh leaves of F_1 (M351) individuals using the modified CTAB method (Wilson, 2009). Approximately 0.1 g tissue was collected from each plant into a 2 ml Eppendorf tube with two stainless steel beads and frozen in liquid nitrogen. Tissue was ground using TissueLyser II (Qiagen) for 2 minutes at 30 Hz frequency. After that, 500 µl CTAB extraction buffer (100 mM Tris pH 8.0, 1.4 M NaCl, 20 mM EDTA, 2% CTAB, 0.2% β-mercaptoethanol) was added to the tissue powder and the mix was ground for another minute. The tube was then incubated at 65°C for 30 minutes. After the tube cooled down to room temperature, 500 µl chloroform was added to it. The tube was briefly vortexed and then centrifuged at 13 000 xg for 5 minutes. The supernatant was transferred to a 1.5 ml

Eppendorf tube and 334 µl isopropanol was then added and the tube contents were mixed gently. The DNA pellet was precipitated by centrifuging the tube at 13 000 xg for 10 minutes. The supernatant was pipetted off the pellet, the tube was left with opened lid in a lamina flow hood for about 1 hour to evaporate the residual isopropanol. To digest RNA, 100 µl TE buffer [10 mM Tris-HCl (pH 8.0), 0.1 mM EDTA] with 0.1 µg/ml of DNase-free RNaseA was added to the pellet and the tube was left at 4°C overnight.

Then 10 µl 3M NaOAc and 250 µl ethanol were added to the tube, and the contents of the tube were mixed gently and centrifuged at 13 000 xg for 10 minutes. The supernatant was pipetted from the DNA pellet and the pellet was washed with 100 µl of 70% ethanol by centrifuging at 13 000 xg for 15 seconds. The ethanol was pipetted off the pellet and the tube was left open in a lamina hood for 1 hour to evaporate all the ethanol. The DNA was then dissolved in 50 µl TE buffer, and stored at -20°C.

2.3.2 Genotyping at *S* locus

The PCR for the F-box component of the *S* locus (Qiao et al., 2004) was conducted in 20 µl reaction containing approximately 50 ng of genomic DNA as template, 4 pmoles of each primer, 0.2 mM each dNTP, 0.2 units of *Taq* DNA polymerase, and 2 µl of PCR buffer solution (10x: 500 mM Tris-HCl pH 8.3, 5% Ficoll, 5 mg/ml BSA, 10% sucrose, 300 mM KCl, 30 mM $MgCl_2$, 10 mM tatrazine). Primers F-box F and F-box R were used to amplify the sequence of the F-box (Table 2.2). The PCR program used for the F-box was as follows: 1 cycle of 2 minutes at 95°C; 35 cycles of 20 seconds at 95°C, 20 seconds at 55°C, 1 minute at 72°C, and a final extension of 5 minutes at 72°C. The F-box allele of *A. charidermi* can be digested twice by *Dpn* II with the recognition site of GATC. The F-box allele of *A. majus* subsp. *majus* contains only one recognition site. The digestion solution contained 4 µl PCR

products, 3 units of *Dpn* II (NEB) and 1µl of 10x buffer supplied with the enzyme and was incubated at 37°C for 1 hour. Digested products were separated in a 2% agarose gel for genotyping.

2.3.3 Pollination

Self- and cross-pollination was conducted as described previously (Hudson et al., 2008). After H^mS^m/h^cS^m plants had been identified, pollen was transferred to the stigma of the same flower with a toothpick after the petals had opened to produce the F_2 population (M430). For cross-pollination, anthers of H^mS^m/h^cS^m plants were removed when flowers were still unopened. Pollen of natural species were collected and transferred to the stigmas of H^mS^m/h^cS^m plants to do allelism test. Pollination of the same flower was repeated at least three times on different days.

2.3.4 Bulked segregant analysis

Self-progeny of an H^ms^m/h^cs^m plant (F_2 population, family M430) segregated 306 bald plants and 80 hairy plants. Genomic DNA was extracted from individuals of the F_2 population as described above (Section 2.3.1), and its concentration was measured by an ND-1000 NanoDrop spectrophotometer. For each phenotype, equal amounts of DNA were pooled from 280 bald plants and 70 hairy plants to make bald pool and hairy pool. Before sequencing, pooled DNA samples were purified with phenol/chloroform extraction. DNA samples were gently mixed well with an equal volume of phenol:chloroform (1:1 by volume), then they were centrifuged at room temperature for 5 minutes at 13 000 xg. The supernatant was transferred to a new 1.5 ml tube and mixed with 1/10 volume of 3 M NaOAc and 2.5 volumes of ethanol. The mixture was left at -20°C overnight for precipitation and centrifuged at 13 000 xg for 15 minutes next day. The supernatant was removed from the pellet and the pellet was washed once with 200 µl 70% ethanol and centrifuged at 13 000 xg for 1 minute. Pellets were dried in a lamina flow hood to remove residual ethanol after

the removal of the supernatant. Pellets were dissolved in nuclease-free water. Concentrations, A260/A280 and A260/A230 ratio were measured with a GeneQuant 1300 spectrophotometer. After samples passed the quality test (concentraton: 40 ng/µl, A260/A280 and A260/A230 ratio: 1.80-2.00), samples were sent to the Genome Analysis Centre, Norwich Research Park for Illumina paired-end sequencing.

The sequencing data was analyzed by Matthew Barnbrook. All reads were mapped to the *A. majus* subsp. *majus* JI.7 reference geneome together with RNAseq data. RNA samples for RNAseq had been extracted from shoot apices of plants in which the node 6 leaves were 5 mm long.

2.3.4 Genotyping at *GRX1*

Once the candidate gene (*GRX1*) was isolated, primers GRX-NR and GRX-F were designed to amplify alleles from *A. majus* subsp. *majus* and *A. charidemi* (primers are listed in Table 2.2). PCR was conducted in 20 µl total reaction reagent volumes as described previously (see Section 2.3.2). The amplification conditions were an initial denaturation of dsDNA template for 10 minutes at 95^{o}C followed by 35 cycles of denaturation at 95^{o}C for 20 seconds, annealing at 56^{o}C for 20 seconds, and extension at 72^{o}C for 60 seconds. An addition final extension at 72^{o}C for 5 minutes was included at the end of the reaction cycle. PCR products (2 µl) were loaded into a 1% agarose gel to estimate the size. The allele of *A. charidemi* has a *Bst*X I recognition site of CCNNNNNNTGG, while the allele of *A. majus* subsp. *majus* does not. CAPS was utilized as described above to genotype plants (see section 2.3.2). After 1 hour incubation with *Bst*X I at 37°C, digested PCR products were loaded into 2% agarose gels for separation. Parental plants *9 and H5, and plants from the F_1 and F_2 population were genotyped to confirm genotypes and co-segregation of hair phenotypes with genotypes.

2.4 Virus-induced gene silencing (VIGS) in *Antirrhinum*

VIGS is a method taking advantage of plant RNAi-mediated antiviral defense mechanism to induce silencing of endogenous genes (Senthil-Kumar & Mysore, 2014). Tobacco Rattle Virus (TRV) has been widely used in VIGS and has a wide range of host. To test whether the candidate gene *GRX1* was *Hairy* gene, it was cloned into pTRV2. To test whether genes from the same family also involved in trichome formation, a homolog of candidate gene (*GRX2*) which shares 73.2% similarity to *GRX1* in nucleotide sequences was also cloned. To test whether the ortholog of *GRX1* play the same function in related species, TRV::*MoGRX1* was constructed and used for infection of *Misopates orontium*. Three potential targets of GRX1, encoding two TGA transcription factors and a GLABROUS11 (GL11)-like member of the homodomain-leucine zipper (HD-Zip) family, were isolated by yeast two-hybrid screening. These three genes and *TGA27*, which is potential to interact with GRX1, were cloned in pTRV2 to find out their function in trichome formation. Phytoene desaturase gene (*AmPDS*) was cloned and used as a reporter gene here, disruption of it causing leaf bleaching. All sequences used for VIGS construction were blasted against *Antirrhinum majus* genome to avoid off-target silencing.

2.4.1 TRV construct

The pTRV1 and pTRV2 Δ 2b vectors (PpK20 strain) were gifts from Molnar's group (Vainstein & Zuker, 2014). To validate the function of genes, *AmGRX1*, *AmGRX2*, *AmPDS*, *AmTGA1*, *AmTGA2*, *AmGL11*, *MoGRX1* were amplified from cDNA by PCR from using primers listed in Table 2.2. *MoGRX1* was amplified from cDNA extracted from the shoot apex forming bald internodes (before inflorescence formation) of *Misopates orontium*. All the other six genes were amplified from cDNA extracted from the shoot apices of bald NILs where the fourth leaves were 5 mm long. For TRV2 to silence *PDS* alone, *AmPDS* was amplified with a forward

primer containing an *Asc* I site, and a reverse primer with a *Bam*H I site and cloned after digestion into the same sites in pTRV2. To generate *AmPDS* fragments fused to other test genes, two rounds of PCR were carried out. In the first round, the *AmPDS* fragment was amplified with a forward primer without an *Asc* I site and the reverse primer with a *Bam*H I site; the other genes were amplified with forward primers with an *Asc* I site, and reverse primers which contained sequence overlapping of *AmPDS* at the 5' ends. PCR was conducted in 20 µl total reaction with Q5 high-fidelity DNA polymerase (NEB). The mixture was prepared with 4 µl 5x Q5 reaction buffer, 4 µl Q5 high GC enhancer, 0.4 µl 10 mM dNTP, 1 µl 10 µM forward and reverse primers, 0.2 µl Q5 DNA polymerase, 1 µl undiluted cDNA template, and nuclease-free water to 20 µl. The amplification conditions were an initial denaturation of cDNA template at 98^{o}C for 30 seconds followed by 35 cycles of denaturation at 98^{o}C for 10 seconds, annealing at 60^{o}C for 20 seconds, extension at 72^{o}C for 30 seconds, with a final extension at 72^{o}C for 2 minutes. First round PCR products (2 µl) were loaded into 1% agarose gel to check amplification. In the second round, *AmPDS* fused fragments were amplified by overlap PCR from first round products with the corresponding forward primer with an *Asc* I site and the reverse *AmPDS* primer with *Bam*H I site. The PCR mixture was prepared as for the first round except primers were added after the first PCR cycle while the PCR machine was held at 4^{o}C. PCR products with overlapping *PDS* sequences annealed together during the first cycle without primers and were extended to produce fused fragments that could be amplified in the following cycles. DNA gel electrophoresis was used to check that a single strong band of correct size was produced after second round PCR. If more than one band could be seen, the band of correct size was cut and gel purified with QIAquick® gel extraction kit (Qiagen) according to the manufacturer's protocol.

To increase the efficiency of cloning, PCR products were firstly inserted into

pJET2.1 vector, which allows selection for inserts, using the ClonJET PCR cloning kit (Thermo Scientific) according to the supplier's manual. Colonies with correct insertions were screened on L Broth (LB) plates containing ampicillin (100 µg/ml) and then cultivated in 5 ml LB medium with antibiotic at 37°C overnight. Plasmids were extracted from 5 ml overnight culture with QIAprep® spin minprep kit (Qiagen). Afterwards, fragments with *Asc* I and *Bam*H I sticky ends were produced by double digestion at 37°C for 2 hours, separated in agarose gels and purified with a QIAquick® gel extraction kit (Qiagen). The concentration of purified fragments and digested pTRV2 vector were measured with a ND-1000 NanoDrop spectrophotometer to ensure that the molar ratio of vector:insert was 1:1 in the ligation. Fragments were then inserted at the *Asc* I and *Bam*H I sites of the pTRV2 vector with T4 DNA ligase (Promega) at 16°C overnight. The ligations were then transformed into *E. coli* competent cell strain DH5α using the heatshock method at 42°C for 45 seconds, followed by 1 hour recovery in SOC broth. Colonies were screened on LB plates containing kanamycin (50 µg/ml). pTRV2 with correct insertions were extracted from 5 ml LB overnight culture with kanamycin. The sequence of pTRV2 plasmids with insertions was confirmed by sequencing with pTRV2 primers.

2.4.2 TRV inoculation

After the construction of pTRV2 plasmids, they were transformed in *Agrobacterium* strain GV3101 using the freeze-thaw method (Koncz & Schell, 1986). Meanwhile, the pTRV1 vector was transformed as well. A single *Agrobacterium* colony was selected and cultivated in 5 ml LB medium containing kanamycin (50 µg/ml), gentamycin (25 µg/ml) and rifampicin (50 µg/ml) at 28°C for overnight to make a 5 ml starting culture. The next day, a main culture was made with 200 µl of starting culture and 10 ml LB medium containing antibiotics, and grown overnight at 28°C. Cells were pelleted and resuspended in freshly prepared infiltration medium (10 mM

MES pH 5.6, 10 mM $MgCl_2$, 150 µM acetosyringone) to a final OD_{600} of 1.5. Prior to infiltration, *Agrobacterium* cell suspensions were incubated at room temperature for 3 hours (Zhu et al., 2008). To increase the efficiency of *Antirrhinum* infection, infective virus was first produced in *N. benthamina*. Tobacco plants were grown for 3-4 weeks at 21^{o}C in a long day room, until 4 to 5 leaves could be seen. They were infiltrated with a 1:1 mixture of TRV1- and TRV2-carrying *Agrobacterium* strains using the needleless syringe method (Senthil-Kumar & Mysore, 2014). The top three leaves of each tobacco plants were collected 5-7 days post infection (dpi) and ground in extraction buffer (1 mM Na_2HPO_4, 1mM NaH_2PO_4) on ice to obtain sap containing TRV virus particles. The sap was then spun down at 3000 xg for 5 minutes at 4°C. The supernatant was transferred to a 1.5 ml Eppendorf tube, and was used for inoculation afterwards or stored at -80°C. Competent cells preparation in this research was followed protocols published from the website OpenWetWare (Pei, 2012, Hill, 2014).

For infection of other species, seeds of bald and hairy NILs were sowed on 1/2 MS plants after sterilization. Seedlings were transplanted to single pots of compost 10 days after sowing and grown in a GrowDome. Seeds of *Misopates orontium* were sowed directly in compost in the GrowDome. All plants used for VIGS were grown in a chamber of the GrowDome to minimize release of TRV to the environment. Seedlings were transplanted to single pots 10 days after seed sowed out and grown in GrowDome. When the first real leaves could be seen from seedlings, usually 7-10 days after transplanting *Antirrhinum*, 3-5 days for *M. orontium*, cotyledons and leaves were inoculated by rubbing them between two fingers after aluminum oxide powder was scattered and sap (10 µl per plant) was dropped on them. Plants were then covered with transparent plastic lids for 5 days. To not disturb the absorption of virus, plants were watered before inoculation. The effect of silencing *AmPDS* was usually visible on the first leaves by 5-7 days post infection. Phenotypes of treated plants were recorded with a Nikon D60 camera and a Nikon M1500

stereomicroscope.

2.5 Phylogenetic analysis

To reconstruct evolution of *GRX*, the gene was amplified from accessions of 24 *Antirrhinum* species and two relatives in the Antirrhineae (*Misopates orontium*, *Chaenorhinum origanifolium*). Sequences from the more distant relatives *Mimulus guttatus*, *Solanum esculentum* and *Arabidopsis thaliana* were identified by BLAST searches of the whole-genome sequence at TAIR or Phytozome. Bayesian inference and maximum likelihood methods were applied to analyze the phylogenetic relationship.

2.5.1 Extraction of genomic DNA from *Antirrhinum* and related species

DNA was extracted from either fresh leaf tissue, or dried leaf tissue from herbarium specimens. For living plants, about 0.1 g fresh leaf tissue was collected in 2 ml Eppendorf tube with two stainless steel beads and frozen in liquid nitrogen. DNA was then extracted followed the method described in section 2.3.1.

For dried tissue from herbarium specimen, about 150 µg leaf tissue was collected and placed in a 1.5 ml Eppendorf tube with two glass beads. Tissue was ground with TissueLyser II for 2 minutes at 30 Hz. DNA was then extracted with DNeasy plant mini kit (Qiagen) according to the manufacturer's protocol.

The DNA concentration was estimated with an ND-1000 NanoDrop spectrophotometer and diluted to the appropriate concentration for subsequent techniques in TE buffer. To check the quality of DNA, 2 µl of each sample were run in a 1% agarose gel.

2.5.2 PCR and sequencing

The *GRX1* sequences of most species were amplified with primers GRX-NR and GRX-L. For species that cannot be amplified with these two primers, GRX-R2 and GRX-L were used. For the outgroup species, *Chaenorhinum origanifolium* and *Misopates orontinum*, sequences were amplified with GRX-CR-R, GRX-RACE-R3. PCR reactions were conducted with Taq polymerase or Veraseq 2x PCR mix containing VeraSeq 2.0 high-fidelity DNA polymerase (Enzymatics), 2 pmole primer mix, 0.5 ng genomic DNA in 10 µl total solution. The PCR was carried out by denaturing genomic DNA at 98^{o}C for 5 minutes followed by 35 cycles of 20 seconds at 98^{o}C, 20 seconds at 56^{o}C, 1 minute at 72^{o}C and by a final extension of 10 minutes at 72^{o}C. Electrophoresis in 1% agarose gel was applied to test the success of PCR amplification. PCR products were then cloned into pJET 1.2 vector according to the manufacturer's protocol, and screened on LB plates containing 100 µg/ml ampicillin. Colony PCR using pJET-forward and pJET-reverse primers, Taq or VeraSeq 2.0 high-fidelity DNA polymerase was applied to screen positive single colonies with insertions. The PCR products (3 µl) were submitted to Edinburgh University Gene-Pool Sequencing facility with 1 µl 10 µM pJET-forward primer, and 2 µl nuclease-free water for Big-Dye sequencing.

2.5.3 Southern blot analysis

For some hairy species, the *GRX1* gene could not be amplified with any combination of primers I tried. One possibility was that the *GRX1* gene had been deleted in these species. To test this, genomic DNA was extracted for Southern blot analysis (method described in section 2.3.1). About 5 µg genomic DNA was mixed with 3.5 µl NEB buffer 2, 1 µl *Eco*R I, 1 µl *Xba* I (NEB), 1.5 µl 5 mM spermidine, and sterilized distilled water to 35 µl. The mixture was incubated at 37^{o}C for 6-8 hour. After digestion, the mixture with addition of 7 µl 6x blue loading buffer (NEB) was loaded into a 0.7% agarose gel (20 cm x 30 cm, without ethidium bromide) to get

better resolution. Electrophesis was conducted at 35 V for 16-24 hours and the gel was then stained in 0.5x TBE containing 0.5 µg/ml ethidium bromide for 1 hour. Afterwards the gel was photographed under UV with a ruler as a scale.

To reduce the size of DNA molecules, to help transfer, and to make DNA single stranded, the gel was treated with depurinating, denaturing and neutralizing buffer with gentle shaking after excess gel was trimmed from it. It was first depurinated in 0.25 M HCl for 10 minutes, and then soaked in 0.5 M NaOH, 1.5 M NaCl for 20 minutes, and was neutralized in 1 M Tris pH 7.5, 1.5 M NaCl for 20 minutes with gentle shaking. The blotting was done via upward capillary transfer of DNA from the agarose gel onto a nylon membrane. A sheet of Hybond^{TM}-N (Amersham) slightly larger than the gel and six sheets of Whatman 3 MM paper of the same size were cut. A platform bigger than the gel was made with three sheets of Whatman 3 MM paper soaked in 20x SSC (1 M NaCl, 0.1 M NaCitrate, pH 7.0). Each sheets of Whatman paper was soaked separately and air bubbles were rolled out with a glass pipette before putting the next sheet on. The gel was then placed upside down on the Whatman paper covered platform. A frame for the gel was made with Parafilm to avoid direct contact between dry paper towels and the wet platform. The sheet of Hybond^{TM}-N membrane was rinsed briefly in the leftover neutralizing buffer and placed on the gel. Air bubbles were rolled out from the filter and the other three sheets of Whatman paper were wetted in neutralizing solution separately, and placed on to the membrane one by one. Air bubbles were removed before the next sheet was placed on. A stack of paper towels cut to similar size of the gel was added. A plastic board and a bottle of water (about 500 g) were placed on top of the stack and they were left overnight for transfer of the digested DNA bands from gel to Hybond^{TM}-N membrane.

The next day, the paper towel and Whatman paper were removed. The

Hybond^{TM}-N membrane was rinsed briefly in 2x SSC, drained and air dried. It was then fixed in a UV Stratolinker (0.4 J/cm^2) with the DNA side up. The fixed membrane was stored at room temperature between sheets of Whatman paper.

To prepare a Digoxigenin-labeled DNA probe, the *GRX1* sequence was amplified from genomic DNA of a bald NIL plant with primers GRX-CR-R and GRX-L. The PCR product was cloned with a cloneJET^{TM} PCR cloning kit (Thermo Fisher Scientific). A labeled DNA probe was generated with the PCR DIG Probe Synthesis kit (Roche) according to the manufacturer's instructions.

Before hybridization, 100 ml hybridization buffer was made with 25 ml 20× SSC (3 M NaCl, 0.3 M sodium citrate, pH 7.0), 1 ml 10% N-lauryl sarcosine, 200 µl 10% SDS, 2 g Blocking reagent (Roche), and distilled H_2O to 100 ml. The membrane was firstly prehybridized in 70 ml hybridization buffer for 2 hours at 65^{o}C. When the prehybridization was almost done, 10 µl of the prepared DIG-labeled DNA probe was denatured by boiling it at 100^{o}C for 10 minutes and added to 20 ml of prewarmed hybridization buffer. The membrane was then hybridized overnight in this solution at 65^{o}C. To remove non-specific bound probe, the membrane was rinsed twice in 100 ml low stringency wash buffer (2x SSC, 0.1% SDS) for 5 minutes at room temperature and twice in 100 ml high stringency wash buffer (0.5x SSC, 0.1% SDS) for 15 minutes at 65^{o}C. Afterwards, the membrane was blocked in 50 ml blocking solution [1% Roche blocking reagent dissolved in maleic acid buffer (100 mM maleic acid, 150 mM NaCl pH 7.5)] for 1 hour at room temperature. To detect the hybridized signal, the membrane was firstly soaked in 20 ml blocking solution with 20 µl anti-Digoxigenin-alkaline phosphatase antibody (Roche) for 1 hour at room temperature. It was then washed twice in 100 ml maleic acid buffer with 0.3% TWEEN 20 for 15 minutes to remove antibody that was not specifically bound and equilibrated in detection buffer (100 mM Tris-HCl pH 9.5, 100 mM NaCl)

for 3 minutes at room temperature. A chemiluminescent assay was done to visualize probe-target hybrids. The membrane was placed onto an acetate sheet with DNA side facing up. Ready-to-use CSPD substrate (Roche) was applied to the surface of the membrane until the entire surface was evenly soaked. Another acetate sheet was used to cover the dampened side of the membrane. Air bubbles and excess liquid between acetate sheets and blot were squeezed out to let the CSPD substrate spread evenly over the membrane before these two acetate sheets were sealed by heating. To enhance the luminescence reaction, the sealed membrane was incubated at 37^{o}C for 10 minutes. A Lumi-film X-ray film (Thermo Scientific) was exposed to the sealed sheets for 4 hours in a cassette. The film was developed and scanned.

2.5.4 Bioinformatic analysis

All the phylogenetic analysis was conducted online by the CIPRES Science Gateway V. 3.3, a public resource for inference of large phylogenetic trees (Miller et al., 2010). Bayesian Inference analyses were conducted with MrBayes 3.2.6 (Huelsenbeck & Ronquist, 2001, Ronquist & Huelsenbeck, 2003), using the best-fit models of nucleotide substitution or amino acid substitution. Two independent Metropolic-coupled MCMC analyses were performed with default settings. Each search was run for 20000000 generations sampled every 1000th generations. The initial 25% of samples of each Metropolis-coupled MCMC run were discarded as burnin.

2.5.4.1 Phylogenetic analysis of *Antirrhinum* and related species

Phylogenetic analysis of GRX sequences from *Antirrhinum* and other species was based on DNA sequences of *Hairy*-like genes and protein sequences predicted from DNA sequences. Sequences were firstly aligned with Clustal Omega via the web

service from EMBL-EBI (Goujon et al., 2010, Sievers et al., 2011, McWilliam et al., 2013), corrected manually, and the alignments exported as Nexus and Phylip files. jModeltest2 was applied to choose the best model for nucleotide substitution (Darriba et al., 2012), and TPM2uf+G was chosen. Prottest2.4 was used to choose the best model for amino acids substitution (Abascal et al., 2005), and JTT+G was chosen.

2.5.4.2 Phylogenetic analysis of GRX family proteins

To resolve the relationship of HAIRY to other known GRX proteins, GRX protein sequences were downloaded from TAIR, GenBank, Phytozome and Sol Genomic Network, or for AmHairy, CoHairy, MoHairy, and AmGRX2 were translated from DNA sequences. Alignment of the amino acid sequences was performed using Clustal Omega. Prottest 2.4 was applied to choose the best model for amino acides substitutions (Abascal et al., 2005) and JJT+G was selected.

2.6 RNA expression analysis

2.6.1 RNA extraction and reverse-transcription (RT)

Total RNA was extracted from tissue of different developmental stages using TRIzol® reagent (Invitrogen, ThermoFisher Scientific) according to the manufacturer's protocol. Extracted RNA was then treated with RQ1 RNase-free DNase (5 units, Promega) at 37ºC for 30 minutes to remove genomic DNA. DNase was inactivated at 65ºC for 10 minutes with the addition of 2 µl RQ1 DNase stop solution provided with the enzyme. The RNA concentration was measured with a NanoDrop spectrophotometer and 2 µl of each sample was separated in a 1% agarose gel to check quality. To conduct the reverse transcription, 2 µg of total RNA was mixed with 10 pmole oligo-dT primer and incubated at 65°C for 5 minutes. The

reaction was cooled to 4°C afterwards, and mixed with 100 nmole of each dNTP, 10 units of RNase inhibitor (Promega), 200 units of M-MLV Reverse Transcriptase (Promega), 1x RT reaction buffer, and RNase-free water to 20 µl in total. The reaction mix was incubated at 42°C for 60 minutes, and then at 65°C for 15 minutes. The reaction product was stored at -20°C or used immediately in PCR.

2.6.2 SYBR green qRT-PCR

Quantitative RT-PCR reactions were performed using LightCycler® 480 SYBR Green I master mix (Roche) in a Lightcycler® 96 instrument (Roche). The housekeeping gene *AmUbiquitin* (*AmUbi*) was used for relative quantification of gene expression (Preston & Hileman, 2010). Usually three biological replicates (RNA extracted from independent tissue samples) and two technical replicates (amplification of the same cDNA) were used. Relative quantification of the expression of each gene was performed using the $2^{-\Delta\Delta CT}$ method. Primers used in this analysis were listed in table 2.2.

2.7 *In situ* hybridization

The expression pattern of *AmHairy*, *AmGRX2* and genes encoding potential substrates were examined by in situ hybridization to RNA in samples at three developmental stages. Samples were prepared as described before (Zachgo et al., 2000, Rebocho et al., 2017).

2.7.1 RNA probe preparation

AmHairy and *AmGRX2* were amplified from genomic DNA of a bald NIL, while *AmTGA1*, *AmTGA1*, *AmTGA27* and *AmGL11* were amplified from cDNA from apices above node 4 of bald NILs. To generate antisense RNA probes, PCR

products were cloned in pJET2.1 vector (ThermoFisher Scientific) in the antisense orientation relative to the vector's T7 promoter. DNA templates with the T7 promoter sequence were generated by PCR with a primer about 100 bp outside the T7 promoter in pJET and a gene specific forward primer. PCR products were loaded in a 1% agarose gel, and purified from separated bands of correct size with QIAquick Gel Extraction kit (Qiagen). DNA templates were eluted with DEPC-treated H_2O from the spin column. To avoid RNase contamination, DEPC-treated H_2O was used instead of sdH_2O during preparation. Primers used for probe synthesis are listed in Table 2.2.

Digoxin (DIG) labeled probes were synthesized using *in vitro* transcription by T7 RNA polymerase. Up to 150 ng DNA template was used in 25 µl total reaction together with 5 µl 5x transcription buffer, 2 µl T7 polymerase (20 units/µl, Thermo Scientific), 2.5 µl ATP, CTP and GTP (5 mM, Thermo Scientific), 2.5 µl digoxigenin-11-UTP (1 mM, Roche), 1 µL RNase inhibitor (20 units/µL, RNasin®, Promega). The reaction was incubated at 37°C for 2 hours. Then 75 µl H_2O, 1 µl tRNA (100 mg/ml), 1 µl RQ1 RNase-free DNase (Promega) were added to it and incubated at 37°C for 10 minutes to degrade DNA template. Afterwards 100 µl ice cold 4M NH4OAc, 400 µl ethanol were added and mixed well, and the mixture was incubated at -80°C overnight for precipitation. The RNA probe pellet was then precipitated by centrifuging at 13 000 xg in an Eppndorf 5417 centrifuge at 4°C for 45 minutes. The pellet was dried in a lamina hood after discarding the supernatant, and then the RNA pellet was dissolved in 100 µl DEPC-treated H_2O. Half of the dissolved probe was used for hydrolysis, the rest kept at -80°C.

To hydrolyze the probe, 50 µl of dissolved probe was mixed gently with 50 µl of carbonate buffer (120 mM Na_2CO_3, 80 mM $NaHCO_3$) and incubated at 60°C for 1 hour. Acetic acid (10 µl of a 10% solution) was added to it to neutralize the solution and then 11 µl of 3M NaOAc (pH 5.2), and 220 µl ethanol. The mixture

was left at -80°C for 1 hour for the probe to precipitate. Hydrolyzed probe was pelleted by centrifuging at 13 000 xg at 4°C for 45 minutes. The supernatant was removed from the pellet. The pellet was dried in a lamina flow hood and dissolved in 50 µl DEPC-treated H_2O. Probes were stored at -80°C.

The quality of probes was tested by northern blotting analysis. To do this, 5 µl of each probe was heated at 80°C for 4 minutes, and then cooled down on ice. NEB 6x blue loading buffer (1 µl) was mixed with each probe and the mixture was then loaded into a 1% agarose mini gel containing ethidium bromide. The comb and tank for electrophoresis were washed with 2 N NaOH to remove possible RNase. After visualization and photography of RNA probes, the gel was trimmed to remove excess gel and placed upside down on Saran wrap. One sheet of Hybond^{TM}-N (Amersham), two sheets of filter paper (Whatman 3MM) slightly bigger than the gel were placed on top of the gel with a stack of paper towels and a weight of about 200 g and left overnight. The Hybond-N filter was fixed with 0.4 J/cm^2 in a UV Stratolinker next morning after one brief wash in 2x SSC. The blot was incubated in 1% Roche blocking reagent in Buffer 1 (100 mM Tris pH 7.5, 150 mM NaCl) for 15 minutes. The blot was then washed briefly in Buffer 1, and then incubated in 5 ml Buffer 1 with 1 µl anti-DIG antibody (Roche) for 20 minutes. Afterwards, the blot was washed twice in Buffer 1 for 10 minutes. The blot was then washed briefly in Buffer 5 (100 mM Tris-HCl pH 9.5, 100 mM NaCl, 50 mM $MgCl_2$). The membrane was then incubated in 5 ml Buffer with 7 µl Nitrotetrazolium Blue Chloride (NBT, 75 mg/ml in 70% dimethylformamide) and 5 µL 5-Bromo-4-chloro-3-indolyl Phosphate (BCIP, 50 mg/ml in 100% dimethylformamide) in the dark until purple signal became visible.

2.7.2 Sample fixation

Samples of different developmental stages (aerial parts of seedlings, vegetative

apices when the forth leaves were 5 mm long and inflorescence apices) were collected with forceps and placed in ice-cooled fixation buffer immediately. To prepare fixation buffer, 20 g of paraformaldehyde was dissolved in preheated buffer (50 ml 10 × PBS, 392 ml distilled H_2O, 3.3 ml 2N NaOH at 65^oC) in a fume hood and the pH adjusted to 7.0 with H_2SO_4 once it had cooled down to room temperature on ice. Then 5 ml 10% Triton X100, 0.5 ml TWEEN 20 and 50 ml Dimethyl Sulfoxide (DMSO) were added to it and mixed well. This buffer was stored on ice afterwards.

After the harvest of tissues, they were poured into M507T-Micromesh^{TM} plastic histology cassettes which were labeled with stage and genotype in pencil and placed in a beaker with 250 ml fixation buffer on ice in a desiccator. Vacuum was applied slowly and kept at 50 kPa for 2 hours to remove air from samples. The samples were then drained and fresh fixation buffer was added. Samples were left overnight at 4^oC with gentle agitation on a rocking platform. The next day, samples were rinsed twice with 1x PBS for 10 minutes, and then stored in 70% ethanol at 4^oC.

2.7.3 Sample embedding and sectioning

Fixed samples were taken to the Histology Department in The Queen's Medical Research Institute for infiltration with paraffin wax. This consisted of dehydration of samples from 70% ethanol to 100% ethanol and then into 100% xylene (three steps for one hour each), then infiltration with liquid paraffin wax (four changes of one hour each at 60^oC) using a Leica ASP300S automated tissue processor. Tissue samples were then embedded in molten paraffin wax in plastic histology moulds on a Leica paraffin embedding station. Embedded samples were stored at 4^oC before sectioning.

Samples were sectioned at 8 μm using a Leica RM2025 microtome. Ribbons were checked underneath a stereomicroscope to find good sections and then placed on

ProbeOn™ Plus microscope slides (Fisher Scientific). Ribbons were floated on water and kept at 42°C for about 3 minutes in a slides incubator to un-wrinkle the sections. Water was removed with paper tissue from the one side of sides. Slides were then baked at 42°C overnight to allow for the paraffin wax sections to stick to the slides. Afterwards, slides were stored at 4°C in slides boxes before hybridization.

2.7.4 Hybridization

During the first day of hybridization, samples slides were arranged in stainless steel slides racks and passed through a series of solutions. For deparaffinization, slides were immersed twice in Histo-Clear (National Diagnostics) for 20 minutes in glass dishes in a fume hood. Histo-Clear was replaced by ethanol and sections were then rehydrated using an ethanol series: two washes for 1-2 min in 100% ethanol, then 1-2 minutes each in 95% ethanol, 90% ethanol, 80% ethanol, 60% ethanol, 30% ethanol and distilled water. Slides were then washed in 2x SSC for 5 minutes after that, and treated with 1 µg/ml proteinase K solution (100 mM Tris pH 8.0, 50 mM EDTA, prewarmed to 37°C; with 15 µl of 20 mg/ml proteinase K stock added to 300 ml of warm buffer just before use) for 30 minutes at 37°C. The reaction was stopped by washing slides in 2% glycine (6 g glycine in 300 ml of 1x PBS) for 10 minutes at room temperature. Slides were then washed twice in 1x PBS for 2 minutes and further fixed in 4% formaldehyde (made as for fixing tissue) for 10 minutes at room temperature. Slides were then washed twice in 1x PBS for 2 minutes. To reduce background signal during hybridization, the positively charged slides were acetylated by incubation in triethanolamine buffer (8 ml triethanolamine in 600 ml H_2O, pH 8.0) for 10 minutes in a fume hood with 3 ml Acetic Anhydride added dropwise into the solution, while stirring with a magnetic stir bar. The slides were then washed twice in 1x PBS for 5 minutes at room temperature and dehydrated by successive 30 seconds incubation in each of the ethanol series concentrations: 30% ethanol, 60%

ethanol, 80% ethanol, 90% ethanol, 95% ethanol, 100% ethanol. Slides were stored in racks over a small amount of 100% ethanol in a closed box while making hybridization mix.

For 250 µl hybridization mix, these reagents were mixed in order: 25 µl 10x in situ salts (3 M NaCl, 100 mM Tris-HCl pH 8.0, 2 M sodium phosphate buffer pH 6.8, 50 mM EDTA), 65 µl DEPC-treated H_2O, 2.5 µl 100× Denhardt's salts (Amresco, USA), 5 µl tRNA (50 mg/ml), 100 µl de-ionised formamide (Sigma), 50 µl 50% dextran sulfate (warmed to 65^{o}C before pipetting), 2.5 µl 10% Trition X100. Probe (1 µl) was mixed with 250 µl hybridization buffer, and denatured by heating the probe mix at 80^{o}C for 3 minutes, and then kept on ice. For a pair of slides hybridized with the same probe, 250 µl of probe mix was added to one slide and the other slid over it, sections inwards. Slides were hybridized overnight at 58^{o}C in closed boxes on four dampened paper towels covered completely with Parafilm. At the same time, 1.5 l 0.2x SSC was placed at 58^{o}C to warm.

After overnight hybridization, pairs of slides were separated in beaker of pre-warmed 0.2x SSC, and placed back into slides racks. Slides were then washed three times in 0.2x SSC for 1 hour at 58^{o}C with gentle agitation. They were immersed in 1% blocking solution (2.8 g Roche blocking reagent dissolved by heating to 65 ^{o}C in 280 ml Buffer 1: 100 mM Tris-HCl, pH 7.5, 150 mM NaCl) for 45 minutes at room temperature. Meanwhile, 4.26 ml of Triton X100 was dissolved in 1420 ml Buffer 1, and 4 g of BSA dissolved in 400 ml of the solution to make 1% BSA. Slides were then washed in 300 ml 1% BSA for 45 minutes (keeping this solution for reuse). At the end of this washing step, 4.8 µl anti-DIG antibody (Roche) was diluted in 6 ml of unused 1% BSA solution. To create a moist environment during antibody binding, two damp paper towels were placed at the bottom of a 245 mm x 245 mm square Petri dishes and pairs of glass rods placed over the towel to support slides.

The antibody mix was introduced between pairs of slides by capillary action induced by the gradual bringing together of two slides held in a pool of antibody solution on Parafilm. Pairs of slides were placed on glass rods and incubated for 2 hours at room temperature. Slides were placed back in racks and washed in the previously used 1% BSA solution for 15 minutes. Afterwards, the unused 1% BSA solution was mixed with remaining Buffer 1 plus Triton X100 and slides were washed three times in this solution for 15 minutes to remove excess and unbound antibody. The slides were washed briefly in buffer 5 and immersed in 100 ml buffer 5 with 200 µl NBT (75 mg/ml) and 150 µl BCIP (50 mg/ml) in the dark for 1-3 days at room temperature, until purple signal was visible. The reaction was stopped by rinsing slides in TE. Slides were treated with 0.01% Calcafluor for 5 minutes to counterstain cell walls. Slides were then washed with H_2O, air dried in a laminar flow hood and mounted in Entellan in a fume hood. After slides were completely dried, they were examined with a Nikon SMZ1500 steromicroscope and a Nikon Eclipse E600 compound microscope equipped with a Leica DFC425 camera.

2.8 Yeast two-hybrid screen

To identify possible targets of AmHairy, and AmGRX2, a paralogue of AmHairy, their coding sequences were cloned into the shuttle vector pGBKT7 (Clontech) in frame with the GAL4 DNA binding domain. A prey library produced by cloning cDNAs from mRNAs of whole *A. majus* subsp. *majus* into pGADT7 next to the GAL4 DNA activation domain was provided by Barry Causier and Brendan Davies, University of Leeds (Weir et al., 2004). Screening of the yeast library was performed with pGBKT7-*AmHairy* as bait, according to the manufacturer's manual (Clontech). Three candidate targets were isolated: two TGA transcription factors, TGA1 and TGA2, one homeodomain (HD) protein, GL11.

2.8.1 pGBKT7-bait construction

AmHairy and *AmGRX2* were cloned in pJET2.1 vector with primers listed in Table 2.2. Primers containing recognition sites were designed to amplify the coding regions and allow in-frame fusion to the GAL4 DNA-binding domain in pGBKT7. The 5'ends of the forward primers contained a *Nde* I site, while 5' ends of reverse primers harbor a *Eco*R I site, which were used for subsequent ligation into pGBKT7. Mutations were introduced into $AmHairy^{C35S}$, $AmGRX2^{C31S}$ by PCR based site-directed mutagenesis using mutated primers (Table 2.2), transforming the second cysteine of the GRX active sites to serine. After amplifying the pJET clones with the mutant primers, non-mutated template plasmid was digested with *Dpn* I, and competent DH5α cells were subsequently transformed. Mutagenized plasmids were extracted, confirmed by DNA sequencing and digested with *Nde* I and *Eco*R I. The mutated fragments were purified and ligated at the *Nde* I and *Eco*R I sites of the pGBKT7 vector. Transformed DH5α colonies were screened on kanamycin (50 µg/ml) selective plates. Recombinant pGBKT7 plasmids were identified by colony PCR, purified and the mutated sites confirmed by DNA sequencing.

2.8.2 pGADT7-prey isolation

After library screening with pGBKT7-*AmHairy* at high stringency, three positive colonies were identified. Yeast colonies were picked and cultivated in 5 ml YMM medium containing synthetic dropout (SD)/-Leu/-Trp at 28^{o}C overnight. To extract plasmids from overnight culture, yeast cells were spun down and digested in 100 µl spheroplast buffer [21.8% (m/v) sorbitol, 100 mM NaPO4 pH7.4, with 1/1500 volume of β-mercaptoethanol and 2.5 mg/ml zymolase added before use] at 30^{o}C for 1 hour. Then 150 µl of resuspension buffer P1 from the Qiagen Plasmid Minprep kit was added to the mixture and plasmid extraction was continued according to the protocol for the kit. Plasmids were eluted from columns with 50 µl of elution

buffer.

Extracted plasmids were then transformed into *E. coli* strain DH5α by heat shock. Cells were screened on LB plates containing ampicillin (100 µg/ml) to select colonies that harbor pGADT7-prey plasmids. Plasmids were extracted, purified and used for DNA sequencing.

2.8.2 Co-transformation

Three baits, pGBKT7-*AmHairy*^{C35S}, pGBKT7-*AmGRX2*^{C31S}, pGBKT7 (negative control), and three preys, pGADT7-*AmTGA1*, pGADT7-*AmTGA2*, pGADT7-*AmGL11*, were co-transformed into Y2HGold (Clontech) using a heat-shock method. The transformants were tested on selective medium afterwards.

To prepare yeast competent cell strain Y2HGold, colonies were recovered from glycerol stock on YPDA medium at 30°C. Single colonies were selected and cultured in 5 ml YPDA medium at 30°C overnight. For each co-transformation, 100 µl overnight culture was diluted in 5 ml YPDA medium and then cultivated at 28°C for 3 hours. It was spun to form cell pellet and the supernatant was removed. The pellet was resuspended in 100 µl LiAc-TE solution (10 mM Tris-HCl pH8.0, 1 mM EDTA, 0.1 M lithium acetate). Boiled salmon sperm DNA (6 µl of a 10 mg/ml solution), 5 µl (about 1 µg) of pGBKT7-bait plasmid and 5 µl of pGADT7-prey plasmid were added to the cell suspension. It was then mixed with 600 µl PEG-TE-LiAc solution [40% (m/v) PEG-4000 in LiAc-TE], and incubated at 30°C for 30 minutes. The mixture was placed at 42°C for 15 minutes, and then spun briefly. The supernatant was pipetted off the pellet and the pellet was resuspended in 100 µl YPDA medium, plated on YMM medium containing SD/-Leu/-Trp, and incubated at 30°C for 48 hours.

After 48 hours incubation, single colonies were selected and grown in 5 ml selective medium at 30^{o}C for 48 hours to reach similar densities. Cultures were diluted with sterilized distilled water to make a series: 1, 1/10, 1/100, 1/1000. Equal volumes were pipette onto SD/-Leu/-Trp medium (which selects for bait and prey plasmids) and SD/-Ade/-Leu/-His/-Trp mdium with X-α-gal (which selects for interaction) and grown at 30^{o}C for 48 hours.

Table 2.2. Primers used in this study.

Catagory	Primer Name	Sequence (5'-3')*	Gene Information†	Remarks
Genotyping	F-box F	GTGCTTTCCTTCCACGATGT	S locus F-box	
	F-box R	CCTGGTTCAAACTGATCAAGC		
	GRX NR	GTAGTCCTATACAAATTAATACGTA	*AmGRX1*	
	GRX F	ACAGAGTATACGCCTCGAT		
VIGS	AscI-AmGRX-F	*a*GGCGCGCCATGCAGTACGACGCAGAACC	*AmGRX1* CR, 324 bp	
	AmPDS&GRXfusion-R	gtaagatcctctgaagcactacTTAGAGCCAAAGAGCACCAGC		
	AscI-AmGRX3'UTR-F	*a*GGCGCGCCATAATACAAGTTGAGCAACAGCG	*AmGRX1* 3'UTR, 237 bp	
	AmPDS&GRX3'UTRfusion-R	gtaagatcctctgaagcactacACAGAGTGATACGCCTCGAT		
	AscI-AmGRX2-F	*a*GGCGCGCCCACCTAATGTACTACGAAAGTGA	*AmGRX2*, 347 bp	
	AmPDS&GRX2fusion-R	gtaagatcctctgaagcactacTATTCTCCTTAGGAACTAGAG		
	AscI-AmPDS-F	*a*GGCGCGCCgtagtgcttcagaggatcttacaa	*AmPDS*, 363 bp	
	AmPDS-R	Gtagtgcttcagaggatcttaca		
	BamHI-PDS-R	*ctca*GGATCCcaatgagccttaccgtgcat		
	AscI-MoGRX-F	*a*GGCGCGCCTGGGCGTAAACACGACGGTCT	*MoGRX*, 214 bp	
	AmPDS&MoGRXfusion-R	gtaagatcctctgaagcactacTAGAGCCAAAGAGCACCAGCC		
	AscI-TGA13'prime-F	*a*GGCGCGCCGAATCCGCATCAGTGCAGTA	*AmTGA1* 3'UTR, 285 bp	
	TGA1&PDS3'prime-fusion	gtaagatcctctgaagcactacAGCAAACTAACTAGAAAGGCTATGA		
	AscI-TGA273prime-F2	*a*GGCGCGCCCTTAGAGCCCTCAGTTCACTTT	AmTGA27 3'UTR, 228 bp	
	TGA27&PDS3'prime-fusion2	gtaagatcctctgaagcactacGAGCAGACTACAAAGGCTAACA		
	AscI-GL113'prime-F	*a*GGCGCGCCCAACTCTCCAACAGCAAGAATG	*AmGL11*, 343 bp	
	GL11&PDS3'prime-fusion	gtaagatcctctgaagcactacGAGAGGTTGTTGTGAACTGTAATG		
	TRV2-forward	TGCTGACCTACTGGTTACTG	TRV2 vector	colony PCR and sequencing
	TRV2-reverse	ACCGTAGTTTAATGTCTTCG		

Catagory	Primer Name	Sequence (5'-3')*	Gene Information†	Remarks
qPCR	AmGRX-qPCR-F2	TCTTGTCTTTTCCACCTGTCA	*AmGRX1*, 174 bp	
	AmGRX-qPCR-R	TGAATATCACCACCGGATTCTC		
	AmGRX2-qPCR-F2	TGGCTCTAGTTCCTAAGGAGAA	*AmGRX2*, 131 bp	
	AmGRX2-qPCR-R	CACAAGCCTACAGAGCTACTAATC		
	AmPDS-qPCR-F2	TCTTTGTAATGGACGGCAAG	*AmPDS*, 133 bp	
	AmPDS-qPCR-R2	ACTTGCCAAACTCTTCCCTG		
	AmUbi-qPCR-F	CCGAACCATCAGACAAACAAAC	*AmUbiquitin, 138 bp*	
	AmUbi-qPCR-R	TACCCTGGCCGACTACAATA		
	TGA27-qPCR-F	TTAGAGCCCTCAGTTCACTTTG	*AmTGA27*, 108bp	
	TGA27-qPCR-R	GCTCGTGAATGTCTATCCATCTT		
	GL11-qPCR-F2	GCCATCCGGTTTCACAATTTC	*AmGL11*, 144 bp	
	GL11-qPCR-R2	GCTGTTGGAGAGTTGCTTACTA		
RT-PCR	MetSynthF	GTTTGATGAGCCCACCCTTG	*AmMet3*, 384 bp	
	MetSynthR	TGTGGAGAAGTGAGCAGGAG		
	GRX40-CR-F	CCATCAATTAACTTCACCAAAATG	*AmGRX3* (pseudomajus), 301 bp	
	GRX40-CR-R	ATCACAAGCATTAGAGCCAAAG		
Phylogenetic analysis	GRX NR	GTAGTCCTATACAAATTAATACGTA		
	GRX F	ACAGAGTATACGCCTCGAT		
	GRX-R2	ACAGTCCTATACAAATTAATATG		
	GRX-RACE-R3	ACCAAGTGGCGTACGAAATTA		
	GRX-CR-R	GAATCCGGTGGTGATATTCA		
in situ Hybridization	GRX-CR-R	GAATCCGGTGGTGATATTCA	*AmGRX1*, 515 bp	
	GRX F	ACAGAGTATACGCCTCGAT		

Catagory	Primer Name	Sequence (5'-3')*	Gene Information†	Remarks
	GRX2-CR-F	TAATGTACTACGAAAGTGA	*AmGRX2* 3'UTR, 347 bp	
	GRX2-CR-R	TATTCTCCTTAGGAA CTAGAG		
	TGA1-F	GAATCCGCATCAGTGCAGTA	*AmTGA1*, 285 bp	
	TGA1-R	AGCAAACTAACTAGAAAGGCTATGA		
	TGA27-F2	CTTAGAGCCCTCAGTTCACTTT	*AmTGA27* 3'UTR, 228 bp	
	TGA27-R2	GAGCAGACTACAAAGGCTAACA		
	GL11-F	CAACTCTCCAACAGCAAGAATG	*AmGL11*, 343 bp	
	GL11-R	GAGAGGTTGTTGTGAACTGTAATG		
	T7-UP-F	GAGCAGGTTCCATTCATTGTT		100 bp upstream of T7 promoter in pJET1.2 vector
Yeast Two Hybrid	GRX express F	GATCACACATATGCAGTACGACG		
	GRX express R	ATAGAATTCAAGTTGAGCAACAGCG		
	NdeI-GRX2-F	ACACATATGTACTACGAAAGTGA		
	EcoRI-GRX2-R	ACACAGAATTCTCTCCTTAGGAACTAGAG		
	GRX-C36-F	CGTGCTATTTGaGCCTTACTGTG		Site directed mutagenesis
	GRX-C36-R	CACAGTAAGGCtCAAATAGCACG		
	GRX2-C31-F	CCACGTGCTACATGaGCCAC		Site directed mutagenesis
	GRX2-C31-R	GTGGCtCATGTAGCACGTGG		
pJET1.2	pJET1.2-forward	CGACTCACTATAGGGAGAGCGGC	pJET1.2 vector	colony PCR and sequencing
	pJET1.2-reverse	AAGAACATCGATTTTCCATGGCAG		

*Underlined sequences are restriction enzyme recognition sites. Lower-case italic bases were added to the 5'ends of recognition site to increase cleavage efficiency of restriction enzymes. Bases in lower case are sequences of *AmPDS*. †Sizes of products are shown when these did not vary.

Chapter 3

3. Trichome morphology

To better understand trichome evolution in the genus *Antirrhinum* and its close relatives, the morphology and distribution of trichomes was examined. The natural species used in this study were collected previously and grown in the glasshouse of the Univerity of Edinburgh or were kindly provided by Pablo Vargas in Real Jardín Botánico de Madrid, Spain. DNA samples were also collected from these plants, to allow trichome phenotypes to be compared to genotypes later.

3.1 Trichome distribution in the genus *Antirrhinum*

The distribution of trichomes was found to differ between species. It was convenient to divide species into bald plants and hairy plants, defined as follows. A bald plant has a decreasing density of trichomes from its base, is completely or nearly free of trichomes in the middle vegetative part, and has dense hairs distributed on the inflorescence. In contrast, the whole body of a hairy plant is covered with very dense trichomes (Fig. 3.1).

Most species from subsection *Antirrhinum* were found to be bald. They commonly became bald from the third internode (where the first leaves are at node one), with some exceptions. The place of the transition to baldness varied under different growth condition. Plants of *A. majus* subsp. *tortuosum* became bald from either the third or the seventh internode, when grown under the same conditions, suggesting genetic variation within the subspecies. Some species showed phenotype polymorphism. Both bald and hairy individuals were identified among accessions of *A. australe*. Bald individuals of *A. australe* have a reducing density of trichomes

until late nodes. The *A. latifolium* plants grown in the glasshouse and herbarium specimen I sampled were hairy, though *A. latifolium* is described as a glabrous or hairy species according to herbarium records (Sutton, 1988). All *A. graniticum* individuals that I sampled were hairy, however, some individuals collected from different populations by Yvette Wilson were recorded as bald (Wilson, 2009). In contrast, all the species from subsection *Kickxiella* are hairy. In subsection *Streptosepalum*, *A. meonanthum* has both bald and hairy individuals, while the sampled *A. braun-blanquetii* plant was bald (Table 3.1).

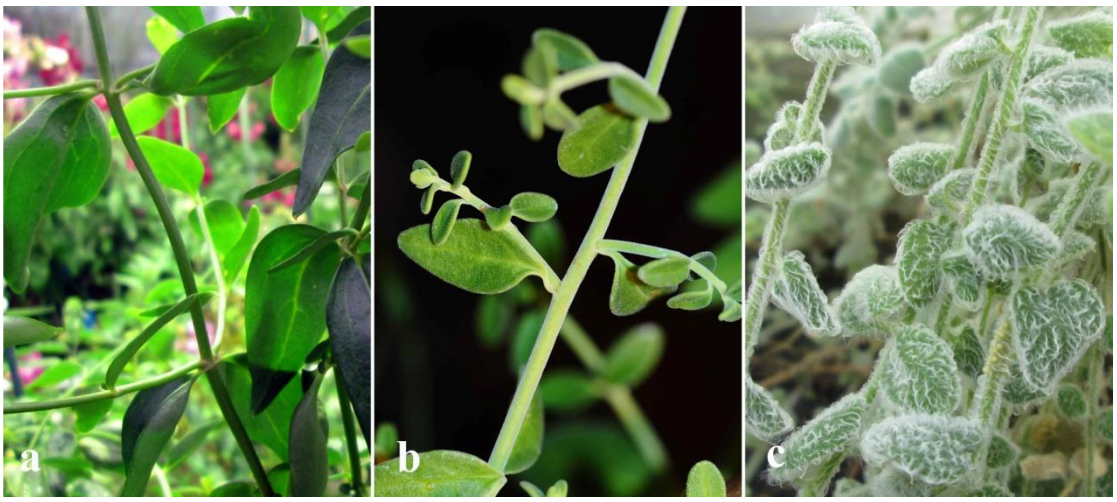

Figure 3.1. Trichome distribution of *Antirrhinum* species in the higher vegetative parts
The higher vegetative parts (later internodes and leaves of later nodes below the inflorescence) of bald species, for example *A. majus* subsp. *majus* (a), are free of hair (except for the adaxial midrib of leaves), while the higher vegetative parts of hairy species are covered with short trichomes, as in *A. charidemi* (b), or long trichomes, as in *A. lopesianum* (c).

3.2 Trichome morphology in the genus *Antirrhinum*

Trichomes of *Antirrhinum* are uniseriate and can be glandular or eglandular. According to length and gland size, trichomes were classified into six types (Figure 3.2): short glandular trichomes (type I), short glandular trichomes with two-neck-cells (type II), glandular trichomes (type III), long glandular trichomes (type IV), long simple trichomes (type V) and short simple trichomes (type VI). All

the glandular trichomes have similar, multicellular, cuplike glands. Well-developed glands have more than 12 secretory cells. Type I trichomes are frequent on the adaxial midrib in all species (Fig. 3.3b). As the leaf grow bigger, the distribution of type I trichomes expands to lateral veins from the leaf base. Glands of some type I trichomes are divide into two layers—apical and basal. Rarely type I trichomes branch from the base of their stalks. Type II trichomes differ from type I trichomes due to the presence of two-neck-cells. Type II trichomes can be found on the adaxial midrib of every species but are usually rare. However, about a quarter of glandular trichomes on the adaxial midrib of *A. siculum* belong to type II (Appendix 1.10). Type III trichomes and long simple trichomes (type V) are commonly distributed on lower internodes and early leaves with a decreasing density apically (Fig. 3.3a). Bald plants become glabrous or nearly glabrous on the later vegetative parts, and have type III trichomes growing on peduncle, bracts, pedicel and sepal, making the inflorescence hairy. The inflorescences of hairy plants exhibit the same trichome types as the middle vegetative parts. It suggests that type III trichomes are supposed to grow in the middle vegetative parts of bald plants, but initiation of them is prohibited due to the genetic difference between bald plants and hairy plants.

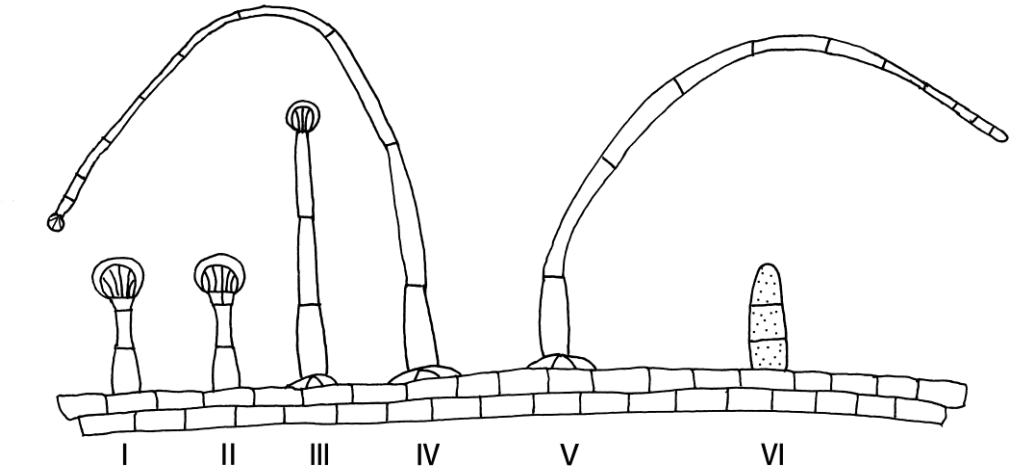

types	Characteristics
I	1-3 stalk cells, diameter of gland 0.03-0.05 mm
II	1-3 stalk cells, diameter of gland 0.03-0.05 mm
III	3-5 stalk cells, diameter of gland around 0.02-0.04 mm
IV	≥6 stalk cells, diameter of gland around 0.02 mm
V	≥6 cells, eglandular
VI	1-4 cells, covered with papillae, eglandular

Figure 3.2. Classification of trichomes in *Antirrhinum*

Trichomes were classified into five categories according to the length and presence of gland. They are short glandular trichome (type I), short glandular trichome with two neck-cells (type II) (mainly distribute on adaxial midrib), glandular trichome (type III), long glandular trichome (type IV), long elgandular trichome (type V) and short eglandular trichome with micropapillae (type VI).

3.2.1 Foliar trichome morphology

3.2.1.1 Foliar trichome morphology in subsection *Antirrhinum*

The majority species of subsection *Antirrhinum* are bald. From the base to the second node, type III and type V are frequent on the stem, both adaxial and abaxial sides of cotyledons and leaves with a density declining from the base (Fig. 3.3a).

These early trichomes are often lost after lignification of the basal stem. Apart from type I trichomes on the adaxial midrib, plants become bald or almost bald at later internodes. Type III trichomes reappeared in the inflorescence. Trichomes on the abaxial side of sepal are always longer than those on the adaxial side.

A. majus subsp. *cirrhigerum*, *A. majus* subsp. *linkianum*, *A. majus* subsp. *majus*, *A. majus* subsp. *pseduomajus*, *A. majus* subsp. *striatum*, are bald species. They have type I trichomes on the adaxial midrib of middle leaves (Fig. 3.2a, Appendix 1.4-1.8). Approximately a quarter of glandular trichomes of *A. siculum* belong to type II (Appendix 1.10). In contrast to other bald species, only a few type III trichomes could be found on the shoot of inflorescences of *A. siculum*. Plants of *A. majus* subsp. *tortuosum* could become bald from the third or seventh internode, the parts of them are covered with type III trichomes (Appendix 1.9).

Both bald and hairy progeny were found for *A. australe* plants. From which internode plant started to become bald varied among individuals: it could be the fifth, sixth, or seventh internode. For hairy siblings, the whole plants were covered with type III trichomes (Appendix 1.1) and a decreasing density of type V (long, eglandular) trichomes were found on the lower stem and leaves.

For *A. graniticum*, both bald and hairy individuals were identified. Hairy individuals frequently had type III trichomes at high density (Fig. 3.2c, Appendix 1.2). In a previous study, *A. latifolium* was reported as a bald species (Doaigey & Harkiss, 1991). However, the individual I sampled was covered with sparse or very dense type III trichomes below the inflorescence, suggesting it has a hairy phenotype (Appendix 1.3).

3.1.1.2 Foliar trichome morphology in subsection *Kickxiella*

Trichome morphology of *Kickxiella* species appeared more complicated. According to trichome morphology and distribution, *Kickxiella* species can be categorized into four groups.

Group 1: Type III trichome

Type III trichomes are frequent on the stem and leaf blades of *A. boissieri* and *A. hispanicum* (Appendix 1.11, 1.3).

Group 2: type IV trichome

Dense type IV trichomes were found on plants of *A. mollisimum* (Fig. 3.3d, Appendix 1.17) and *A. rupestre* (Appendix 1.20). Glandular trichomes of *A. mollisimum* exhibit stalks with micropapillae, like those of type VI trichomes.

Group 3: Glandular trichome and non-glandular trichome coexist

Type III and type V trichomes, up to 1 mm in length, were observed together in *A. lopesianum*. Only type III trichomes can be found on very young leaves indicating that glandular trichomes initiate earlier than long simple trichome in *A. lopesianum* (Fig. 3.3f-g, Appendix 1.14). Leaves of *A. molle* are extremely hairy due to dense distribution of type IV and type V trichomes (Fig. 3.3e, Appendix 1.16).

Group 4: Mainly type VI trichome

Type VI trichomes are frequent in many species, for example, *A. charidermi* (Appendix 1.12), *A. microphyllum* (Appendix 1.15), *A. pertegasii* (Fig. 3.3h, Appendix 1.18), *A. pulverulentum* (Appendix 1.19), *A. sempervirens (*Appendix 1.21), *A. subbaeticum* (Appendix 1.22), *A. valentinum* (Fig. 3.3i, Appendix 1.23). These short simple trichomes exhibit cell walls with papillae. In *A. pertegasii*, more short glandular trichomes appear during the process of leaf growth. These

type I-like trichomes may be formed by production of a gland from the top cell of type VI trichomes. In the other five species of in this group, glandular trichomes were observed at low frequency.

3.2.1.3 Foliar trichome morphology in subsection *Strepsepalum*

For hairy plants of *A. meonanthum*, type III and type VI trichomes were found on both sides of leaf blades (Appendix 1.24).

Table 3.1. Foliar tricome types in the genus *Antirrhinum*. '-' indicates no trichome present.

subsection	Species	Phenotype	Midrib, lateral vein		Lamina	
			adaxial	abaxial	adaxial	abaxial
Antirrhinum	*A. majus* subsp. *cirrhigerum*	Bald	I	-	-	-
	A. majus subsp. *linkianum*	Bald	I	-	-	-
	A. majus subsp. *majus*	Bald	I	-	-	-
	A. majus subsp. *pseudomajus*	Bald	I	-	-	-
	A. majus subsp. *striatum*	Bald	I	-	-	-
	A. majus subsp. *tortuosum*	Bald	I	-	-	-
	A. siculum	Bald	I,II	-	-	-
	A. australe	Bald	I	-	-	-
		Hairy	I	III	III	III
	A. graniticum	Hairy	I	III	III	III
	A. latifolium	Hairy	I	III	III	III
Kickxiella	*A. boissieri*	Hairy	I	III	III	III
	A. hispanicum	Hairy	I	III	III	III
	A. mollisimum	Hairy	I	IV	IV	IV
	A. rupestre	Hairy	I	IV	IV	IV
	A. lopesianum	Hairy	I	III,V	III,V	III,V
	A. molle	Hairy	I	IV,V	IV,V	IV,V
	A. charidemi	Hairy	I	VI	VI	VI
	A. microphyllum	Hairy	I	VI	VI	VI
	A. pulverulentum	Hairy	I	VI	VI	VI
	A. sempervirens	Hairy	I	VI	VI	VI
	A. subbaeticum	Hairy	I	VI	VI	VI
	A. valentinum	Hairy	I	VI	VI	VI
	A. pertegasii	Hairy	I	I,VI	I,VI	I,VI
Streptosepalum	*A. meonanthum*	Bald	I	-	-	-
		Hairy	I	III，V	III，V	III，V
	A. braun-blanquetii	Bald	I	-	-	-

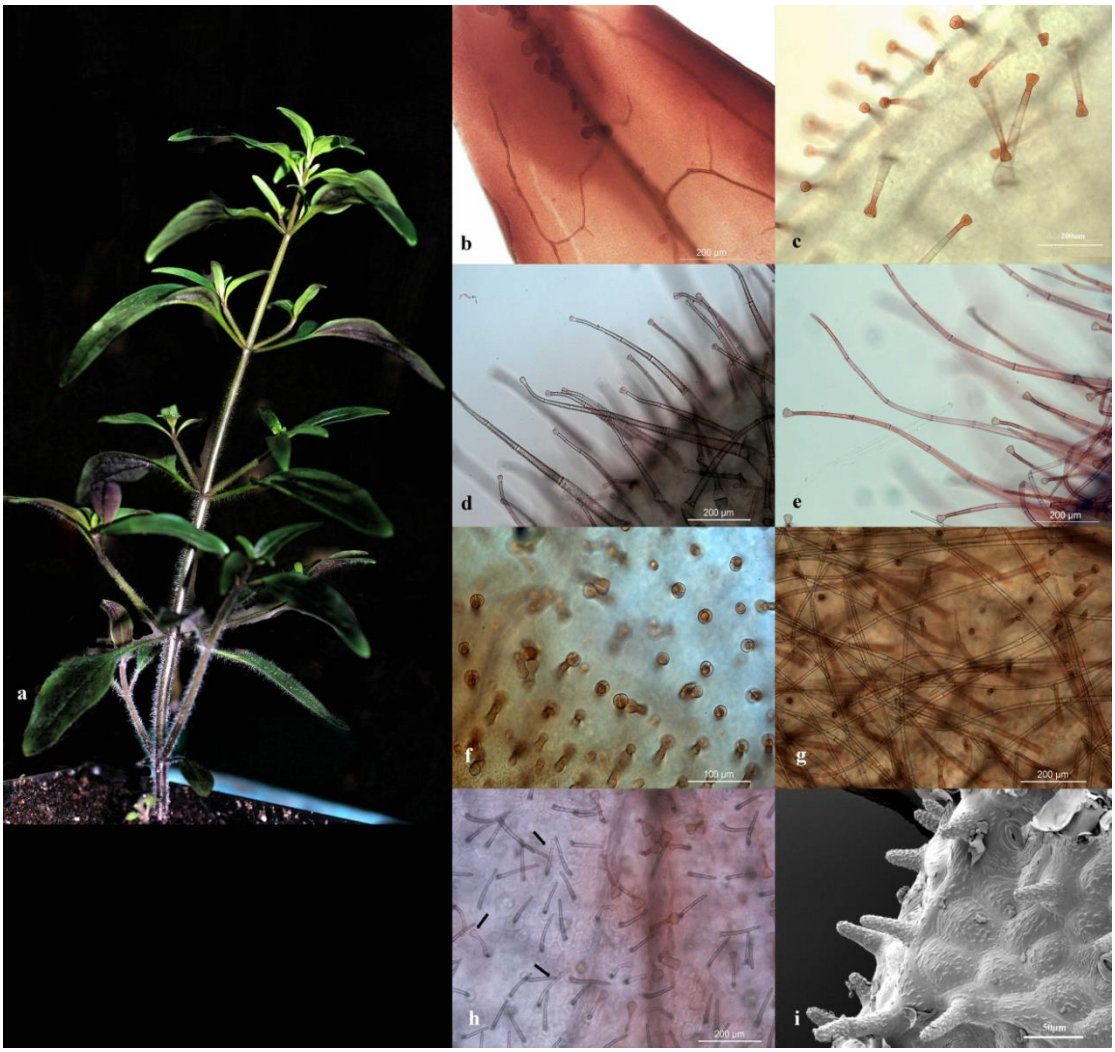

Figure 3.3. Trichome distribution and foliar trichome morphology of *Antirrhinum* species
(a) A bald plant of *A. australe* starts to be free of trichomes from the sixth internode. Type III trichomes and type V trichomes are distributed on the lower stem and leaves with a decreasing density apically; (b) Type I trichomes on the adaxial midrib of *A. majus* subsp. *majus*; (c) Type III trichomes on the lamina of *A. graniticum*; (d) Type IV trichomes in *A. mollisimum* exhibit micropapillae on stalk cells; (e) *A. molle* has type IV and V trichomes; (f) Type III trichomes initiate first on the young leaves of *A. lopesianum*; (g) Type V trichomes occur later in *A. lopesianum* leaves; (h) Adaxial leaf surface of *A. pertegasii*, arrows indicate glandular trichomes with similar stalks to type VI trichomes; (i) An SEM picture of *A. valentinum* shows that type VI trichomes are covered with papillae.

3.2.2 Sepal trichome morphology

Sepals of 15 species were examined (Appendix 2). Most of them show similar trichome types to leaves. Abaxial trichomes are longer than adaxial trichomes,

except in *A. subbaeticum* and *A. valentinum*, where adaxial trichomes are longer. Trichomes in the middle part of adaxial side are similar to type I trichomes found on the adaxial midrib of leaves of all species, while trichomes on the adaxial leaf margin and abaxial trichomes resemble trichomes on the lamina of each species. For species with type III foliar trichomes, e.g. hairy *A. australe*, *A. graniticum*, *A. boissieri*, and *A. hispanicum*, their sepals are covered with glandular trichome similar to type III (Appendix 2.1, 2.2, 2.7, 2.8). Bald species have similar type of trichomes on their lowest leaves and sepals (Appendix 2.3-2.6). A few type VI-like trichomes were found in the middle adaxial part of sepals in all species, possibly abnormally shaped type I trichomes (Appendix 2.1, 2.3, 2.7). Two-neck-cell glandular trichomes occur on the adaxial side in *A. siculum*. Although hairy *A. meonanthum* plants have type III and V trichomes on the leaf blade, their sepal trichome morphology is the same as bald *A. meonanthum* - type III trichomes with very cuplike glands (Appendix 2.15). *A. molle* has type IV and V trichomes on the abaxial side of sepals (Appendix 2.9). *A. rupestre* has type IV trichomes on the abaxial side (Appendix 2.12). *A. pertegasii*, *A. pulverulentum*, *A. subbaeticum* and *A. valentinum* have very similar foliar trichome morphology (group 4). No type VI trichomes can be found on sepals of *A. pertegasii* (Appendix 2.10), while for the other three species, type VI trichomes cover the abaxial side and adaxial margin. The majority of type VI trichomes in *A. subbaeticum* and *A. valentinum* are unicellular (Appendix 2.13-14).

3.2.3 Trichome morphology of seedlings

There is no significant difference in trichome morphology of seedlings between species. Therefore, trichome type in seedlings is not related to foliar trichome morphology. Not only species with glandular foliar trichomes, but also species with simple foliar trichomes, like *A. subbaeticum*, have glandular seedling trichomes. The type III trichome is the predominant type on cotyledons and first and second

leaves. Unlike foliar glandular trichomes, which have multicelluar glands, most type III trichomes of seedlings present unicellular glands. Long, eglandular (type V-like) trichomes also occur on seedlings (Fig. 3.4). Compared to trichomes from inflorescence and later vegetative parts, these trichomes are longer and denser, possibly helping young plants survive from drought, UV radiation or herbivores.

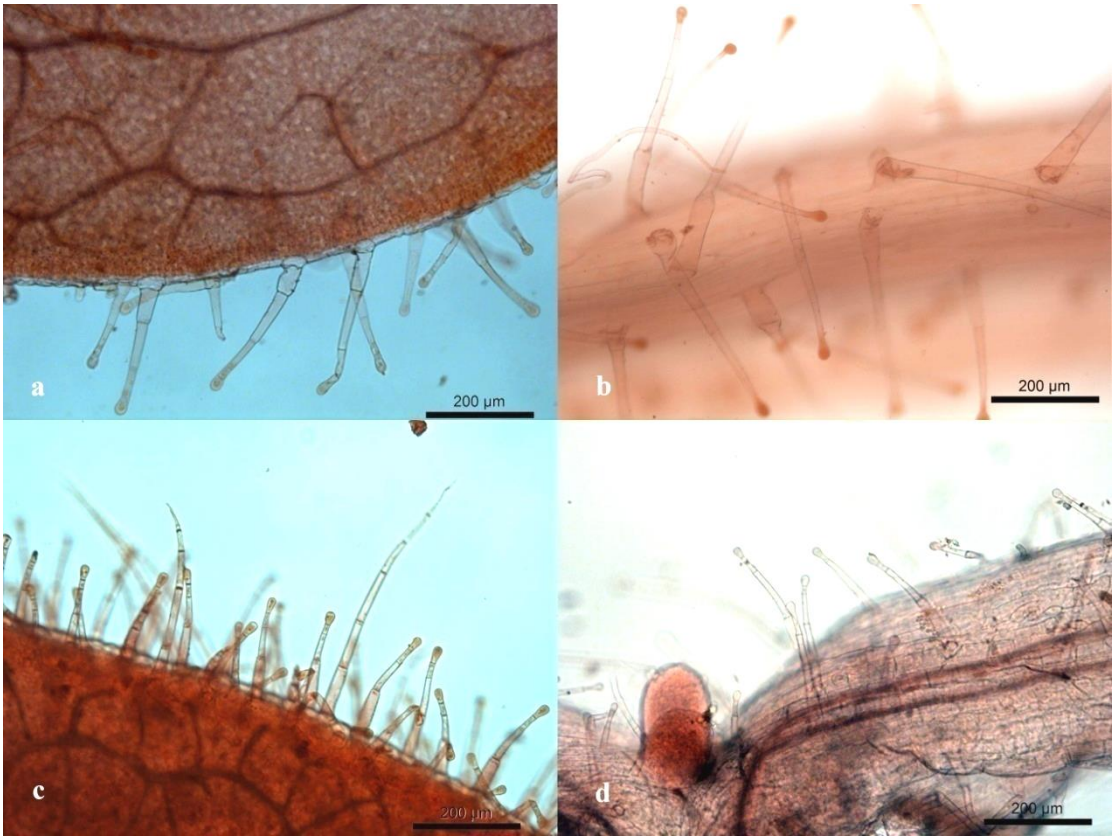

Figure 3.4. Trichome morphology of seedlings
Glandular trichomes with unicellular gland are the predominant type on seedlings of all species. (a) *A. australe*, (b) *A. graniticum*, (c) *A. molle*, (d) *A. subbaeticum*.

3.3 Trichome distribution and morphology of NILs

The main difference between bald species and hairy species is that trichomes are absent or nearly absent from the middle vegetative parts (usually above the third internode and below the inflorescence). To isolate the genes underlying trichome density, a near-isogenic line was generated by crossing *A. majus* subsp. *majus* (line

JI.7, which was bald) to *A. charidemi* (which was hairy) and backcrossing to *A. majus* subsp. *majus* for 8 generations. The progeny segregated as bald NILs and hairy NILs. The whole plant of hairy NILs is covered with trichomes, while the phenotype of the bald NIL is similar to *A. majus* subsp. *majus*. Bald plants start to become bald from the third internode and go back to being hairy in the inflorescence (Fig. 3.5). Type I trichomes are distributed on the adaxial midrib of all leaves (Fig. 3.6c). For hairy individuals, type III trichomes are commonly distributed on both sides of the lamina and stem of the middle nodes and internodes (Fig. 3.6d). No significant difference of trichome morphology occurs on lower leaves, basal parts of the stems and inflorescence between bald and hairy individuals. Seedlings of NILs appear similar to seedlings of natural species—type III trichomes with one secretory cell are the predominant type. Glands of most early leaf trichomes do not go through further division and remain unicellular (Fig. 3.6a, b). Type III trichomes are distributed on the peduncle, pedicel and bract of the inflorescence. For sepals, short glandular trichomes are distributed on the adaxial side, long glandular trichomes on the abaxial side. It suggests that the middle vegetative parts of bald NILs should have type III trichomes which are stopped by the expression of some gene or genes from *A. majus* subsp. *majus*; the type III trichome growth in the middle vegetative parts of hairy NILs can occur because of the introduction of *A. charidemi* gene or genes in the *A. majus* subsp. *majus* genetic background. The NILs possess the same trichome types to *A. majus* subsp. *majus* rather than *A. charidemi.* The trichome distribution of bald NILs is the same as *A. majus* subsp. *majus*, while the trichome distribution of hairy NILs is similar to *A. charidemi*, suggesting that the genetic difference between NILs affects trichome distribution but not trichome morphology.

Figure 3.5. Phenotypes of hairy and bald NILs

(a, d) inflorescence, (b, e) middle vegetative part, (c, f) basal stem.

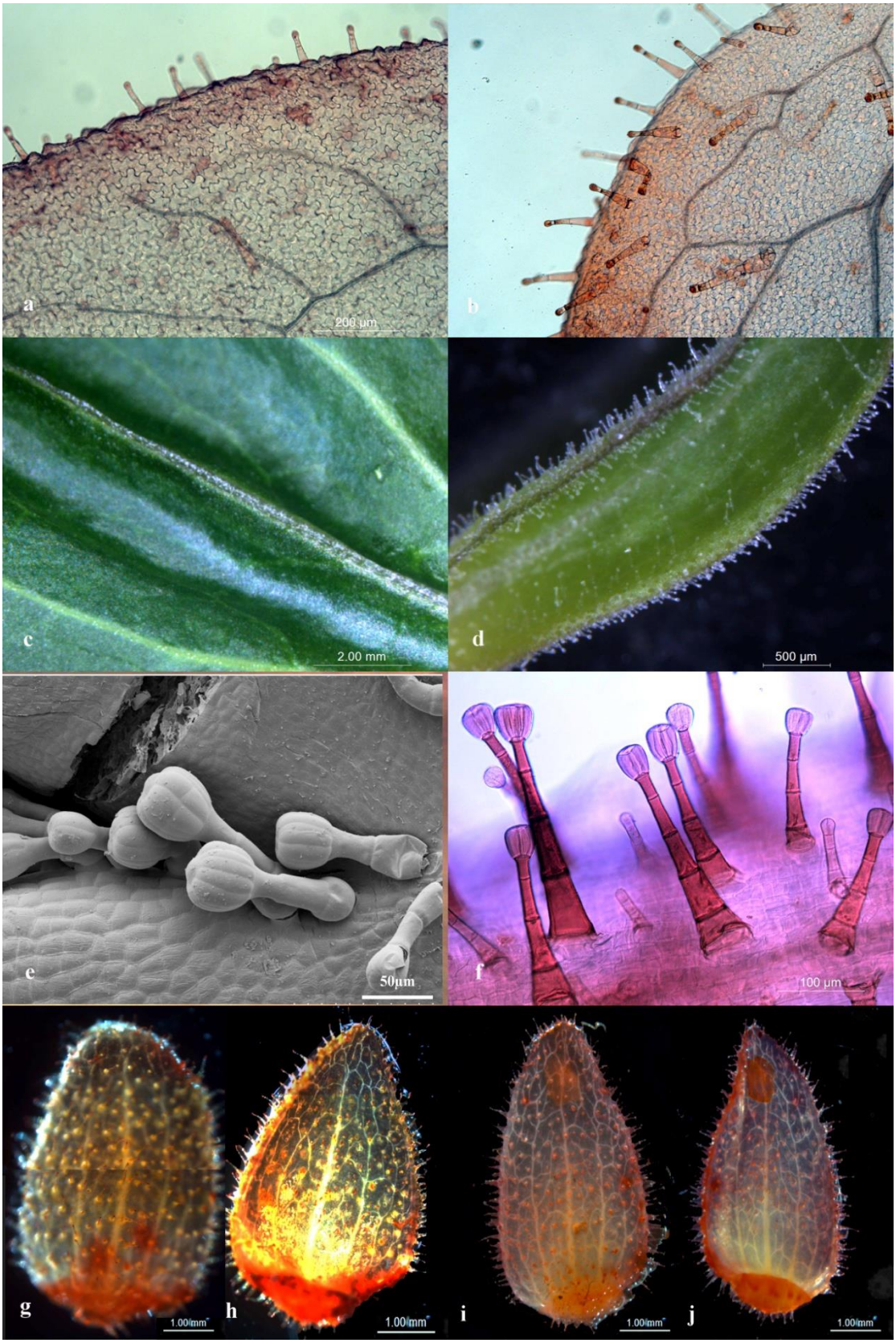

Figure 3.6. Trichome morphology of NILs

(a) the first leaf of a bald NIL, (b) the first leaf of a hairy NIL; (c, e) trichomes on the adaxial midrib of a bald NIL, (d, f) trichomes on the blade of a hairy NIL; (g, h) sepals of a bald NIL, (g)

shows the abaxial side and (h) shows the adaxial side; (i, j) sepals of a hairy NIL, (i) shows the abaxial side, (j) shows the adaxial side.

3.4 Phenotypes and trichome morphology of hybrids

To test whether the genes underlying variation in trichome distribution between *A. majus* subsp. *majus* and *A. charidemi* were also responsible for variation throughout the genus *Antirrhinum*, allelism tests were conducted by crossing bald NILs with different *Antirrhinum* species. The progeny from the bald NIL crossed with bald species were all bald with one exception (bald NIL × *A. siculum* only produced one hairy progeny), while the progeny of the bald NIL crossed with hairy species segregated bald progeny and hairy progeny at a 1:1 ratio. The results are listed and discussed in Chapter 4. Here I focus on the trichome distribution and morphology of the hybrids generated in allelism test.

The place of the baldness transition varied in the bald progeny. Most of them become bald from the third internode, except for the hybrids of *A. molle*, where the middle parts of plants were not free of trichomes, but had a few scattered hairs. Although a plant of *A. majus* subsp. *tortuosum* that was bald from the sixth node was chosen to provide pollen, their progeny become bald from the second node. It suggests the alleles from *A. majus* subsp. *majus* are dominant.

Trichome morphology of seedlings was consistent in all hybrids, showing the same types to the wild parents. All the progeny also have type I trichomes on the adaxial leaf midrib. According to the trichomes presented on inflorescences, segregating bald progeny and hairy progeny have the same trichome types. Usually, hybrids exhibit both trichome types found in their parents. This is consistent with multiple genes acting additively to determine trichome type. As we know, NILs possess type III trichomes which are prohibited in the middle vegetative parts of bald NILs.

Hairy progeny of *A. hispanicum* have type III trichomes covering the middle parts of plants (Fig. 3.7a), as in the *A. hispanicum* and NILs parents. However, the *A. molle* hybrids, unlike *A. mole*, which possesses type VI and V trichomes, have type III and V trichomes (Fig. 3.7b). One explanation is that glandular trichomes may be determined by one gene or genes and their length by other factors. This could explain why type IV was lost in hybrids, so all glandular trichomes develop as type III. Although *A. pulverulentum*, *A. subbaeticum* and *A. valentinum* have the same trichome type (type VI) and similar trichome distribution, their crosses present distinct trichomes phenotypes. *A. pulverulentum* or *A. subbaeticum* hybrids possess type III (inherited from bald NILs) and VI trichomes (Fig. 3.7c). The stalks of type III trichomes are covered with micropapillae like type VI trichomes, suggesting that micropapillae develop independently to trichome types. Hybrids of *A. valentinum* are similar to the wild species, only possessing type VI trichomes (Fig. 3.7d), suggesting the growth of type III trichomes is prohibited by the introduction of some genes from *A. valentinum*.

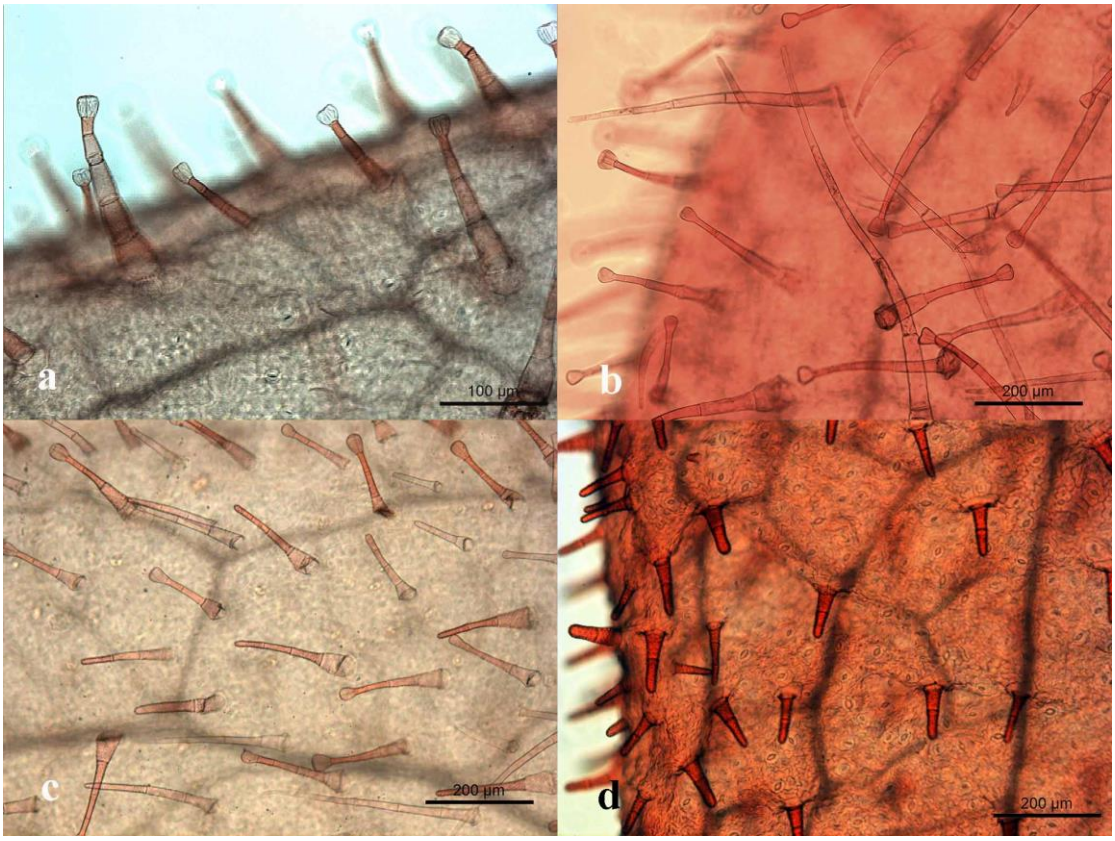

Figure 3.7. Foliar trichome morphology of hairy hybrids

(a) Cross of bald NIL × *A. hispanicum*, (b) Cross of bald NIL × *A. molle*, (c) Cross of bald NIL × *A. subbaeticum*, (d) Cross of bald NIL ×*A. valentinum*. Leaves shown here are from the fourth or fifth node.

3.5 Trichome development

To investigate trichome development, leaves at different stages of development were examined. The youngest trichomes were found towards the base of the developing leaf and more mature trichomes towards the tip (Fig. 3.8a). As trichomes mature, they are separated through pavement cell division and enlargement. Trichomes of all types initiate from one epidermal cell. A model of trichome development was developed based on observation (Fig. 3.8i). For types III, IV, V, the foot cell underlying the trichomes keeps rising and dividing to form an epidermal cell complex as the trichome is elongating (Fig. 3.8f). Glandular trichomes and elandular or glandless trichomes do not appear different at early developmental

stages. Glands develop from the top stalk cell, which begins to swell laterally. For the majority of type I, II and III trichomes, glands begin to form at the three stalk cell stage (Fig. 3.8b, c, d). The two-neck-cell of type II trichome is formed by a vertical division of the stalk cell below the cell which forms the gland. Glands of type IV trichomes are formed when they have more than 5 stalk cells (Fig. 3.8a). New type VI trichomes are not covered with micropapillae, these develop as the trichome matures.

Apart from glandular trichomes on lower leaves, all glandular trichome types have multicellular, cuplike glands. Secretions are probably stored in the space between the apical secretory cells and the cuticle. There can be more than 12 cells in the glands of well-developed glandular trichomes with four shorter secretory cells enclosed by a larger number of peripheral cells to form the cuplike gland (Fig. 3.8g, h). The four middle cells may play an important role in secretion. The multicellular gland develops from the single apical cell, which divides three times to form eight cells. At the eight-cell stage, the four middle cells divide inwardly to give the four shorter cells in the center. Peripheral cells can undergo further division (Fig. 3.8j).

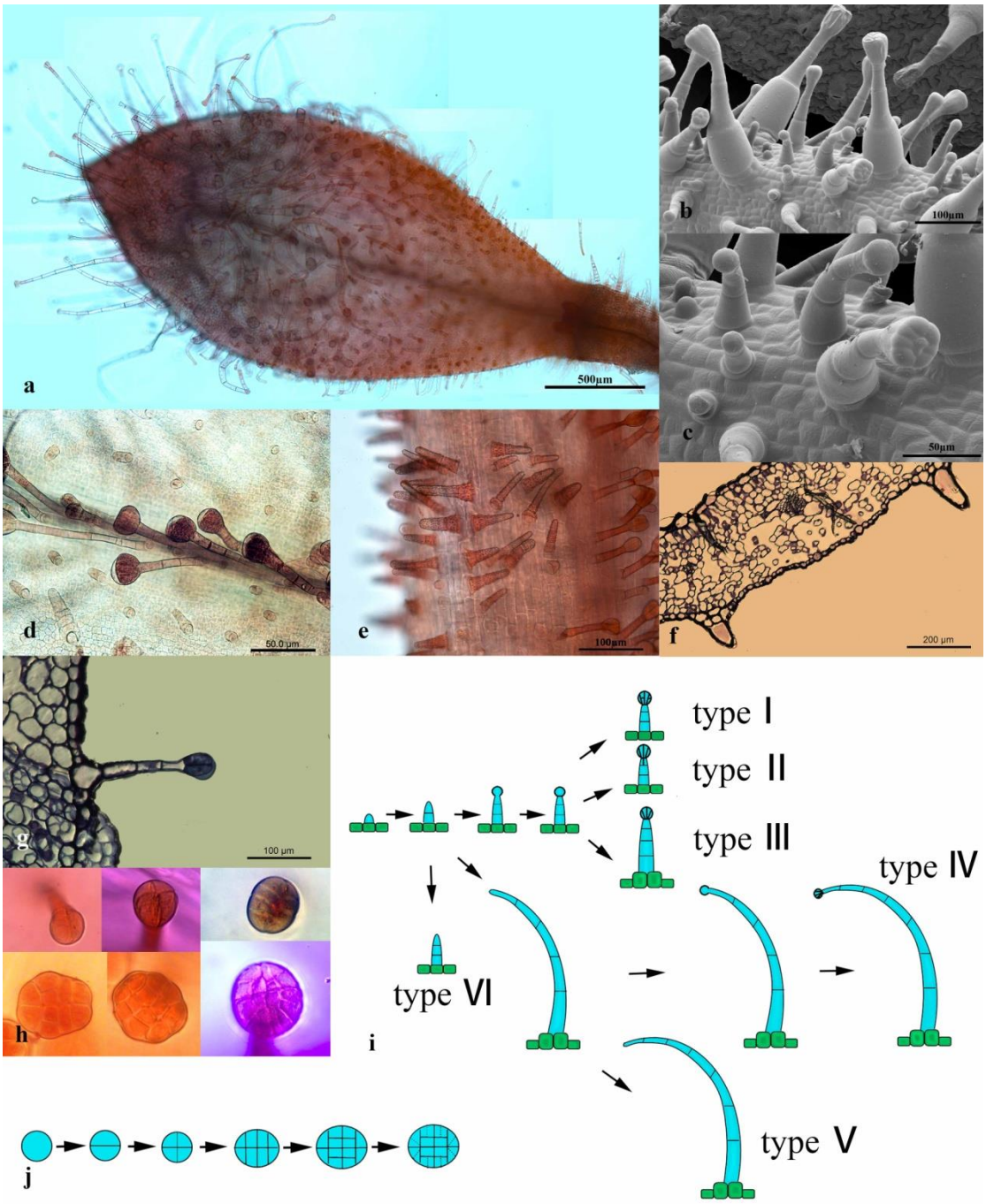

Figure 3.8. Development of trichomes in *Antirrhinum*

(a) Trichomes of the lamina mainly initiate from the base of a young leaf of *A. molle*. Type IV and V trichomes show no difference at early stages. (b, c) SEM pictures show that type III trichomes of different developmental stages can be found on leaves of a hairy NIL. (d) Type I trichomes initiate from the base of the midrib in *A. meonanthum* (e) Newly-initiated type V trichomes are not covered with micropapillae in *A. charidermi*. (f, g) resin sections show the division of foot cells at the base of type III trichomes. (h) Top views of glandular trichomes showing glands at different developmental stages. (i) A model of trichome development. (j) A model of gland development. Dashed lines indicate potential division.

3.6 Trichome distribution and morphology of related species

The genus *Antirrhinum* belongs to the tribe Antirrhineae (Plantaginaceae). Recent phylogenetic analysis identified six main lineages in the tribe Antirrhineae: *Anarrhinum*, *Maurandya*, *Gambelia*, *Chaenorhinum*, *Antirrhinum*, *Linaria* (Vargas et al., 2004, Yousefi et al., 2016). Trichome presence is an important taxonomic character in Antirrhineae. Some species have similar trichome types and trichome distribution to *Antirrhinum* species. Glandular trichomes, similar to the type III trichome in *Antirrhinum*, are found on the base of stems, early leaves and the inflorescence or throughout whole plants in the genus *Linaria* (Gabriel & Isabel, 2001, Saez & Crespo, 2005). For some of the related species I sampled, *Maurandya scandens*, a bald species, has glandular trichomes (type I-like) distributed on the adaxial veins (Appendix 1.25); *M. antirrhiniflora*, a hairy species, is covered with very dense long glandular trichomes (type IV-like) and long eglandular trichomes (type V-like) (Appendix 1.26); and *Gadoria falukei*, a recently published species situated in subtribe *Maurandya* (Güemes & Mota, 2017), shows the similar phenotype and trichome types to *M. antirrhiniflora* (Appendix 1.27)—long glandular trichomes and long eglandular trichomes were found throughout the whole plants. In this study, I focused on *Misopates* and *Chaenorhinum*, which were selected as outgroups in phylogenetic analysis.

3.6.1 Trichome distribution and morphology of *Misopates orontium*

Misopates orontium, known as linear leaf snapdragon, is an herbaceous annual plant placed in subtribe *Antirrhinum* with genus *Antirrhinum* (Vargas et al., 2004, Yousefi et al., 2016). *M. orontium* is a bald species showing descending trichome density from the base to the internode beneath the inflorescence (Fig. 3.9a). The internode underneath inflorescence is almost bare, though sparse trichomes can be seen (Figure 3.9c). Like bald *Antirrhinum* species, trichomes are produced again from the

inflorescence (Fig. 3.9b). Long eglandular trichomes (type V-like) and glandular trichome (type III-like) are distributed on the stem, leaves and inflorescence (Fig. 3.9d, e, g, h). Type I-like glandular trichomes are present on the adaxial midrib of all leaves, which is the same in *Antirrhinum* species (Fig. 3.9f). From bottom to top, leaves show a decreasing number of long eglandular trichomes (type V-like). Only glandular trichomes (type III-like) could be found on the top leaves (Fig. 3.9g). Both trichome distribution and morphology of *M. orontium* is similar to those of *Antirrhinum* bald species, suggesting that *M. orontium* may share the same genetic control as *Antirrhinum*.

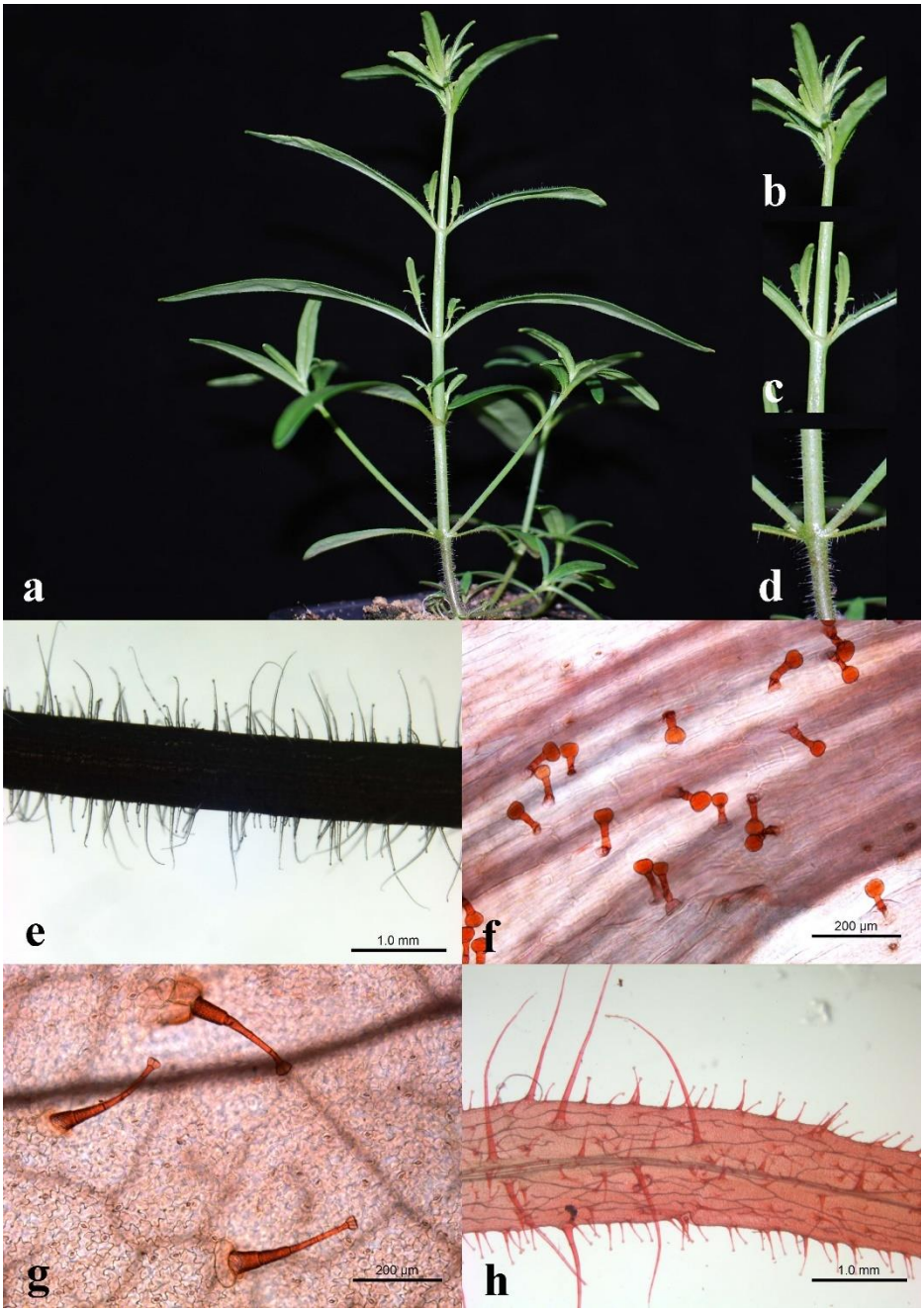

Figure 3.9. Trichome distribution and morphology of *Misopates orontium*

(a-d) Trichome distribution. (a) A plant of *M. orontium* showing a descending density of trichomes from its base to the internode beneath the inflorescence. (b) The inflorescence of *M. orontium* is hairy. (c) The internode beneath the inflorescence is almost bald. (d) The early internodes are covered with dense glandular trichomes and eglandular trichomes. (e-h) Trichome morphology. (e) Type III and V trichomes on the stem. (f) Type I trichomes on the adaxial midrib. (g) Type III trichomes on the leaf. (h) Type III and V trichomes on the sepal.

3.6.2 Trichome distribution and morphology in *Chaenorhinum*

The genus *Chaenorhinum* belongs to the *Chaenorhinum* group, which is sister to *Antirrhinum* group (Vargas et al., 2004, Vargas et al., 2009). It is therefore more distantly related to *Antirrhinum* than *Misopates* is. *C. origanifolium*, which was included in phylogenetic analysis, appears bald except for the inflorescence (Fig. 3.10a). An increasing number of long eglandular trichomes and long glandular trichomes can be seen from where the inflorescence forms to the tip (Fig. 3.10b, f). Although leaves and stem initially look to be free of hairs, trichomes were observed after leaf clearing and safranin O staining. Glandular trichomes comprised of one to two stalk-cells and two gland-cells are scattered on leaves and distributed along the adaxial midrib (Fig. 3.10c, d). Glandular trichomes of this type were also found on stems together with short non-glandular trichomes (Fig. 3.10e). Most of the trichomes on the leaf and stem bend towards the leaf tip or shoot apex. Because hairs are bent and at low density, they are not observable with the naked eye. Morphologically, these trichomes differ from long glandular trichomes and long eglandular trichomes of the inflorescence. Trichomes on the lower nodes were not sampled, they disappeared after the lower stem lignified. Unlike *C. origanifolium*, *C. rubrifolium* was found to be a hairy species (Fig. 3.10g). Long glandular trichomes and long eglandular trichomes are distributed throughout the plant, including leaves, stem and inflorescence (Fig. 3.10h-j). It supports the idea that *C. origanifolium* had a bald phenotype.

Figure 3.10. Trichome distribution and morphology of *Chaenorhinum*

(a-f) Trichome distribution and morphology of *C. origanifolium*. (a) To the naked eyes, plants of *C. origanifolium* are visually bald except for the inflorescence. (b) The inflorescence of *C. origanifolium* shows increasing number of trichome apically. (c, d) Glandular trichomes present on the adaxial midrib and blade. (e) Eglandular trichomes and glandular trichomes distributed on the stem. (f) Long eglandular trichomes and long glandular trichomes can be found in the inflorescence. (g-j) Trichome morphology and distribution of *C. rubrifolium*. (g) *C. rubrifolium* is a hairy species. (h-j) Long eglandular trichomes and long glandular trichomes present on the aerial parts of plants—(h)

leaf, (i) stem.

3.7 Conclusion

Eglandular and glandular trichomes were observed in *Antirrhinum* species. They were classified into five types: short glandular (type I) and short glandular with two-neck-cells (type II) on the adaxial midrib, glandular (type III), long glandular (type IV), long eglandular (type V) and short eglandular with micropapillae (type VI). Bald species and hairy species exist in the genus *Antirrhinum*. The main difference between the two phenotypes is that the middle vegetative parts (usually from the third internode to just below inflorescence) are free of trichomes in the bald phenotype except for the type I and type II trichomes on the adaxial midrib. Bald species usually start to be bald after the second node, though some bald species becomes bald from later nodes, exhibiting a descending density of type III trichomes from the second node. The formation of type III trichomes returns in the inflorescence of bald species. For hairy species, the trichomes in the inflorescence are the same types of trichomes present in the middle vegetative parts. It suggests that the growth of type III trichomes is prohibited in the middle vegetative parts of bald plants. Surprisingly, the lower leaves and internodes of all the species possess type III and type V trichomes with decreasing density apically (Figure 3.11). Other species in the tribe Antirrhineae also exhibit similar trichome distribution and trichome types to *Antirrhinum* species, suggesting that the control of trichome distribution and morphology is conserved within the tribe.

To identify genes underlying trichome distribution in *Antirrhinum*, a near isogenic line was generated by introducing *A. charidemi* genes into an *A. majus* subsp. *majus* background. It segregated bald progeny which have the same trichome distribution to *A. majus* subsp. *majus* (the later vegetative parts are free of hairs except for adaxial midribs) and hairy NILs which have a similar trichome distribution to *A.*

charidemi. The NILs possess type III trichomes, which is the trichome type of *A. majus* subsp. *majus*, has rather than the type VI trichomes that *A. charidemi* has, suggesting that trichome morphology evolved independently to trichome distribution and is controlled by different genes.

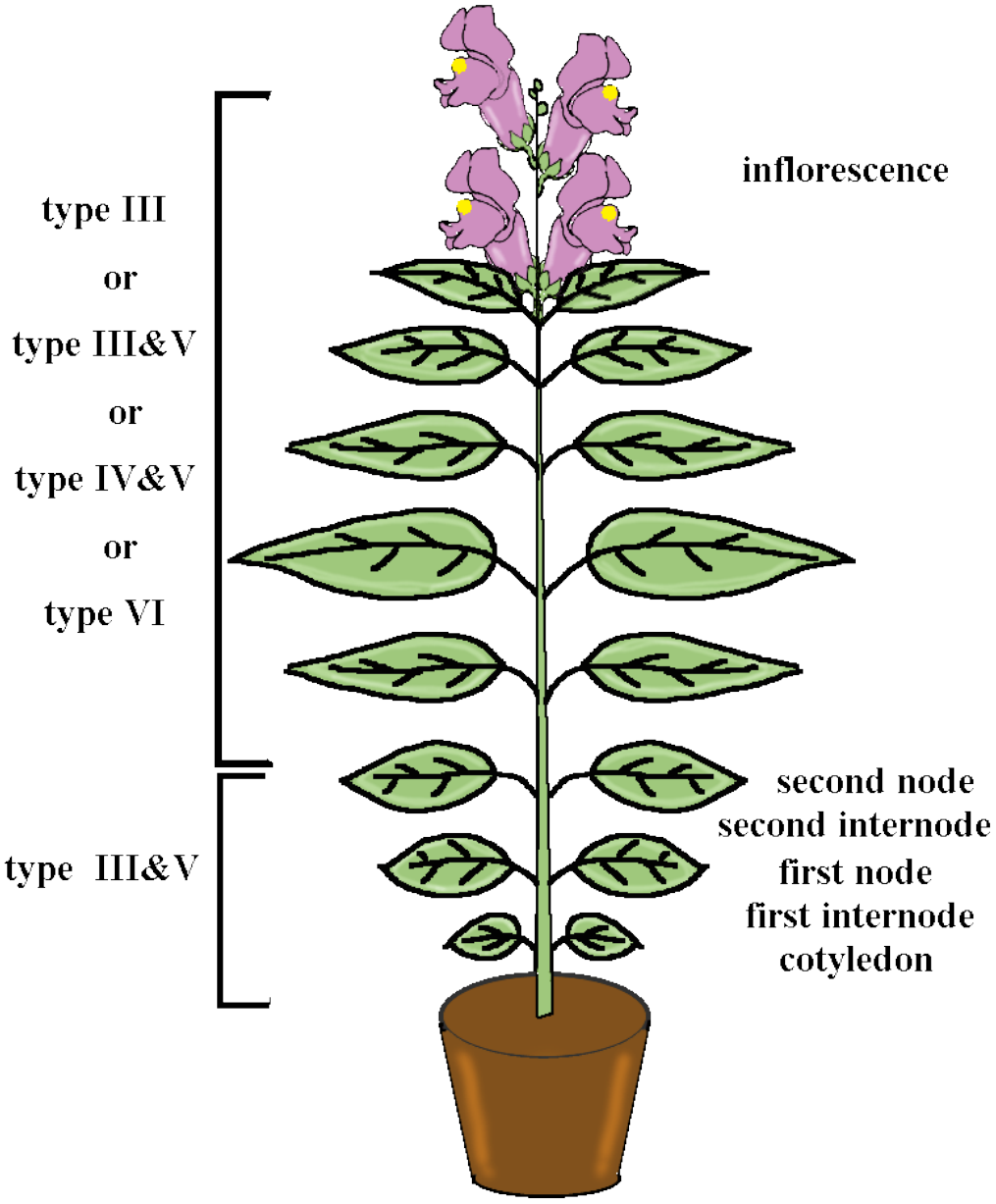

Figure 3.11. Trichome types and distribution in *Antirrhinum*

For all species, hybrids and NILs, type III and V trichomes occur on lower stems and leaves. Trichome types distributed on later vegetative parts and inflorescence vary between species.

Chapter 4

4 Identification and validation of the *Hairy* gene

Crosses between bald species and hairy species suggested that hairiness is a recessive trait controlled by a single locus in *Antirrhinum*. Molecular markers like CAPS and SSLP had been applied previously to map the locus to Chromosome 6, near the centromere, between the self-incompatibility *(S)* locus, responsible for preventing self-pollination, and *CYCLOIDEA* (*CYC*), a gene encoding a TCP transcription factor involved in flower asymmetry. Since the recessive alleles of the locus are responsible for hairiness, we named it *Hairy* (*H*). To isolate *Hairy* in *Antirrhinum*, a near isogenic line (NIL) had been generated by crossing *A. majus* subsp. *majus* (bald) to *A. charidemi* (hairy), and backcrossing to *A. majus* subsp. *majus* for eight generations with selection for the *A. charidemi CYC* allele, using a CAPS marker. One of the resulting NILs produced a low proportion (~5%) of hairy progeny when it was self-pollinated, suggesting that it was heterozygous for *H* alleles form *A. majus* subsp. *majus* (H^m) and *A. charidemi* (h^c). All the bald progeny were assumed to carry at least one H^m allele from *A. majus* subsp. *majus*, while both alleles of the hairy progeny would be from *A. charidemi* (genotype h^c/h^c). *A. charidemi* shows gametophytic self-incompatibility, so extension of pollen tubes carrying the functional *A. charidemi S* allele S^c will be halted and S^c/S^c homozygotes not produced. *A. majus* subsp. *majus* is self-compatible, carrying the inactive allele, s^m. The NIL ($H^m s^m/h^c S^c$) would therefore produce hairy progeny only when recombination had happened between h^c and S^c.

Next-generation sequencing (NGS)-based bulked-segregant analysis and RNA-seq were conducted to identify the *Hairy* gene in this study. To generate segregants for resequencing, a bald NIL individual that was heterozygous at *Hairy* locus and

homozygous for the *A. majus* subsp. *majus* s^m allele (genotype $H^m s^m/h^c s^m$) was self-pollinated. Its progeny segregated approximately three bald to each hairy phenotype and these phenotypes were used to make two bulks for resequencing.

A comparison of bald and hairy progeny of the NIL, showed that the only difference was in the middle parts (between the third internode and the inflorescence), which are free of trichomes in bald plants, except for adaxial midribs. One explanation for this is the *Hairy* gene, which is needed to repress trichome formation, is only expressed in the middle parts of bald plants. Hairs might form on adaxial midribs either because they cannot be repressed by *Hairy* or because *Hairy* is not active in the adaxial midrib. Trichomes can always be found from adaxial midrib throughout the genus. The distribution of hairs in hairy species further suggests that they might lack *Hairy* activity. These assumptions were used to test candidates for *Hairy* on the basis of RNA expression.

4.1 Construction of a population to map *Hairy*

A bald NIL (*9), as mother, had been crossed to a hairy sibling (H5). Seeds were available from a previous member in the group and my work started from this generation. Bald and hairy phenotypes were found in the progeny (population M351) in a 1:1 Mendelian ratio (p = 0.919, chi-squared test). This suggested that the bald *9 parent had the genotype $H^m s^m/h^c S^c$, and the hairy H5 parent had the genotype $h^c s^m/h^c S^c$, so that pollen carrying the $h^c S^c$ chromosome was rejected (Table 4.1). The *9 and H5 parents were genotyped at the *S* locus by sequencing the F-box component of *S* locus and were confirmed to be heterozygous (s^m/S^c). The two *S* alleles could be distinguished by a CAPS marker, because S^c has two *Dpn* II sites and s^m has only one (Fig. 4.1). CAPS genotyping of the progeny showed that most (46) bald plants in the F_1 population were $H^m s^m/h^c s^m$, having probably inherited the

recombinant $h^c s^m$ haplotype from the hairy H5 parent. From these, one plant, M351-3, was chosen to be self-pollinated to generate an F_2 population (family M430). The F_2 population consisted of 306 bald plants versus 80 hairy plants, corresponding to a 3:1 ratio (p = 0.052). The segregation ratio supports M351-3 being heterozygous at the *Hairy* locus. DNA was extracted from 280 bald F_2 plants separately and equal amounts were pooled. Equal amounts of DNA from 70 hairy F_2 individuals were also pooled. DNA samples were sent to the Earlham Institute, Norwich for Illumina paired-end sequencing. Sequencing data was analyzed by Matthew Barnbrook.

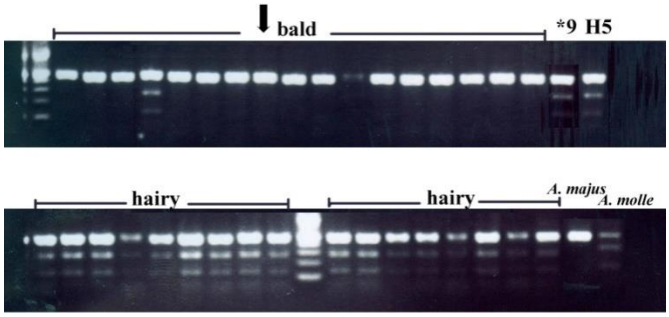

Figure 4.1. CAPS genotyping of F_1 plants at the *S* locus
The *S* locus F-box sequence of *A. charidemi* can be digested into three fragments with *Dpn* II. The F-box of *A. majus* subsp. *majus* is digested into only two fragments. Most bald plants of the F_1 population are S^m homozygotes, while most hairy plants are heterozygotes. The arrow indicates M351-3 that was self-pollinated to generate an F_2 population for mapping.

Table 4.1. Formation of the F_1 population. '-' indicates pollen grains carrying the $h^c S^c$ chromosome were rejected.

♀ ♂			H5 $h^c s^m/h^c S^c$	
			$h^c s^m$	$h^c S^c$
*9 $H^m s^m/h^c S^c$	Non-recombinant	$H^m s^m$	$H^m s^m/h^c s^m$	-
		$h^c S^c$	$h^c s^m/h^c S^c$	-
	Recombinant	$H^m S^c$	$H^m S^c/h^c s^m$	-
		$h^c s^m$	$h^c s^m/h^c s^m$	-

Making the assumptions that the middle parts of bald plants would express the *Hairy* gene and that the S^c allele might be expressed at a lower level, the hairy NIL ($h^c S^c/h^c s^m$) and a bald NIL, homozygous for $H^m s^m$, were used for RNA sequencing by Matthew Barnbrook. RNA was extracted from shoot apices where the sixth leaves

were 5 mm long and sent to Glassgow Polyomics for cDNA library production and Illumina single-end sequencing. Sequencing reads were mapped onto the JI.7 reference genome and alignments visualized using Integrative Genomic Viewer (IGV) (Robinson et al., 2011, Thorvaldsdóttir et al., 2013)

4.2 Identification of a candidate *Hairy* gene

Whole-genome resequencing reads of bald and hairy bulks were aligned to the reference genome of *A. majus* subsp. *majus* line JI.7. The bald population used for resequencing was produced by self-pollination a heterozygous plant (M351-3), as confirmed by its 3:1 segregation ratio of bald to hairy progeny. Therefore, about two out of three plants in the bald bulk would be heterozygotes carrying the h^c allele. h^c should therefore be one third of the alleles in the bald bulk, but the only allele in the hairy siblings. We also hypothesized that the *Hairy* gene would be expressed in the middle parts of bald plants preventing trichome initiation here, and its expression might be reduced in hairy plants. Based on these hypotheses, we found one candidate gene belonging to the *Glutaredoxin* (*GRX*) family from Scaffold 1097 on Chromosome 6 (Fig. 4.2). This gene was named *GRX1*. In the hairy pool, all the *GRX1* alleles have only the polymorphisms from *A. charidemi*, while about two thirds of the alleles are identical to the reference sequence in the bald pool. In addition, expression of *GRX1* was found only from the bald RNA samples. The *GRX1* gene was therefore a strong candidate for *Hairy* and the mutations of *GRX1* in *A. charidemi* may be a loss-of-function resulting in no RNA expression.

Two related *GRX* genes, from Scaffold 40 and Scaffold 123, were identified by blasting the DNA sequence of *GRX1* against the reference genome. One of them, in Scaffold 40, appeared to be closely linked to *Hairy* because *A. majus* subsp. *majus* polymorphisms were not found in the pool of hairy plants, the other, in Scaffold 123, had only *A. majus* subsp. *majus* sequences so appeared unlinked. The RNA-seq

results showed that the gene in Scaffold 40 was not expressed in either bald or hairy NILs, while the gene on Scaffold 123 showed the same expression level in bald and hairy NILs. Independent RT-PCR tests of the gene in Scaffold 40 (*GRX40*) suggested that it is a pseudogene since no expression could be found in any of the tissues tested (Appendix 3). The *GRX* gene from Scaffold 123 was named *GRX2*.

Figure 4.2. Screenshot of whole-genome resequencing of bulked segregants and RNA-seq in Intergrative Genomic Viewer

Whole genome resequencing and RNA-seq results were aligned to the reference genome (*A. majus* subsp. *majus* line JI.7). One candidate gene, *GRX1*, was identified from Scaffold 1097 and is shown here. In the hairy pool, all the genome sequence reads have the same polymorphisms; while about one third of reads show these mutations in the bald pool. The expression of *GRX1* was found only in RNA samples extracted from the apices of bald NILs producing bald leaves. Grey arrows indicates sequences identical to the reference with both paired-end reads mapped; vertical colored lines indicate SNPs relative to the reference genome, black horizontal lines indicate deletions, and colored bars show sequenced fragments with only one read mapped to this region.

4.3 Validation of the *Hairy* gene

Three further tests were used to validate *GRX1* as a candidate for *Hairy*. First F_1 and F_2 populations and parent plants were genotyped at *GRX1* to confirm that their *GRX1* and *Hairy* genotypes were consistent. This was important for the F_2

population because bulked-segregant analysis was unlikely to have sequenced all alleles in the hairy pool and might have failed to detect recombination between *GRX1* and *Hairy*. Secondly, the pattern of *GRX1* expression was studied further using quantitative RT-PCR and *in situ* hybridization. Thirdly, VIGS was used to confirm that *AmGRX1* was needed to repress trichome formation in bald plants and also to test the function of *GRX2*.

4.3.1 Genotyping mapping populations

A Cleaved Amplified Polymorphic Sequences (CAPS) marker was used for genotyping *GRX1*. The *A. charidemi* allele has a *Bst*X I recognition site (5'CCANNNNNNTGG3'), while the allele of *A. majus* subsp. *majus* does not. The sequence of *AmGRX1* was amplified (*A. majus* subsp. *majus* 703 bp, *A. charidemi* 732 bp), and then incubated with *Bst*X I. The sequence of *AcGRX1* was cut in the middle and generated two smaller fragments (432 bp and 300 bp). The sequence of *AmGRX1* was not digestible and remained the same size (Fig. 4.3).

As predicted, the bald mapping parent *9 (H^m/h^c) was heterozygous for the *AmGRX1* and *AcGRX1* sequences and the hairy parent H5 (h^c/h^c) homozygous for *AcGRX1*. All the hairy plants genotyped in the F_1 and F_2 population proved to be homozygous *AcGRX1* (43 in F1, 70 in F2)), while all the bald plants carried at least one *AmGRX1* sequence. In the F_2 population, bald plants consisted of 94 homozygous plants and 170 heterozygous plants (1:2, p=0.433). Therefore, no recombination was detected between *GRX1* and *Hairy*, consistent with *Hairy* being *GRX1*. Homozygous bald and hairy F_2 NILs were selected at this stage and used for the rest of the studies.

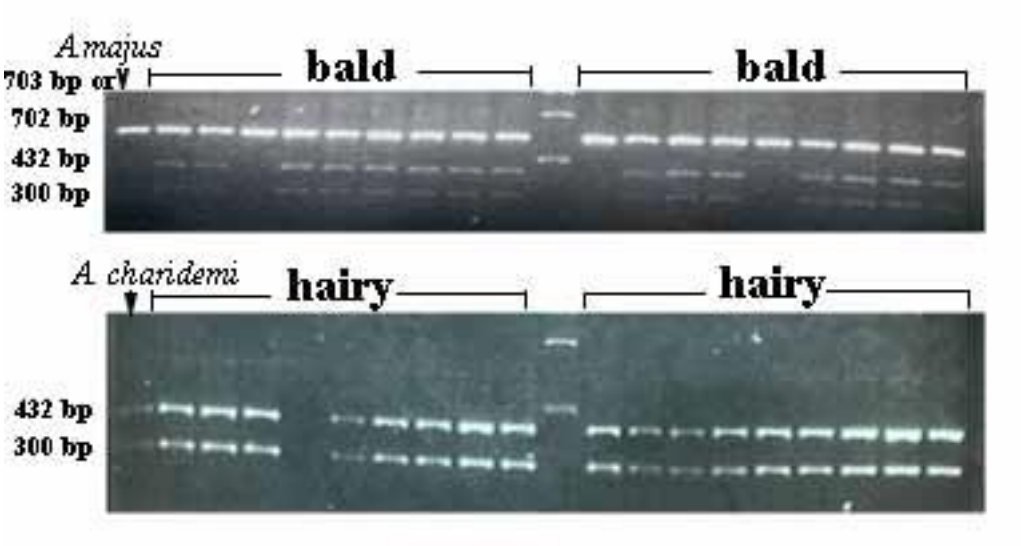

Figure 4.3. An example of CAPS genotyping of F_2 plants at the *GRX1* gene
The *AcGRX1* of *A. charidemi* can be digested into two fragments (432 bp and 300 bp) with *Bst*X I. The *AmGRX1* of *A. majus* subsp. *majus* was digestible. Bald plants of the F_2 population are heterozygous or homozygous for *AmGRX1*, while all the hairy plants carry only *AcGRX1* from *A. charidemi*.

4.3.2 Expression patterns of *GRX1* and *GRX2*

Quantitative RT-PCR and *in situ* hybridization were used to study the expression patterns of *GRX1* and *GRX2*. Samples were prepared from different developmental stages (aerial parts of seedlings, shoot apices where the fourth leaves were 5 mm long and inflorescence apices) of bald and hairy NILs.

For RT-PCR of *GRX1*, primers were designed to regions that were identical in the *AmGRX1* and *AcGRX1* alleles. Quantitative RT-PCR failed to detect *GRX1* expression in all samples, except shoot apices of bald NILs forming bald vegetative parts (Fig. 4.4a). This supported *GRX1* being *Hairy*, the idea that h^c/*AcGRX1* is a null allele and that H^m/*AmGRX1* is expressed only in bald tissues. Even in shoot apices of bald NILs, expression of *AmGRX1* appeared low (Cq value around 40, compared to ~16 for the reference gene *Ubiquitin*). One explanation for this is that *AmGRX1* expression is confined to a limited number of cells in the shoot apex.

In contrast to *GRX1*, expression of *GRX2* was detected in all samples, and increased during development from seedlings to inflorescences (Fig. 4.4b). Expression was significantly higher in inflorescences of hairy NILs compared to bald NILs (around six-fold higher). This obervation does not have a simple explanation, Neither inflorescence expresses *GRX1*, so increased *GRX2* expression seems unlikely to reflect repression of *GRX2* by *AmGRX1*.

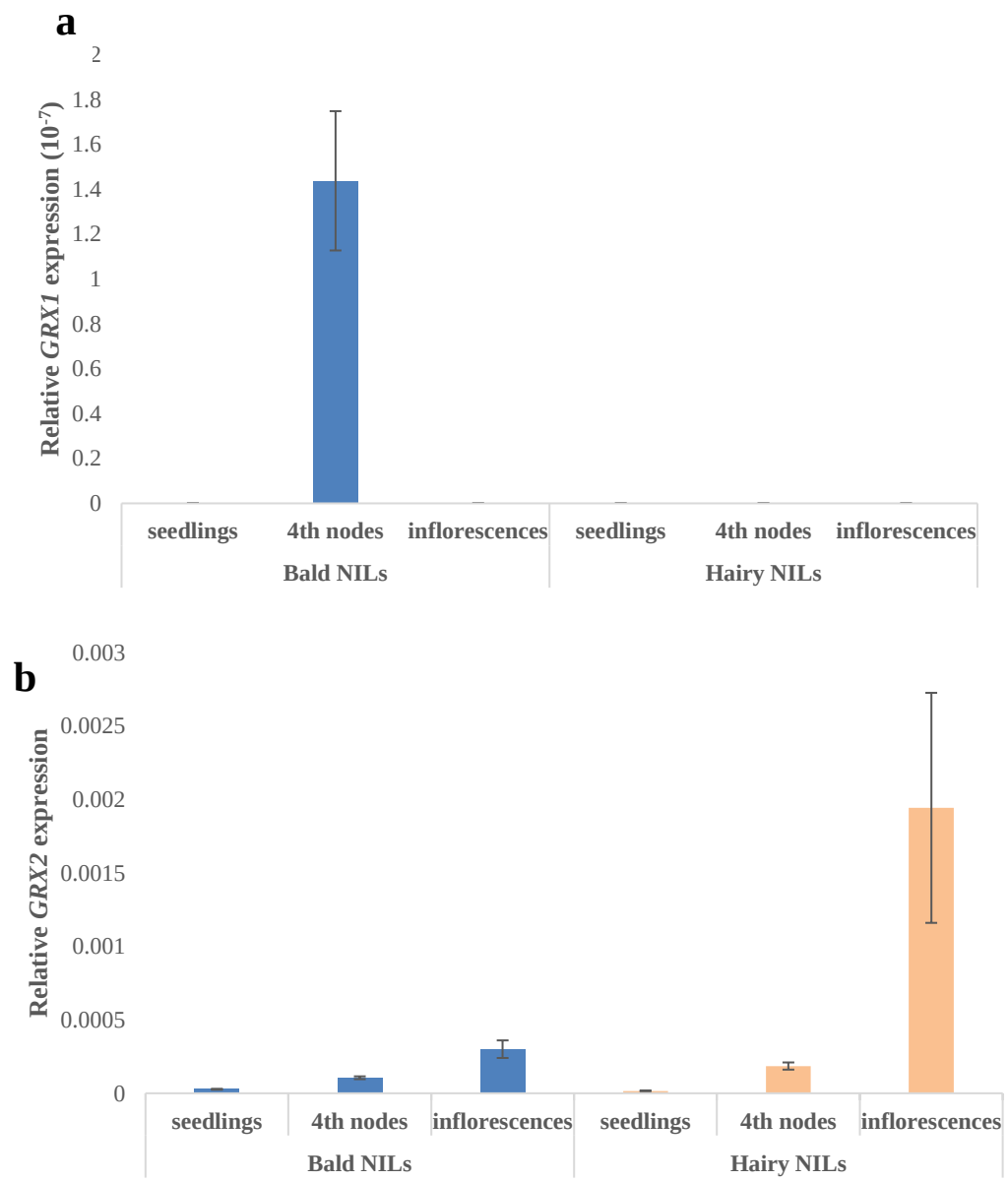

Figure 4.4. Expression of *GRX1* and *GRX2*

Abundance of *GRX1* (a) and *GRX2* (b) RNA in different tissues of bald and hairy NILs estimated using quantitative RT-PCR. RNA samples were extracted from seedlings, shoot apices where the fourth leaves were 5 mm long (4th nodes), and inflorescences. Data are displayed as the ratio of *GRX1* or *GRX2* expression to *Ubiquitin*, given as mean ± SE (*n* = 3 biological replicates).

I carried out RNA *in situ* hybridization to analyze further the sites of *GRX1* and *GRX2* expression. *GRX1* expression was detected only in vegetative apices producing the middle parts of bald NILs. It appeared to be restricted to the

epidermis of bald leaves and stems (Appendix 4.2), which forms trichomes in hairy species. In leaves, expression was stronger in the abaxial epidermis and no expression was detected in the adaxial midrib (Fig. 4.5, Appendix 4.1). The spatial pattern of *AmGRX1* is consistent with the region in which *Hairy* is needed to repress trichomes – bald leaves are glabrous except for the adaxial midrib – further supporting that idea that *GRX1* is the *Hairy* gene that prohibits trichome formation. It also suggests that trichomes on the adaxial midrib survive because *GRX1* is not expressed there.

GRX2, in comparison, was expressed in internal cells of developing organs (Fig. 4.5), consistent with its involvement in a different process to trichome development. In leaves and sepal, it appeared stronger in abaxial cells, especially in spongy mesophyll. *GRX1* and *GRX2* did not show overlap in spatial expression pattern that might suggest similar developmental roles.

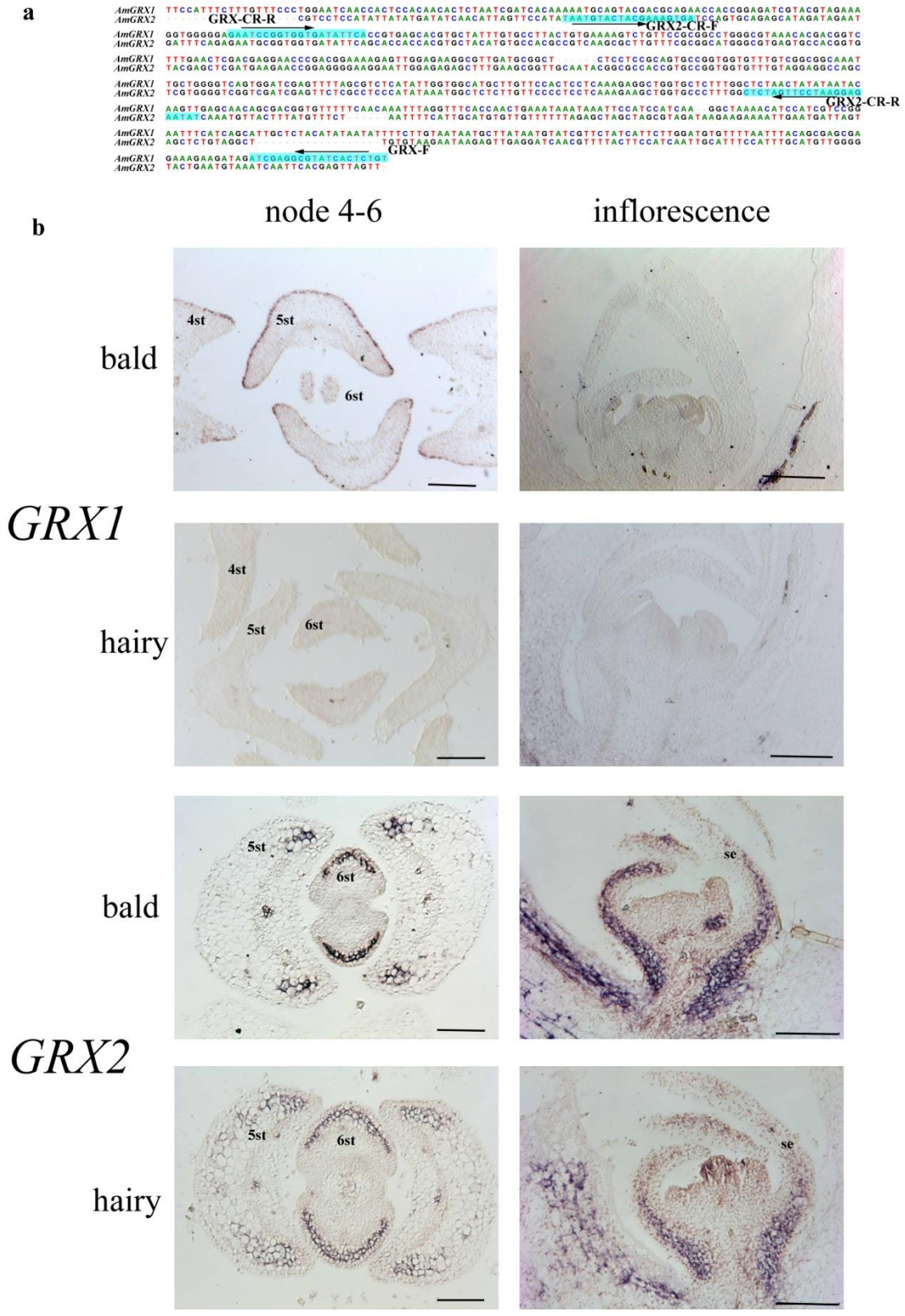

Figure 4.5. Sequence comparsion of *GRX1* and *GRX2* probes and spatial localization of *GRX1* and *GRX2* in young leaves and inflorescence meristem by *in situ* hybridization

(a)*AmGRX1* and *AmGRX2* share 71% identity in the coding region. Primers labeled in blue were used to prepare probes for *in situ* hybridization. Arrows indicate the 5' to 3' orientation of primers.

(b) *GRX1* expression was only detected in the epidermis of bald tissue, while GRX2 expression was detected in the internal cells of vegetative reproductive tissue. And these two genes don't show overlap in expression pattern. That means two probes are specific to each gene. Staining in the vascular tissue of inflorescences probed with *GRX1* appears to be background, because it is seen in bald and hairy genotypes. 4st, the fourth real leaves; 5st, the fifth leaves; 6st, the sixth leaves. Scale bars represent 200 μm.

4.3.3 VIGS in *Antirrhinum*

VIGS is a powerful method to discover the function of genes by reducing their expression that is less time-consuming than genetic transformation. It was therefore an ideal tool to test whether *GRX1* is needed to suppress trichome formation in *Antirrhinum*, which had proved difficult to transform. Although VIGS using Tobacco Rattle Virus (TRV) had been reported for *Antirrhinum*, very few of the infected plants were found to show silencing of the target gene. I therefore developed a more efficient method for producing infective virus (method described in Chapter 2) and a marker for gene silencing.

Silencing of the endogenous *Phytoene desaturase* (*PDS*) gene, which causes photobleaching, has commonly been used to test VIGS efficiency. PDS is an enzyme of the carotenoid biosynthetic pathway in chloroplasts (Linden et al., 1993, Grünewald et al., 2000), and reducing its activity results in photo-oxidative damage and tissue bleaching (Sandmann et al., 1991, Qin et al., 2007), making the effects of VIGS clearly visible in photosynthetic tissues. I identified a single *PDS* gene in the *A. majus* subsp. *majus* reference genome and used part of this as a reporter for VIGS, either on its own or fused to parts of the test genes *AmGRX1* or *AmGRX2*. For *GRX1*, the coding region or part of the 3'-UTR were used, and for *GRX2*, only the coding region was used. TRV virus carrying each construct were used to infect more than 30 plants.

4.3.3.1 VIGS phenotypes

Compared to uninfected plants, infection with TRV carrying the *Antirrhinum PDS* sequence resulted in slower plants growth, shorter internodes, curly stems and leaves (Fig. 4.6). Silencing of *PDS* was revealed as tissues bleaching in almost all infected plants.

Uninfected plants in these conditions showed a reduction in the density of trichomes in the third internode and third leaf and then became bald. Silencing the *PDS* gene alone did not alter the transition to baldness. However, infection with virus carrying *PDS* and either the coding region of *AmGRX1* (c*GRX1*) or the 3'-UTR sequence (3'*GRX1*), allowed trichome growth in bleached areas experience VIGS between the second node and inflorescence. In all cases, the ectopic trichomes were type III (Fig. 4.6, Appendix 5). Trichome growth was not restored from all the bleached areas, possibly because *GRX1* and *PDS* genes are expressed in different tissues (*GRX1* in the epidermis, *PDS* in in photosynthetic cells), so it would be possible to have epidermal cells in which *GRX1* remained active above bleached cells in which *PDS* was silenced. These observations suggested that *GRX1* is needed to repress trichome formation in later vegetative nodes, and therefore that *GRX1* was very likely to be *Hairy*.

In contrast to *GRX1*, infection with virus carrying *GRX2* and *PDS* did not cause any changes in trichome growth (Fig. 4.6) or any other effects that were not seen with *PDS* alone.

None of the treatments affected production of trichomes from early internodes or inflorescences of bald NILs, consistent with *AmGRX1* expression and *Hairy* activity being confined to later vegetative nodes. I also infected hairy NILs with virus containing each VIGS construct. No obvious changes to hair development were

observed.

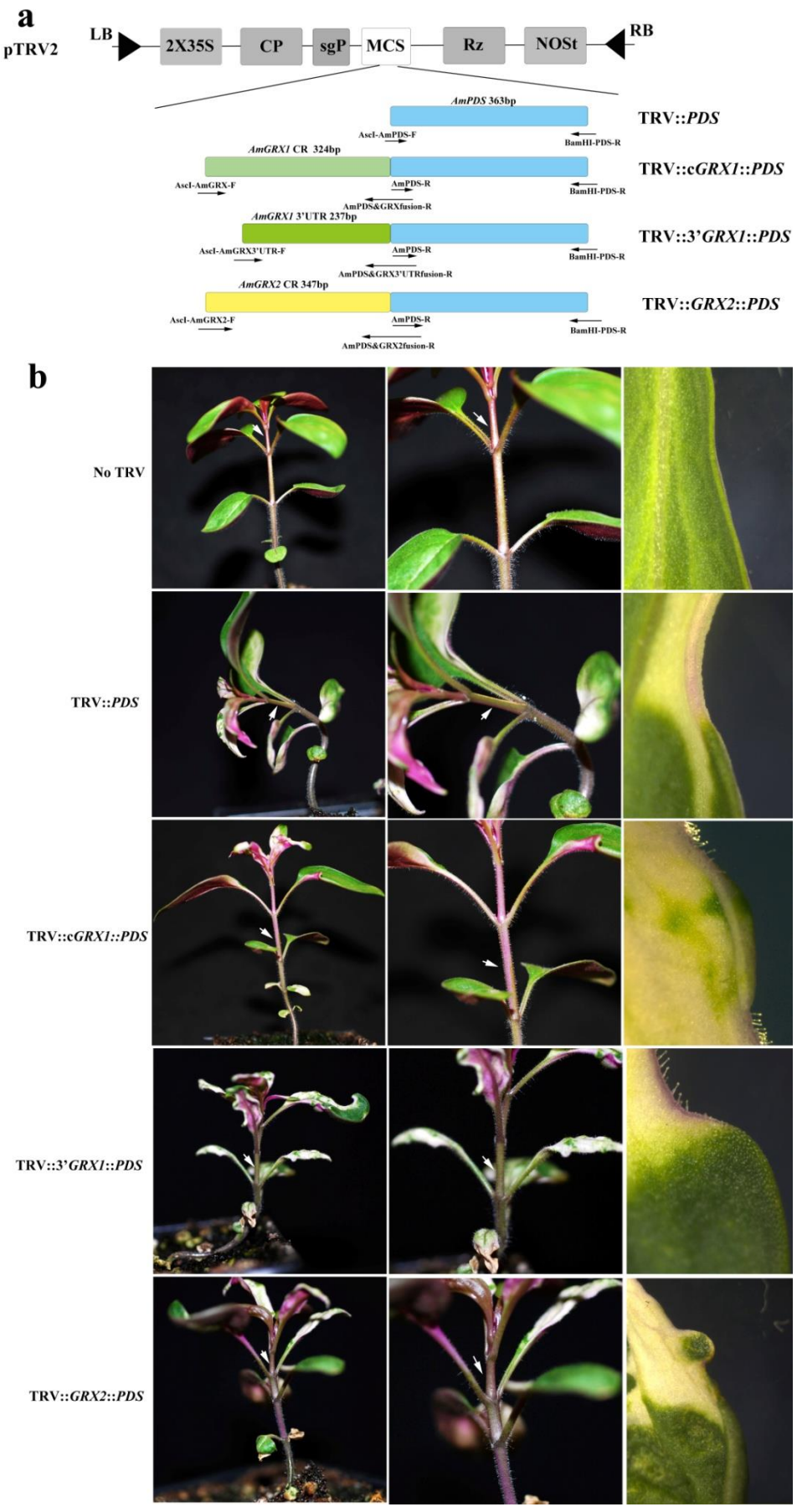
a
pTRV2
LB
2X35S
CP
sgP
MCS
Rz
NOSt
RB
AmPDS 363bp
AscI-AmPDS-F
BamHI-PDS-R
TRV::PDS
AmGRX1 CR 324bp
AscI-AmGRX-F
AmPDS-R
BamHI-PDS-R
AmPDS&GRXfusion-R
TRV::cGRX1::PDS
AmGRX1 3'UTR 237bp
AscI-AmGRX3'UTR-F
AmPDS-R
BamHI-PDS-R
AmPDS&GRX3'UTRfusion-R
TRV::3'GRX1::PDS
AmGRX2 CR 347bp
AscI-AmGRX2-F
AmPDS-R
BamHI-PDS-R
AmPDS&GRX2fusion-R
TRV::GRX2::PDS
b
No TRV
TRV::PDS
TRV::cGRX1::PDS
TRV::3'GRX1::PDS
TRV::GRX2::PDS

Figure 4.6. VIGS constructs and phenotypes of VIGS treated plants

(a) For TRV2 to silence *PDS* alone, *PDS* was amplified with a forward primer containing an *Asc* I site, and a reverse primer with a *Bam*H I site. Coding sequence and 3'UTR of *GRX1* and coding sequence of *GRX2* were fused to *PDS* sequence by overlapping PCR. To do this, they were amplified from bald NIL plants with forward primers with an *Asc* I site and reverse primers containing sequence overlapping of *PDS* at the 5' ends. Fragments were then inserted between the *Asc* I and *Bam*H I sites of TRV2 vector. Arrows indicate the 5' to 3' orientation of primers. CP, coat protein; sgP, subgenetic promoter; MCS, multiple cloning site; Rz, self-cleaving ribozyme; NOSt, NOS terminator; LB, left border; RB, right border. (b) Infection with virus carrying *GRX1* and *PDS* allows trichome develoment in bleached areas (above the second node), whereas *PDS* alone or *GRX2* and *PDS* have no effect on trichome formation. Arrows indicate the third internodes where the bald NILs usually become glabrous from. Infection with virus carrying *GRX1* and *PDS* allows trichomes to grow there.

4.3.3.2 Effects of VIGS on RNA levels

To confirm that VIGS results in reduced levels of *GRX1* transcripts, samples were chosen from the later vegetative parts of bald NILs, which are usually free of trichomes except for the adaxial midrib. RNA was extracted from shoot apices where the fourth leaves were 5 mm long. For most VIGS treated plants, samples were chosen from well photo-bleached individuals.

PDS expression was reduced to very low levels in plants infected with virus carrying *PDS* alone, *PDS* and *GRX1*, or *PDS* and *GRX2*, compared to uninfected bald NILs, consistent with the observed photo-bleaching of infected plants (Fig. 4.7b). VIGS of *PDS* alone did not reduce the expression of *GRX1*, consistent with the observation that it had no effect on trichome formation. VIGS of *PDS* and *GRX1* using either its coding region or 3'-UTR significantly reduced *GRX1* expression (Fig. 4.7a), as expected from the hairy phenotype of silenced tissue. However, it did not reduce expression of *GRX2*, its most similar expressed paralogue, suggesting that VIGS with *GRX1* sequence was specific to *GRX1* (Fig. 4.7c).

The mean estimate of *GRX2* RNA was higher in all VIGS treatments, relative to

uninfected plants. However, none of the differences proved significant because the variation between replicates of infected samples was high (Fig. 4.7c). The same high level of variance was found in repeated experiments using different tissue samples and PCR primers, so might reflect an effect of virus infection on *GRX2* expression that varies between plants or tissues. Therefore, it is currently not clear whether virus carrying *GRX2* reduced *GRX2* expression.

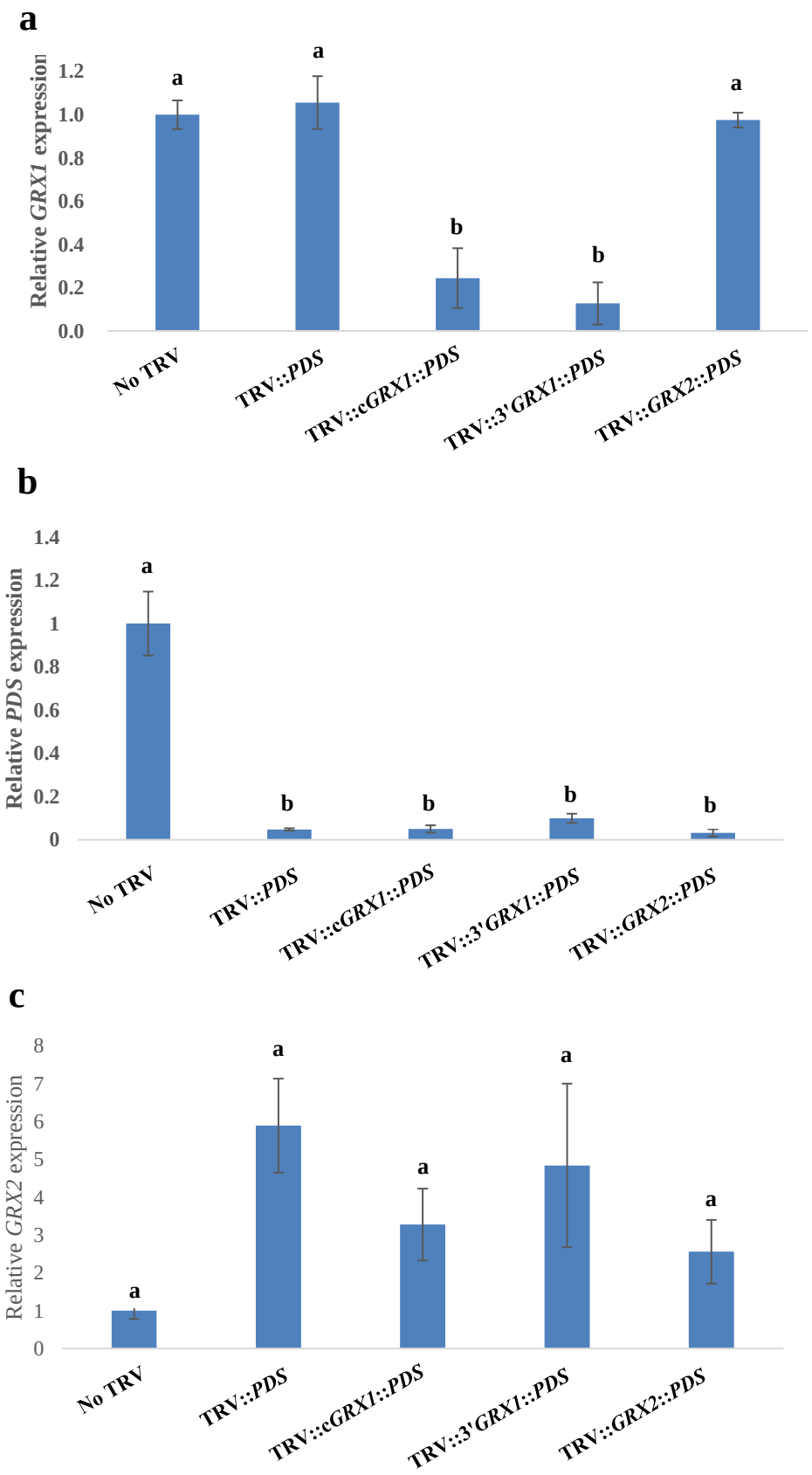
a
Relative GRX1 expression
1.2
1.0
0.8
0.6
0.4
0.2
0.0
a
a
b
b
a
No TRV
TRV::PDS
TRV::cGRX1::PDS
TRV::3'GRX1::PDS
TRV::GRX2::PDS
b
Relative PDS expression
1.4
1.2
1
0.8
0.6
0.4
0.2
0
a
b
b
b
b
No TRV
TRV::PDS
TRV::cGRX1::PDS
TRV::3'GRX1::PDS
TRV::GRX2::PDS
c
Relative GRX2 expression
8
7
6
5
4
3
2
1
0
a
a
a
a
a
No TRV
TRV::PDS
TRV::cGRX1::PDS
TRV::3'GRX1::PDS
TRV::GRX2::PDS

Figure 4.7. Effect of VIGS on RNA levels

Expression of *GRX1* (a), *PDS* (b) and *GRX2* (c) in VIGS treated plants. Data are displayed as the ratio of expression to *Ubiquitin* and normalized to expression in TRV-free plants, given as (mean ± SE for three biological replicates). Bars with different letters are significantly different from each other at $P \leqslant 0.05$ (by one-way ANOVA).

4.4 Reconstruction of *Hairy* evolution in *Antirrhinum*

All available evidence supported *GRX1* being the *Hairy* gene: *GRX1* had not been separated from *Hairy* by recombination, *AmGRX1* expression was restricted to cells in which *Hairy* represses trichome formation, VIGS revealed that *GRX1* was, like *Hairy*, needed to repress trichome formation, and *AcGRX1* was not expressed in hairy NILs.

Identification of *Hairy* opened up the possibility of reconstructing its evolution in the genus *Antirrhinum* and relating this to evolution of the trichome distribution. This was done in two ways. First, allelism tests were used to examine whether the baldness or hairiness of different species reflected their *Hairy* genotype. Secondly, a phylogeny was estimated for the *Hairy* gene in the genus *Antirrhinum.*

4.4.1 Allelism tests

Bald or hairy *Antirrhinum* species were crossed to a bald NIL of genotype $H^m s^m/h^c s^m$. Progeny of bald species crossed with the bald NIL were all bald, except in the case of *A. siculum*, discussed below. In contrast, progeny from hairy species crossed with the bald NIL segregated bald and hairy in a 1:1 Mendelian ratio ($p > 0.05$) (Table 4.2). This suggests that dominant *H* alleles exist in bald species, so that all progeny of the cross carry at least one dominant *H* allele and are bald, and that recessive *h* alleles exist in all hairy species, so that half of their progeny are h/h^c homozygotes and the other half are bald H^m/h heterozygotes. The one exception was that the

cross of the bald species *A. siculum* to the bald heterozygote generated only one viable seedlings, which was hairy. *A. siculum* was also crossed to *A. molle* which is hairy and suggested by the allelism test to have genotype *h/h*. All six progeny were hairy (Appendix 8). A simple explanation for this is that *A. siculum* is homozygous *h*/*h* but is bald because it carries a recessive mutation in a second gene (*Bald*, *B*) needed for formation of hairs (genotype *h*/*h b*/*b*). The single hairy progeny of the cross to the heterozygote (*H*/*h B*/*B*) would have had genotype *h*/*h B*/*b*. This hypothesis could be tested by following segregation of phenotypes in the next generation. However, the *A. molle* x *A. siculum* hybrids produced no viable seeds when self-pollinated, inter-crossed or back-crossed in both directions to *A. siculum*. The hybrid with the NIL was self-pollinated and yielded 477 hairy progeny with varied trichome density and 122 bald progeny. Among the hairy progeny, there were 171 individuals covered with very dense trichomes which were similar to hairy NILs, and 305 individuals with intermediate trichome density that was similar to their mother. Therefore, it produced 171 hairy plants, 305 less hairy plants and 122 bald plants, corresponding to 1: 2: 1 ($p = 0.0160$, chi-squared test). The generation of intermediate phenotype in the progeny suggested that the *Bald* alleles from *A. majus* and *A. siculum* could be co-dominant.

Most of the bald progeny of the NIL crossed to different species became bald above the second node, except for the hybrids of *A. molle*, where the middle parts of plants were not free of trichomes but had a few scattered hairs. This suggests either that the *hairy* allele of *A. molle* has a stronger effect than that of *A. charidermi* or that *A. molle* carries alleles at other loci that can affect hair density. Because the *A. charidemi* allele produces no detectable RNA, suggesting that it is null, a stronger effect would presumably have to involve a dominant-negative effect on the H^m allele in heterozygotes. Although a plant of *A. majus* subsp. *tortuosum* that became bald from the seventh internode was chosen to provide pollen, all progeny become bald

from the third internode. It suggests that the dominant *H* allele of *A. majus* subsp. *tortuosum* has a similar effect to the *A. majus* subsp. *majus* H^m in a genetic background that is partly from *A. majus* subsp. *majus*, and therefore that the later transition to baldness in *A. majus* subsp. *tortuosum* is due to other, possibly recessive genes.

Hybrids, with some exceptions, possessed a mixture of the trichome types found in their parents, as described in section 3.3. The trichomes on basal parts (below the second node) were the same in bald progeny and hairy progeny, dense glandular and nonglandular trichomes as in all the species. The later hairy vegetative parts and inflorescence of bald progeny, higher vegetative parts and inflorescence of hairy progeny produced type III hairs, as in the NIL, mixed with the types of trichomes found at higher nodes in the other parent. This suggests three things. First, that trichome type at higher nodes is not determined by *Hairy*, otherwise the progeny of crosses to hairy species with type VI trichomes would have the same phenotype as the hairy NIL which has the h^c allele from a species with this type of trichome. Secondly, that there is no dominance of trichome type, so it could be determined by a single locus with co-dominant alleles, or by multiple loci acting additively. Thirdly, that *Hairy* is able to suppress development of the different types of trichome, because different types are formed in the absence of *Hairy* activity. One exception was the bald heterozygote and *A. molle* hybrid, that produced medium sized glandular trichomes and long nonglandular trichomes (type V), but *A. molle* possesses long glandular (type IV) and type V trichome. It suggests that glandular trichomes are controlled by the same mechanism, but the length of them is regulated independently, possibly by a single locus with co-dominant alleles, therefore medium length trichomes between type III and type V trichomes were produced. Another exception is the progeny of cross to *A. valentinum*. Unlike the progeny of crosses to *A. pulverulentum* and *A. subbaeticum* which possessed type III and short eglandular

(type VI) trichomes, the *A. valentinum* hybrid only produced type VI trichomes, suggesting that mutations in *A. valentinum* prevented the formation of type III trichomes.

Table 4.2. Phenotype segregation of hybrids. P values were calculated by chi-square test between the actual ratio and a 1:1 ratio.

Pollen supplier			Number of Bald plants in F_1	Number of Hairy plants in F_1	P values
Species	**Accession**	**Phenotype**			
A. majus subsp. *linkianum*	L108	bald	30	-	-
A. majus subsp. *pseudomajus*	L53	bald	31	-	-
A. majus subsp. *striatum*	AC1125	bald	37	-	-
A. majus subsp. *tortuosum*	L92	bald	63	-	-
A. siculum	AC1177	bald	-	1	-
A. boissieri	L104	Hairy	16	21	0.411
A. hispanicum	L99	Hairy	17	14	0.590
A. graniticum	L116	Hairy	20	22	0.757
A. lopeisanum	*	Hairy	6	6	1
A. molle	E51	Hairy	19	15	0.493
A. rupestre	L139	Hairy	9	11	0.655
A. pulverulentum	L70	Hairy	27	22	0.475
A. subbaeticum	E72	Hairy	7	6	0.781
A. valentinum	AC1173	Hairy	19	17	0.739

4.4.2 Sequence analysis of *Antirrhinum Hairy* genes

Allelism testes had suggested that differences in activity of Hairy were responsible for the differences in trichome distribution between most *Antirrhinum* species and that hairy species appeared to carry recessive *hairy* alleles, consistent with loss-of-function mutations. This raised the questions of whether the hairy phenotype was derived from bald by mutation, and whether the hairy phenotype had evolved once, or involved multiple, independent mutations.

To test this, *Hairy* sequences were amplified from accessions of 24 *Antirrhinum* species and two other species in the tribe Antirrhineae (*Misopates orontium*, *Chaenorhinum origanifolium*) as potential outgroups. It was not possible to amplify full-length coding sequences of the two outgroup species using primers for regions conserved within *Antirrhinum*, so the sequences encoding their N-terminal regions are unknown.

The *Hairy* gene could not be amplified from four closely related, endemic *Antirrhinum* species from subsection *Kickxiella* (including *A. pertegasii*, *A. sempervirens*, *A. subbaeticum* and *A. valentinum*) or from some accessions of their close relatives (*A. pulverulentum* and *A. microphyllum*). Genome resequenceing of *A. sempervirens* gave no sequence reads that mapped to *AmHairy* in the reference genome (Annabel Whibley, personal communication), suggesting that the whole locus had been deleted in these endemic species. Southern hybridizations with the *AmHairy* coding region and 3'UTR sequence as a probe failed to detect *Hairy* sequences in *A. valentinum* and *A. subbaeticum*, supporting deletion of the *Hairy* locus in these species (Appendix 6). Given the close evolutionary relationships between these species within subsetion *Kickxiella*, it seems likely that a single deletion occurred in their common ancestor. Identification of the deletion break-points would allow this to be tested in the future.

Some populations of *A. meonanthum*, *A. australe* and *A. graniticum* are polymorphic for trichome distribution. Allelism tests had suggested that this was because they were polymorphic for functional and non-functional *Hairy* alleles. *Hairy* sequences were amplified from both hairy and bald members of these species.

4.4.3 Phylogenetic analysis of *Hairy* alleles in *Antirrhinum*

To reconstruct the evolutionary history of the Hairy gene in *Antirrhinum*, *M. orontium* was set as the outgroup because it had been identified as a closer relative than *Chaenorhinum* (Vargas et al., 2004, Ezgi et al., 2017). DNA sequences were aligned and used to construct Bayesian tree (Appendix 7.1). They were also translated, and the amino acid sequences of their products were aligned (Appendix 7.2).

In the most likely Bayesian tree of DNA sequences, two well-supported clades were identified for *Antirrhinum* (Fig. 4.8). One clade contained sequences that were mostly from hairy species in subsection *Kickxiella*, the other contained mainly sequences from bald species in subsection *Antirrhinum*. This is consistent with a single loss-of-function mutation at the base of the *Kickxiella* clade having given rise to hairiness in this group of species.

The sequences in the *Kickxiella* clade share a number of non-synonymous substitutions relative to the subsetion *Antirrhinum* clade that could have been responsible for the ancestral loss-of-function (Appendix 7.1, Appendix 7.2). However, no *Hairy* RNA expression was detected for the sequences in this clade that were tested using RT-PCR: *A. siculum* (AC1066), *A. boissieri* (L104), *A. molle* (E51) or *A. mollisimum* (L21), suggesting that an ancestral loss-of-function might have involved loss of expression. Allelism tests, RNA expression and sequence analysis

suggest that *A. siculum*, which is bald, carries inactive *hairy* alleles, supporting our hypothesis that there is a second gene or genes repressing the trichome formation in *A. siculum*.

A number of additional amino-acid substitutions and deletions were identified in the *Kickxiella* clade (Appendix 7.1, Appendix 7.2). This included a deletion of 12 bp from the coding region of *A. mollisimum* (positions 103-114) and a T to A substitution in *A. charidemi*, which resulted in a premature stop codon. If the ancestral mutation in the *Kickxiella*-like clade removed Hairy function, these mutations could have accumulated without purifying selection. This might also be true of the deletion/s of *Hairy* in the endemic *Kickxiella* species.

Sequences from hairy members of polymorphic populations of two species from subsection *Antirrhinum*—*A. graniticum* (accessions TM25 and L116), and *A. australe* (accessions L91, 2 L95, and TM7)—were also found in the *Kickxiella*-like clade. This suggested that the polymorphisms might have come from hybridization with species in subsection *Kickxiella*.

The presence of a *Kickxiella*-like sequence in *A. majus* subsp. *cirrhigerum* accession TM41 and *A. majus* subsp. *linkianum* accession TM23 was also anomalous because these accessions, samplesd at the Real Jardín Botánico, Madrid, appeared bald. Their *Hairy* sequence, which was the same in both taxa, had an insertion of 3 bp in the coding regions, which potentially added one amino acid to the Hairy protein (Appendix 7.2). The same allele was isolated from a herbarium specimen of *A. majus* subsp. *linkianum* accession MA865666 which was bald and possibly from the same location as TM24. It is therefore not clear whether the allele would be functional, even if it could produce protein. Sequences from other accessions of these species were placed in the subsection *Antirrhinum* clade. One explanation for

the anomalous plants is that they were heterozygous and also had a functional *Hairy* allele. However, this seems unlikely because no other alleles were detected by direct sequencing of PCR products. Other possibilities are that another gene was responsible for baldness as in *A. siculum*, or that the sequence was from another species. Because the plants were not available for further examination, allelism tests or DNA extraction, these possibilities were not investigated further.

In the second major clade, most sequences were from bald species in subsection *Antirrhinum*, but it also included seven sequences from hairy plants. All except one of these had at least one non-synonymous mutation or deletion that might account for a loss-of-function. *A. boissieri*2 L104 shares an amino acid substitution in the C-terminal region with non-functional *Kickxiella*-like alleles. *A. grosii* L175, *A. meonanthum* L118 and *A. australe*1 L95 shared the same F78L substitution and, in addition, the *A. australe*1 L95 allele carried a 24 bp deletion that would remove eight amino acids from the protein. *A. hispanicum* L99 had a unique non-synonymous (R13I) substitution. No RNA expression from this allele could be detected, suggesting that it also carried a regulatory mutation that could account for loss-of-function. Only the *A. australe*2 L91and *A. latifolium* MA633610 alleles had the potential to encode a protein identical to the product of a functional *Hairy* allele. However, expression of the *A. australe*2 L91 allele was not tested, so it could have a mutation in another region (e.g. promoter region) that affects expression. The *A. latifolium* MA633610 allele was from an herbarium specimen which was hairy. It is impossible to extract RNA from this sample and find the expression of this allele. This allele could be inactive due to another mutation. Samples from the same location as the specimen could be collected for future work.

These findings suggest that several independent loss-of-function mutations in *Hairy* have given rise to the hairy mutant phenotype.

The sequence from the hairy plant *A. latifolium* AC1066 was placed at the base of subsection *Antirrhinum* clade. This could reflect its evolution from an ancestor shared with the rest of the *Antirrhinum* clade by stepwise accumulation of mutations. However, a more likely explanation is that it is the result of recombinations between *Antirrhinum*-like and *Kickxiella*-like alleles, because the 5' region of the sequence (position 1-38 relative to the ATG initiation codon) and the 3' region (position 274 onwards) have SNPs characteristic of *Kickxiella* alleles while the middle part of the coding sequences had subsection *Antirrhinum*-like SNPs (Appendix 7.1). This also suggests that the mutation/s responsible for loss of function at the base of the *Kickxiella* clade lies outside positions 38 to 274 of the coding region.

Another potential recombinant was detected in *A. boissieri* L104, which is hairy and heterozygous at the *Hairy* locus. One allele (*A. boissieri*1 L104) has *Kickxiella*-like features throughout. The other allele (*A. boissieri*2 L104) has *Kickxiella*-like SNPs from position 97 onwards, the rest of the sequence being subsection *Antirrhinum*-like. These two recombinant alleles were possibly formed after hybridization between subsections.

In the Bayesian phylogeny generated using predicted protein sequences, subsection *Antirrhinum* sequences formed a supported clade (Fig. 4.9). However, subsection *Kickxiella* sequences did not form a separate clade and their relationships were poorly resolved, probably because the amino acid alignments provided fewer informative sites than DNA alignments.

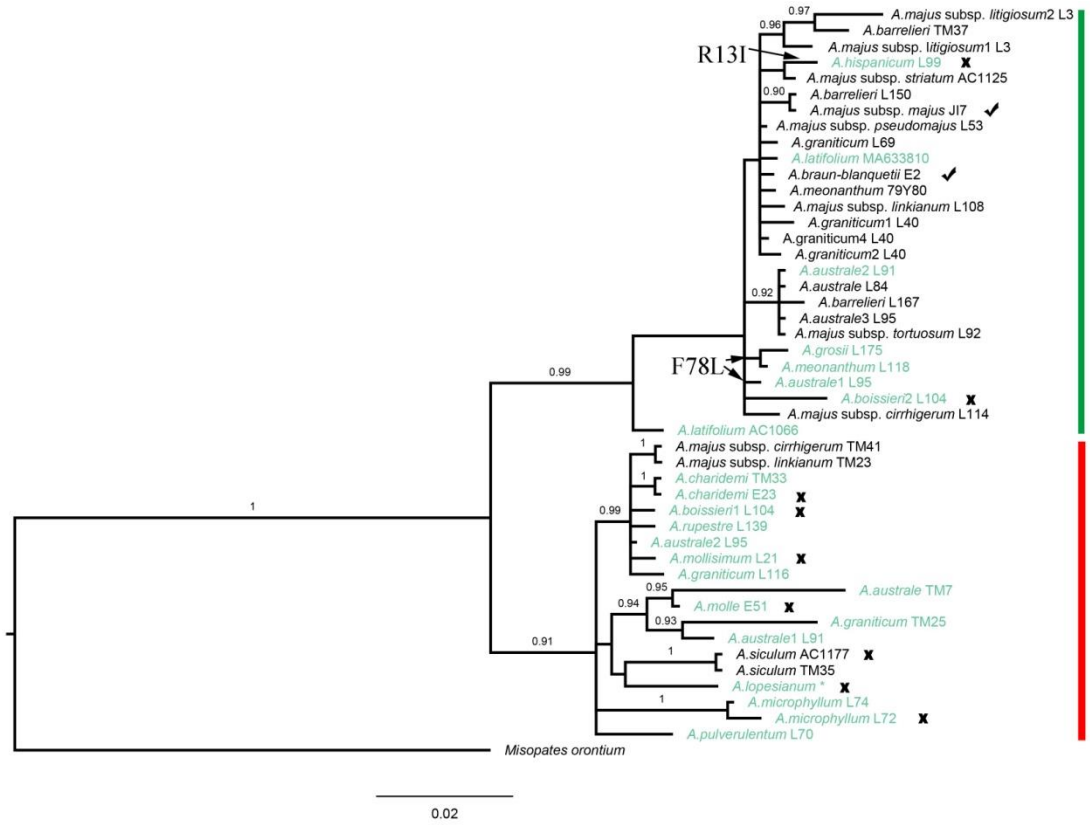

Figure 4.8. Bayesian analysis of *Antirrhinum Hairy* sequences

A Bayesian maximum clade credibility (MCC) tree is shown, with posterior probabilities ≥0.90 shown over the branches. Alleles isolated from the same accession are numbered and shown after the species name and followed by accession number. The Bayesian phylogeny is consisted of two clades: *Antirrhinum*-like (green bar) and *Kickxiella*-like (red bar). Alleles in the *Kickxiella*-like clade share a number of non-synonymous substitutions that responsible for the loss-of-function (Appendix 7.2, 7.3). Hairy species alleles placed in *Antirrhinum*-like clade has unique mutations or share some of the *Kickxiella*-like mutatations. Sequence analysis, allelism test and quantitative PCR result suggested that bald species carry functional alleles and hairy species have null alleles, with an exception of *A. siculum*. The phenotype of plants is represented by color: black, bald; green, hairy. Hairy expression in some species was tested. Expressed alleles were marked with check marks and non-expressed alleles were marked with cross marks.

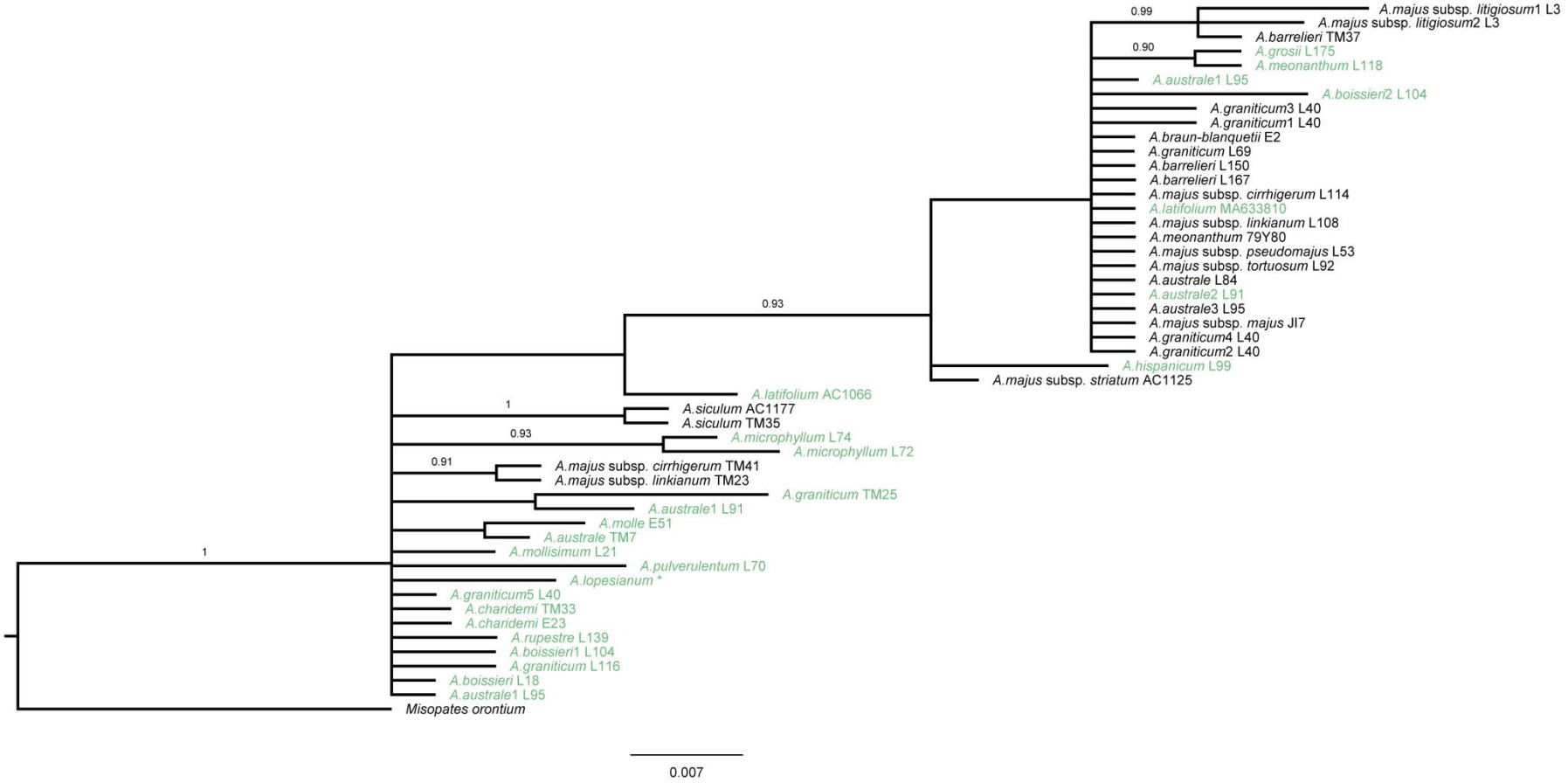

Figure 4.9. Bayesian phylogeny of *Antirrhinum* based on predicted GRX amino acid sequences

The tree was generated with Mr Bayes using *M. orontium* as outgroup. Posterior probability values over 0.9 are shown on branches. Sequences are labelled as in Fig. 4.8.

4.4.4 Hairy function in *Misopates orontium*

Part of the *M. orontium Hairy* (*MoHairy*) sequence was fused with *AmPDS* in pTRV2 to conduct virus-induced gene silencing experiments using *AmPDS* as reporter gene. *M. orontium* is a bald species with decreasing trichome density from the bottom to the top and is nearly bald in the internode beneath inflorescence (Fig 4.10a, b). Infection with the virus containing *AmPDS* and *MoHairy* caused photobleaching in *A. orontium* (Fig. 4.10c), presumably because the *AmPDS* sequence has enough similarity to *M. orontium PDS* to form double-stranded RNA and initiated VIGS. Higher vegetative internodes experiencing VIGS were able to produce dense trichomes on the bleached sites, revealing that *Hairy* orthologues of *Antirrhinum* and *Misopates* have conserved role in repressing trichome formation (Fig. 4.10d-f). Two types of trichomes, glandular and long eglandular, were produced ectopically, as at lower nodes of uninfected plants, suggesting that *MoHairy* does not underlie difference in trichome morphology in *M. orontium*.

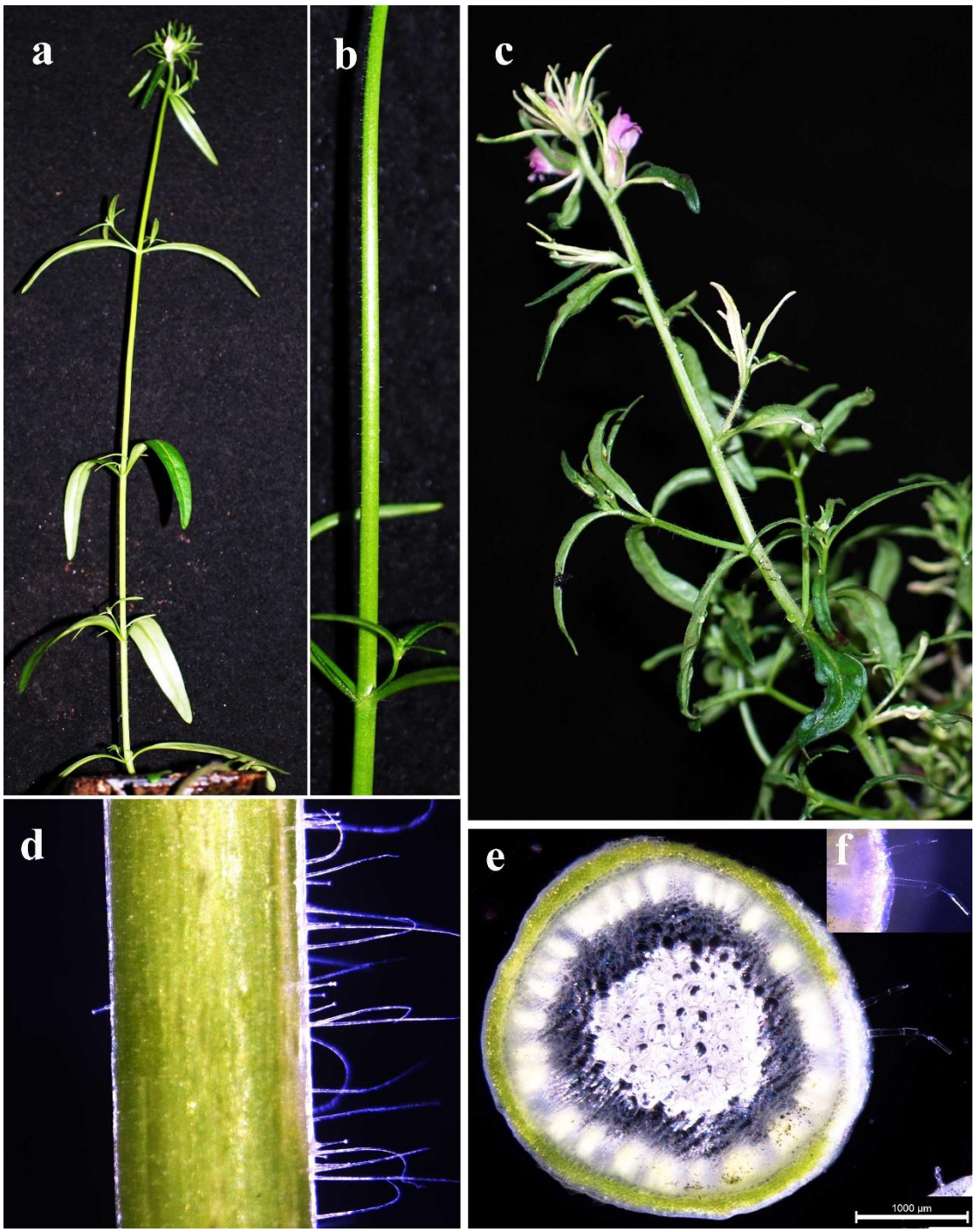

Figure 4.10. Phenotype of *MoHairy* silencing in *Misopates orontium*
M. orontium was infected with tobacco rattle virus carrying TRV::*MoHairy::AmPDS*. (a) An uninfected *M. orontium* plant showed a decreasing density of hairs from the bottom to top. (b) The higher internodes of uninfected plants were nearly glabrous, with a few scatterd trichomes. (c) Infected *M. orontium* plants showed bleached leaves, stem and inflorescence. (d,e) VIGS of *AmPDS* and *MoHairy* allowed more trichomes to form growing in the bleached area of stem. (f) Ectopic trichomes were formed from regions of the stem showing VIGS of *PDS*.

4.4.5 Phylogeny of GRX proteins

Hairy orthologues had been amplified from two members of the tribe Antirrhineae in addition to *Antirrhinum—C. origanifolium* and *M. orontium*. *M. orontium Hairy* was shown to be needed for repression of trichome development. This raised the questions of how the *Hairy* gene originated. This was also relevant to understanding when it acquired its trichome-repressing role, because other *GRX* genes are known to regulate a range of other processes, including defense.

Sequences similar to *AmHairy* were identified from *Antirrhinum majus*, *Mimulus guttatus*, *Solanum lycpersicum*, and *Arabidopsis thaliana* genomes by blast searching and from species in the family Orobanchaceae (*Lindenbergia philippensis*, *Orobanche aegyptiaca*, *Striga hermonthica* and *Triphysaria versicolor*). The majority of these sequences contain conserved active site motif of Cysteine-Cysteine-Methionine-Cysteine (CCMC). The rest of them have a Cysteine-Phenylalanine-Methionine-Cysteine (CFMC) motif. All belong to the CC-type GRXs, which normally possess CC(M/L)(C/S) active site motifs in *Arabidopsis* (Ziemann et al., 2009). It suggested Hairy and its close paralogues are CC-type GRXs even though their ative site motifs are Cysteine-Tyrosine-Lysine-Cysteine (CYLC). Predicted GRXs from *A. majus* were named after the scaffold number except for the *AmHairy* and *AmGRX2*. Bayesian analysis was conducted with alignment of translated amino acid sequence using JTT+G model of substitution. In the phylogeny, AmHairy was placed in a stongly-supported clade formed by Antirrhineae sequences (pp = 0.99), and this clade was sister to GRXs identified from *M. guttatus* (Fig. 4.11). Within this Antirrhineae clade, AmHairy clustered with MoHairy and CoHairy. MoHairy shares conserved function in repressing trichome initiation with AmHairy, supporting their orthology, though the function of CoHairy in trichome formation is still unknown. *Antirrhinum* GRXs at basal nodes of the clade seem unlikely to be involved in trichome development—expression of *AmGRX40* was not detected in shoots and *AmGRX2* was expressed in internal tissues and did not alter trichome development in VIGS experiments. The sequence relationships in this clade and the absence of members from other species suggests that duplication of an ancestral GRX predated

speciation of *Antirrhinum*, *Misopates* and *Chaenorhinum*, but came afer divergence of the Antirrhineae and the lineages leading to *Mimulus* and the Orobanchaceae, and that Hairy gained its trichome-repressing function within the Antirrhineae. The most similar *Arabidopsis* GRXs are ROXY1 (AtROX1) and ROXY2 (AtROX2), which are required for flower development in *Arabidopsis* (Xing & Zachgo, 2008). And their orthologous proteins in rice and basal land plant *Marchantia polymorpha* are also involed in reproductive organs formation (Wang et al., 2009, Gutsche et al., 2017). Most of the known glutaredoxins participate in stress response. AtROX1, AtROX2 and their orthologous proteins are the only ones shown to be responsible for fundamental development, though Hairy is a newly identified glutaredoxin with a similar role. GRX amino acid sequences alignments are listed in Appendix 7.3.

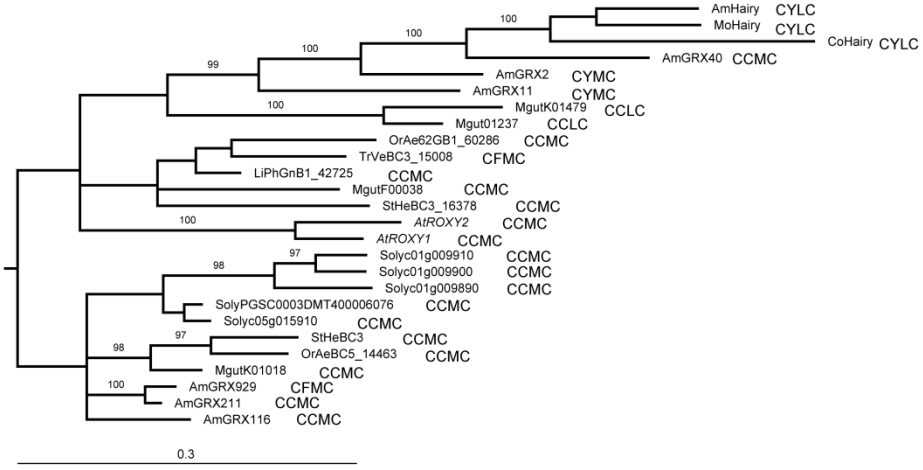

Figure 4.11. Bayesian phylogeny of GRX proteins
The most probably tree, made with Mr Bayes, is shown for an alignment of Hairy-like amino acid sequences from the genomes of the Asterids *Antirrhinum majus* (Am), *Mimulus guttatus* (Mgut), *Solanum lycopersicum* (Soly) and the Rosid *Arabidopsis thaliana* (At). Homologous sequences from transcriptomes of the Orobanchaceae species (*Lindenbergia philippensis* (LiPh), *Striga hermonthica* (StHe), *Orobanche aegyptiaca* (OrAe) and *Triphysaria versicolor* (TrVe) were also included. AmHairy and its orthologous were placed in the clade with CC-type GRXs. Active site motifs of GRX proteins are labelled. Posterior probabilities greater than 0.9 are shown above internal branches.

4.6 Possible substrates of AmHairy

GRXs are small oxidoreductases of the thioredoxin family, and they share a conserved Cystein-X-X-Cystein (CXXC) motif, where X is any amino acid, at their

active site. Their redox activity is based on a dithiol exchange mechanism. The N-terminal cysteine residue of the CXXC motif initiates a nucleophilic attack on a disulfide target in the substrate, resulting in the formation of a mixed disulfide (GRX disulfide-bonded to its substrate). The intermolecular disulfide bond is subsequently cleaved by the C-terminal cysteine residue of the active site, yielding reduced substrate and the oxidized GRX with its cysteine residues disulfide-bonded (Holmgren, 1989, Prinz et al., 1997, Gutsche et al., 2015). The substitution of the C-terminal cysteine with serine can prevent resolution of the disulfide bond between GRX and its substrate. This had been exploited as a method to isolate potential substrates of GRXs (Rouhier et al., 2005).

One explanation for the role of Hairy in repressing trichome formation is that it modifies the activity of substrate proteins that control trichome formation—either activating a trichome repressor, or to de-activating a protein that promotes trichome development. A yeast two hybrid screen was used to identify potential substrates of AmHairy and of its paralogue AmGRX2, using the serine substitution at the C-terminal cysteine to stabilize the interactions.

4.6.1 Yeast two-hybrid Screening

To identify proteins that interact with AmHairy, the C35S substitution at the active site was introduced by site-directed mutagenesis and the *AmHairy*^{C35S} coding sequence fused to the GAL4 DNA-binding domain. The resulting bait plasmid was introduced into yeast and used in mating with a yeast library expressing cDNAs, made from the mRNA of *A. majus* subsp. *majus* whole plants, fused to the GAL4 activation domain. The screen was problematic, because AmHairy^{C35S} appeared to interact with the product of a strongly expressed ATPase subunit gene, giving a high frequency of false-positives. After eliminating prey clones carrying the ATPase sequences, three additional genes were identified as encoding proteins that interated with AmHairy^{C35S}. Two encoded TGA transcription factors, *TGA1* in Scaffold 18 and *TGA2* in Scaffold 202, and one in Scaffold 95 encoded a class IV homeodomain-leucine zipper (HD-Zip IV) transcription factor similar to GLABROUS11 (GL11) of *Arabidopsis*, *GL11*. Each was represented by one

positive clone, and it is unlikely that the screen detected all cDNAs encoding potential interacting proteins.

Although was no evidence that *AmGRX2* is involved in trichome formation in *Antirrhinum*, and it does nto appear to be expressed in the same cells as AmHairy, it might be capable of interacting with the same substrates as AmHairy. To test this possibility, baits consisting of $AmHairy^{C35S}$ or $AmGRX2^{C31S}$ in pGBKT7 or empty pGBKT7, were tested with preys carrying *AmTGA1*, *AmTGA2* or *AmGL11* by co-transforamtion of yeast. All co-transformants grew on medium lacking leucine and tryptophan, which selectes for bait and prey plasmids (Fig. 4.12). On mediu also lacking adenine and histidine, which select for protein interaction, yeast with empty pGBKT7 as bait did not grow. However, other combinations of baits and preys grew well and colonies turned blue on media with X-α-Gal (which provides a third marker for interaction), suggesting that both AmHairy and AmGRX2 could interact with AmTGA1, AmTGA2 and AmGL11.

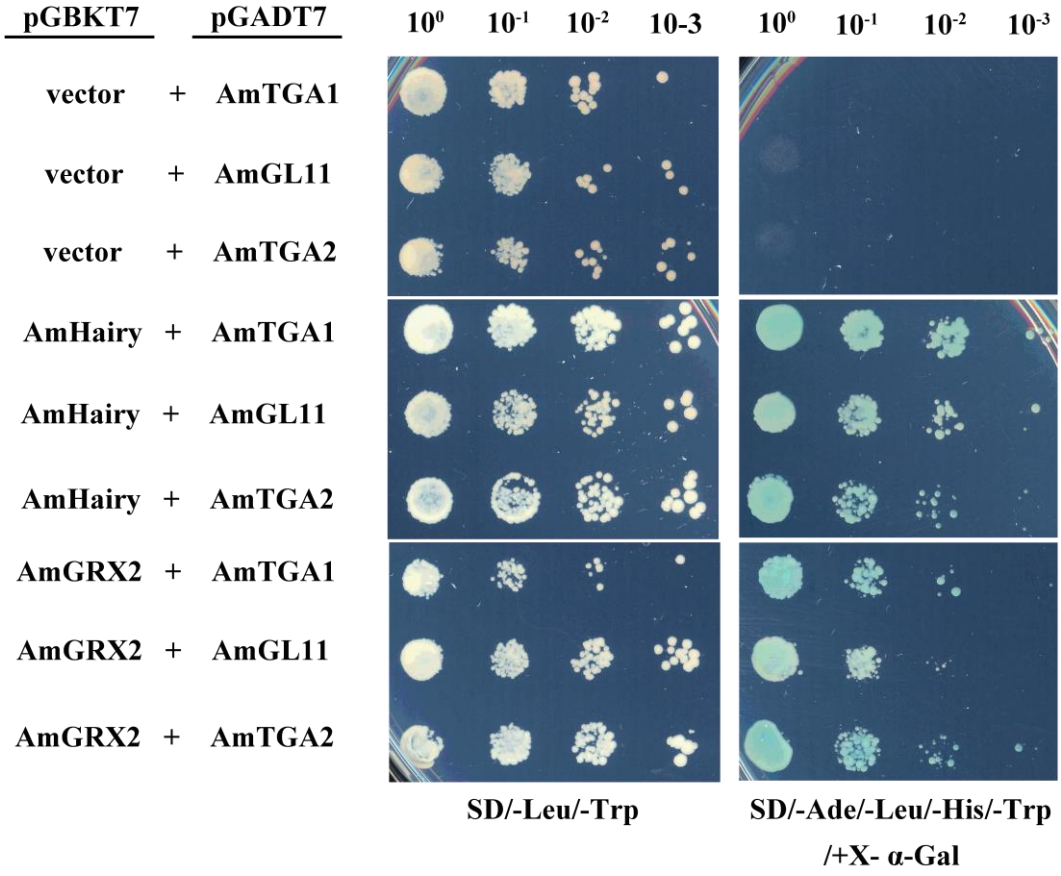

Figure 4.12. Identification of possible substrates of AmHairy and AmGRX2 by a yeast two-hybrid assay
Three possible targets of AmHairy (AmTGA1, AmTGA2, AmGL11) were tested in two-hybrid analysis for interaction AmHairy and its most similar, expressed paralogue AmGRX2. Three baits in pGRBKT7 -- *AmHairy*^{C35S}, *AmGRX2*^{C31S} or empty pGBKT7 (negative control), and three preys in pGADT7 -- *AmTGA1*, *AmTGA2*, *AmGL11*, were co-transformed into strain Y2HGold. Co-transformants were serially diluted and grown on selective medium containing standard-dropout medium without leucine or tryptophan (SD/-Leu/-Trp) to select for bait and prey plasmids and medium also lacking adenine and histidine but containing X-α-Gal (SD/-Ade/-His/-Leu/-Trp/+X-α-Gal) to test for protein interaction. All bait and prey combinations grew well and turned blue when selected for interaction, suggesting that both AmHairy and AmGRX2 could interact with AmTGA1, AmTGA2 and AmGL11.

4.6.2 Expression patterns and roles in trichome formation of possible substrate genes

One paralogue of *AmTGA2*, *AmTGA27* in Scaffold27, was included in this study, because RNA-seq suggested that it was expressed in vegetative shoot tips and it was possible that it shared the sequences needed for interaction with AmHairy or AmGRX2. The expression of *AmTGA1*, *AmTGA2*, *AmTGA27* and *AmGL11* was first investigated further by quantitative PCR. For all genes, expression was seen at

all stages of shoot development. No significantly differences in expression could be found between the same developmental stage of the bald NILs and the hairy NILs, suggesting that none of the genes was expressed only in trichomes and that expression of their RNA was not regulated by Hairy. *AmTGA1* expression was higher in young seedlings compared to other stages (Fig. 4.13a). *AmTGA2* and *AmTGA27* were detected expressing at similar level in three developmental stages (Figure 4.13b, c) while the expression of *AmGL11* was detected higher in later vegetative apices (Fig. 4.13d).

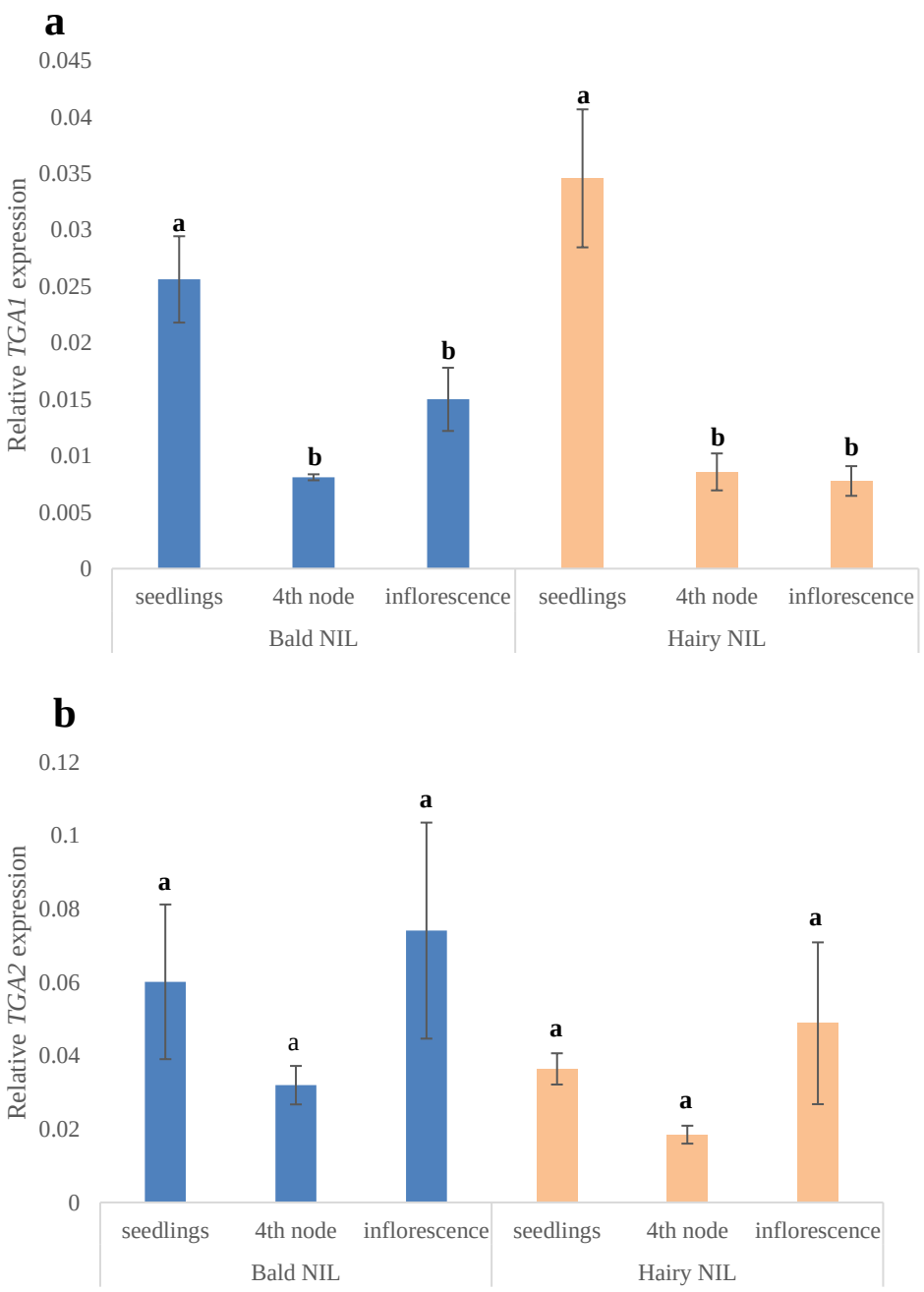

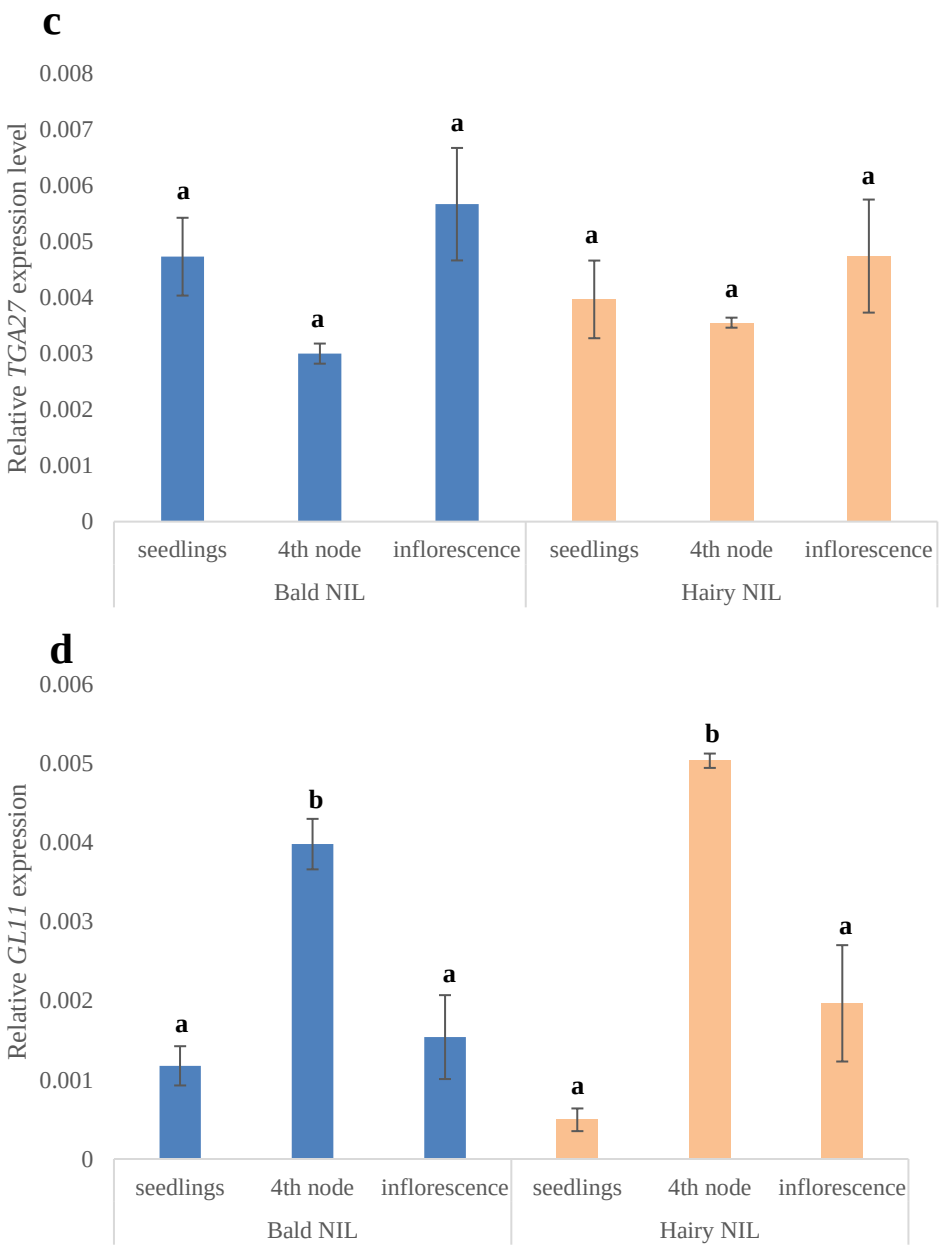

Figure 4.13. Expression of genes encoding potential substrates of Hairy in bald and hairy NILs
RNA expression is shown for *AmTGA1* (a), *TGA2* (b), *TGA27* (c) and *GL11* (d) at three developmental stages in bald and hairy NILs. Data are displayed as the ratio of expression to *Ubiquitin*, given as mean ± SE (n=3 biological replicates). Bars with different letters are significantly different from each other at $p \leq 0.05$ by one-way ANOVA.

The RNA expression of *AmTGA1*, *AmTGA27* and *AmGL11* was then investigated by *in situ* hybridization. Sequences of them were acquired from RNA-seq data of NILs (RNA prepared from shoot apices when the 6th leaves were 5 mm long). The same sequences were used as probes and conduct VIGS. All these three genes showed similar spatial pattern in all lateral organs types. Their expression was

detected in newly initiated leaves or floral meristem. It became mainly restricted to the abaxial mesophyll of older leaves or sepal primordia (Fig. 4.14a). The signal could also be detected from adaxial mesophyll of leaf primordia, but much weaker than in the abaxial side. This pattern was strikingly similar to the expression pattern of *AmGRX2* and markedly different to *AmHairy*—none of the potential substrates showed strong expression in the epidermis. Because the products of three of these genes also interact with AmGRX2 in the yeast two-hybrid assay, there is a possibility that they are involved in the same process as AmGRX2, rather than Hairy.

To test the functions of the substrate genes further, *AmTGA1*, *AmTGA2*, *AmTGA27*, and *AmGL11* sequences were cloned into TRV2 with *AmPDS* sequence as a reporter for VIGS and used to infect bald and hairy NILs. None of the infected hairy NILs showed any phenotype change, except for bleaching and reduced growth, which can be explained by *PDS* silencing and virus infection. However, some bald plants inoculated with TRV carrying *AmTGA27* (three out of 10 infected plants) or *AmGL11* (three plants out of 10 infected plants) initiated trichomes from bleached tissue in the third internode—the position where bald NILs usually became glabrous (Fig. 4.14b). Because *AmPDS* does not affect trichome formation, this suggests that *AmTGA27* and *AmGL11* might be needed for trichome repression—consistent with Hairy acting to promote their repressive activity. However, these observations need to be treated with caution because effects on RNA expression of the target genes and their paralogues were not tested to confirm that VIGS was effective and specific.

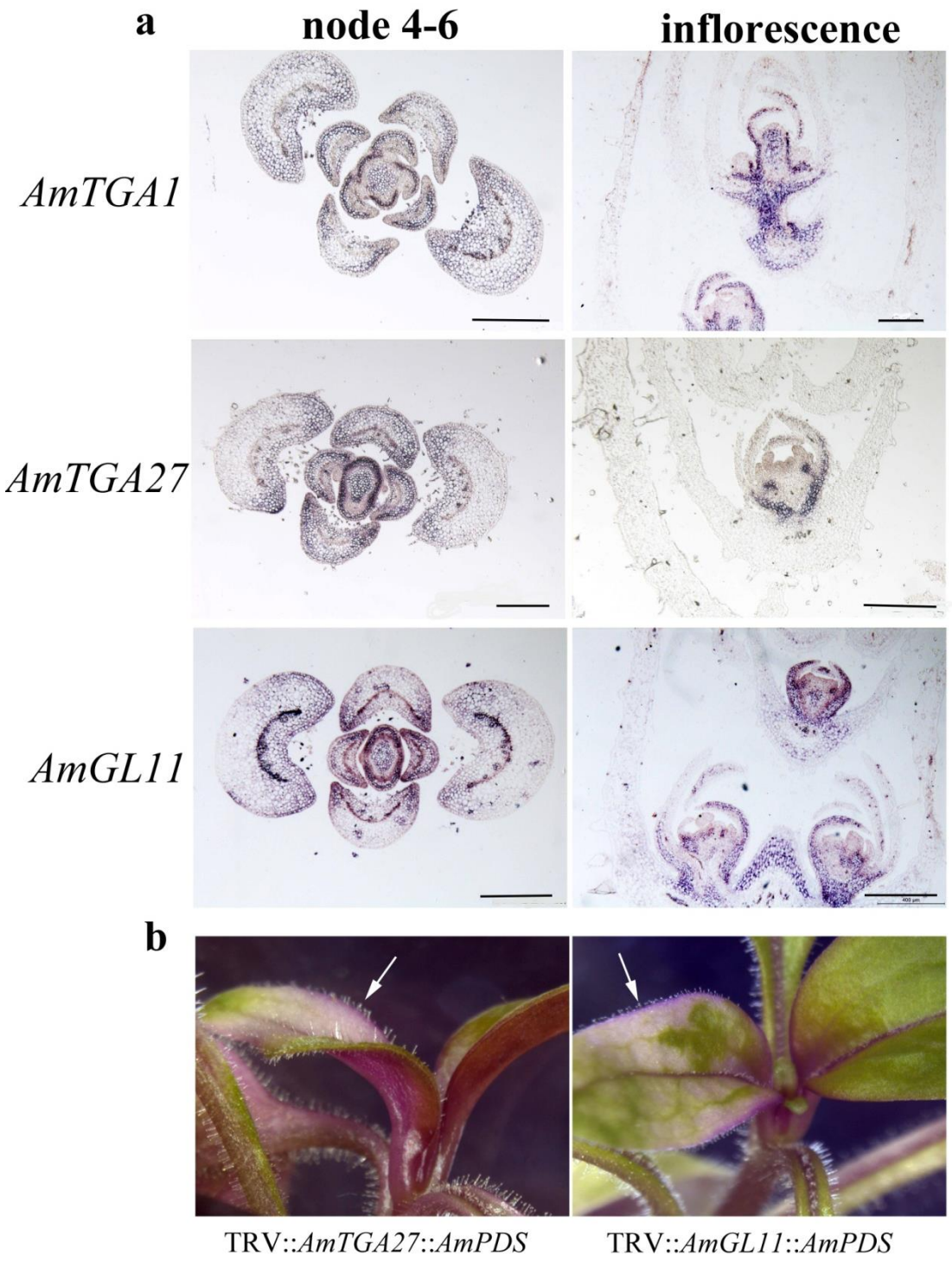

Figure 4.14. Expression pattern and VIGS of three potential target genes
(a) *In situ* hybridization with probes for *AmTGA1*, *AmTGA27* and *AmGL11*. Samples were collected from vegetative apices where the leaves at node 4 were 5 mm long and sectioned transversely. Inflorescence apices were sectioned longitudinally. Photos showed here were from bald NILs, except for *AmTGA27*, which was from a hairy NIL. Scale bars are 400 µm. (b) Phenotypes of bald NILs infected with TRV carrying *PDS* and either *TGA27* or *AmGL11* sequences**.** Arrows indicate the bleached leaf which was hairy, while the green leaf of the same node was bald.

4.7 Conclusion

GRX1 is the *Hairy* gene prohibiting trichome development in the higher vegetative parts of bald plants. It was strongly supported with the evidence that TRV virus carrying *AmGRX1* reduced *AmGRX1* expression and restored trichome growth in the higher vegetative parts of bald NILs, which are free of trichome except for the adaxial midrib. The NILs were generated by introducing regions of the genome of *A. charidemi* (hairy, subsection *Kickxiella*) into the genetic background of *A. majus* subsp. *majus* (bald, subsection *Antirrhinum*). h^c is a null allele, while expression of *AmHairy* is restricted to the epidermis of bald vegetative internodes and leaves. Expression of *AmHairy* is very low or undectable in the epidermal cells of adaxial midrib, which could explain the presence of type I trichomes on adaxial midrib of bald leaves. The hairy NILs (genotype h^c/h^c) possess type III trichomes, which is the type of trichomes *A. majus* subsp. *majus* has. Silence of *AmHairy* allowed type III trichomes rather than type V trichomes (distributed at the higher vegetative parts and in the inflorescencs of *A. charidemi*) to grow in the virus infected bald tissue. It suggests that the *Hairy* gene is required to repress trichome formation, but does not determine for trichome morphology.

In *Antirrhinum*, *Hairy* is responsible for the variation of trichome distribution, except for *A. siculum*, which has a bald phenotype. Allelism test and RNA expression suggested *A. siculum* has inactive alleles which are similar in sequence to the ones most hairy species have. Therefore, a second gene might be required to repress the trichome growth in *A. siculum*. Hairy species have recessive *hairy* alleles which are not expressed. Most of the hairy species have *hairy* alleles that possess *Kickxiella*-like SNPs that might result in loss-of-fucntion mutations. *A. linkianum* plants from some accessions, which are bald, also possess *Kickxiella*-like alleles. They are possibly in the same situation as *A. siculum*. I do not have evidence to support this idea, because they were not living plants and I cannot conduct allelsim test on them. The majority of bald species have alleles similar to H^m (*Antirrhinum*-like alleles). However, some hairy species also possess *Antirrhinum*-like alleles, non-synonymous mutations and mutations in other region may cause the loss-of-function. The phylogeny of Hairy nucleotide sequences

suggests bald is the ancestral state in *Antirrhinum* and independent mutations resulted in the inactivity of *hairy*, implying that hairy species have evolved the hairy phenotype independently possibly to adapt to similar habitats.

Silence of *MoHairy* resulted in ectopic trichome growth in *M. orontium*, implying that *Hairy* orthologues of *Antirrhium* and *Misopates* have conserved roles in repressing trichome formation. A phylogeny of GRX proteins suggests that duplicaton of an ancestral GRX predated speciation of Antirrhineae species, and the Hairy gained its trichome-repressing function within the tribe.

The paralogue of *AmHairy*, *AmGRX2*, is expressed in all phases and mainly in internal cells of organs. There is no evidence supporting its involvement in hair development. Two TGA transcription factors, AmTGA1 and AmTGA2, and a HD-Zip IV transcription factor AmGL11, were identified as potential substrates of AmHairy, and they are also able to interact with AmGRX2. Surprisingly, *AmTGA1*, *AmTGA27* (a paralogue of *AmTGA2*) and *AmGL11* all have similar expression patterns to *AmGRX2*. Ectopic trichomes grew in some bald plants inoculated with TRV carrying *AmTGA27* or *AmGL11*, suggesting that they may act redundantly in repressing trichome growth. However, there is no data to support that reduction of their expression in the infected plants.

Chapter 5

5 Discussions

In this study, *Hairy* was identified as a repressor of trichome development in *Antirrhinum*. *Hairy* encodes a glutaredoxin, and is only expressed in the epidermis of bald internodes and leaves. The trichome-suppressing role of Hairy appears to have evolved relatively late in the history of the Lamiales and sequencing and expression studies suggest that multiple loss-of-fuction mutations have been involved in parallel evolution of the hairy phenotype in *Antirrhinum*. Potential substrates of Hairy, which include TGA and HD-Zip transcription factors and might play roles in trichome regulation, were identified in a yeast two-hybrid screen. The function and evolution of *Hairy* are discussed further here.

5.1 The function of the *Hairy* gene

Comparison of bald and hairy phenotypes suggests that *Hairy* suppresses trichome formation only in the middle parts of the plant. This is consistent with the expression of *Hairy* RNA being confined to this region. This raises the question of how *Hairy* expression is restricted to this phase of development. Recent studies reported that many GRX genes exhibited tissue-/developmental stage-specific expression patterns (Li et al., 2009, Garg et al., 2010). Plant hormones play a vital role during the different life cycle stages and consequently affecting hormone biosynthesis or signaling pathways alters plant morphology and development (Estelle & Somerville, 1987, Poethig, 1990). *Hairy* may have a role in affecting hormone signaling, therefore regulating the phase. However, no significant flowering time difference has been observed between bald NILs and hairy NILs. And leaves of hairy NILs above the fifth node till the first bract (the position where *Hairy* expresses in bald NILs) were bigger than those of bald NILs in terms of leaf area (internal data). It is possible the pleiotropic effect of *Hairy*, affecting hormone or other signaling to surpress leaf growth.

In *Arabidopsis*, genes and microRNAs (miRNAs) which regulate developmental

phase change, also play important roles in regulating the distribution of trichome pattern (Shikata et al., 2009, Wu et al., 2009, Huijser & Schmid, 2011). In *A. thaliana*, trichomes are distributed only on the adaxial side of early rosette leaves and on both sides of later vegetative leaves (Telfer et al., 1997). After entering into the reproductive stage, the number of trichomes is gradually reduced along the inflorescence stem. Development of the plant is accompanied by an increase in abundance of miR156, which targets *SQUAMOSA PROMOTER BINDINGPROTEIN-LIKE* (*SPL*) genes (Schwarz et al., 2008, Wu et al., 2009, Huijser & Schmid, 2011). *SPLs* regulate different aspects of developmental phase change and flowering, including repression of trichome formation on the inflorescence through activation of *TCL1* and *TRY* (Yu et al., 2010). *TCL1* and *TRY* have been proved to be negative regulator of trichome formation (Kirik et al., 2004a, Kirik et al., 2004b, Wang et al., 2007). Reduced activity of SPLs, some of which promote expression of a second miRNA (miR171), results in a reduction in miR171 levels as plants develop (Wu et al., 2009, Huijser & Schmid, 2011). A group of GRAS family members, LOST MERISTEMS (LOM), which are targeted by miR171, promote trichome formation through modulating the *SPL* activity by direct protein-protein interaction. Overexpression of miR171 reduced LOM activity and led to decreased trichome density in the inflorescence (Xue et al., 2014).

The phase-related development of trichomes in *Antirrhinum* is similar, but more complicated than in *Arabidopsis.* In bald *Antirrhinum* species, the lower stem and leaves show a decreasing trichome number from the bottom to the second node. However, unlike *Arabidopsis*, trichomes are restored with increasing density on the inflorescence of bald *Antirrhinum* plants. The expression of the *Hairy* gene, which is restricted to later vegetative development, appears to be related to this phase change. However, *Hairy* does not affect other phase change phenotypes, such as flowering; therefore it is unlikely to have a primary role in the process and is more likely to be regulated by it. Because the sequence and role of miR156 is conserved among flowering plants (Wang et al., 2009), *Hairy* could be directly regulated by it. However, *Hairy* RNA did not contain obvious miR156 binding sites, so this seems unlikely.

The possible advantage of restricting trichome development to some parts of the plant is discussed further below (Section 5.2).

Hairy expression is also limited to epidermal cells, consistent with a cell-autonomous role in repressing trichome development. In *Arabidopsis*, paralogous HD-Zip IV genes, *ARABIDOPSIS THALIANA MERISTEM LAYER1* (*ATML1*) and *PROTODERMAL FACTOR2* (*PDF2*) are expressed only in the epidermis and required to regulate epidermal cell differentiation. They activate expression of other genes and themselves by binding to an L1 promoter motif, which is responsible for L1 layer-specific gene expression (Abe et al., 2001, Abe et al., 2003). Related transcription factors might control expression of *Hairy* in *Antirrhinum* and the presence of an L1 motif could be tested after identification of the *Hairy* promoter.

Crosses of NILs to other species suggested that *Hairy* can repress development of different trichome types in *Antirrhinum*. This raised the question of whether all types of *Antirrhinum* trichome share a common developmental mechanism that can be affected by *Hairy*.

Hairy does not appear to affect development of trichomes in lower leaves and the stem, on the adaxial midrib or in the inflorescence. However, this can be explained by its restricted domain of expression in later blades and stem, rather than *Hairy* being unable to repress trichomes in other parts of the plants. Ectopic expression of *Hairy* in transgenic plants could be used to test whether Hairy can repress development of trichomes in other positions.

However, *A. siculum* provides evidence that development of trichomes with similar morphologies might involve different mechanisms. *A. siculum* appears to carry recessive *hairy* alleles, supported by sequence and lack of expression, and by allelism crosses. However, *A. siculum* has a bald phenotype. This can be explained by a loss-of-function mutation in a second gene (*Bald*) that is needed for trichome formation only in higher vegetative parts of the plant. *A. siculum* also has

fewer trichomes on the peduncle and pedicel of its inflorescence compared to other species (Appendix 8), suggesting that *Bald* might also promote formation of these trichomes. In contrast, the lower internodes and leaves of *A. siculum* are hairy like other species, suggesting that trichome development here is not dependent on the *Bald* gene. Similarly, flower trichomes are produced normally in *A. siculum*, suggesting that they are also not regulated by *Bald*. This suggests that trichomes with similar morphologies are different because some (in the lower parts of the plant, the adaxial midrib and the inflorescence) do not need *Bald*, while the rest do. Identification of the *Bald* gene or genes and investigation of its expression and dominance of its alleles will allow this to be tested further.

Hairy encodes a member of the glutaredoxin (GRX) family: small oxidoreductases that transfer electrons from glutathione to oxidized cysteine redidue in the active motif (Holmgren, 1989). All *Antirrhinum* Hairy-like proteins have the active site CYLC motif, therefore they have the potential ability to function in redox regulation of other proteins. Plant GRXs have known role in defense and stress responses and in development (Gutsche et al., 2015). The most similar *Arabidopsis* GRXs to Hairy are the paralogous ROXY1 (ROX1) and ROX2 proteins, involved in flower development (Xing & Zachgo, 2008).

Yeast two hybrid screens identified two TGA transcription factor, AmTGA1 and AmTGA2, and a HD-ZIP IV protein, AmGL11 that were able to interact with AmHairy or AmGRX2. Hairy and GRX2 can be classified as CC-type Glutaredoxins (GRXs) specific to land plant. Previous studies showed that plant CC-type GRXs can interact with basic leucine-zipper (bZIP) transcription of TGACG (TGA) motif-binding family. In *Arabidopsis*, ROX1 and ROX2, which are required for flower development, interact in the nucleus with the TGA transcription factor PERIANTHIA (PAN) to promote petal development (Li et al., 2009), or with TGA9 and TGA10 to regulate anther development (Murmu et al., 2010). Similarly, ROX1 and ROX2 in *Marchantia polymorpha* are able to interact with MpTGA. All the interactions of ROXs with TGAs are through conserved motifs at their C-termini (LxxL/xL and ALWL motifs) (Li et al., 2011, Gutsche et al.,

2015, Gutsche et al., 2017). Functional *Hairy* alleles in *Antirrhinum* plants encode a conserved C-terminus with LxPxL and ALWL motifs, the latter are identical in all tested samples, though the LxxL/xL motif, which encodes an α helix, varied between *Antirrhinum* accessions. All accessions had the sequence LVPLL, with the exceptions of LDPLL in *A. litigiosum* L3, LVPVL in *A. linkianum* TM23 and *A. cirrhigerum* TM41. The alleles from bald plants appear to be active (except in *A. siculum*), therefore, conservation of these conserved motifs is consistent with a requirement for interaction with TGA substrates.

The conserved C-terminus together with the phylogenetic analysis support that Hairy belongs to CC-type GRXs, even though the active site of it is CYLC rather than CC(M/L)(C/S) motifs. All the *Arabidopsis* CC-type GRXs have CC(M/L)(C/S) active site motifs. The first N-terminal cysteine, which is required for both protein disulfide reduction and reduction of mixed protein-glutathione disulfides (Bushweller et al., 1992), is strictly conserved in known CC-type GRXs. The second N-terminal cysteine could also be replaced by G/F/Y/P in other known CC-type GRXs (Xing et al., 2006, Xing & Zachgo, 200 8). Mutagenesis of the second cysteine into a serine in the AmROXY1 protein did not affect the function of AmROXY1 severely, and it was still able to complement the *roxy1* mutant (Wang et al., 2009), suggesting that the second cysteine may not contribute to the catalytic activity.

Specific interactions between GRXs and HD-Zip IV transcription factors have not been reported. However, members of the HD-Zip IV family are known to affect trichome development in *Arabidopsis*, cotton, *Artemesia annua* and maize. Their expression is usually confined to the epidermal cell layer of plant organs (Szymanski et al., 1998, Vernoud et al., 2009, Walford et al., 2012, Yan et al., 2017), so their role in trichomes might be related to epidermal cell identity, and therefore the location of trichome development, rather than in direct control of trichome identify. However, the expression of *AmGL11* did not appear to be restricted to the epidermis, and VIGs experiment with *AmGL11* did affect trichome formation, so any involvement of *AmGL11* in *Antirrhinum* trichome development is currently unclear. One possibility

is that the interaction between Hairy or AmGRX2 and GL11 which was detected in yeast two-hybrid does not occur in plants. Instead, Hairy might interact with another HD-Zip IV family member that shared the interaction domain and is expressed in the epidermis and involved in trichome development. Candidates could be identified by testing interaction of Hairy with other HD-Zip IV family members and by examining their patterns of expression.

In VIGS experiments, infection with TRV carrying *AmTGA27*, a paralogue of *AmTGA2*, allowed ectopic trichome formation in some leaves. A similar effect was seen with TRV carrying *AmGL11* sequence. Although only a small number of inoculated plants showed ectopic trichomes, and they were restricted to the first leaves that would normally be bald, it provides some evidence that these sequences are required as repressors of trichome development. One possibility is that the *AmTGA27* and *AmGL11* sequences in TRV had enough similarity to trigger silencing of other *TGA* or *HD-Zip* family members. This could be tested by examining the effects of infection on expression of all family members. It seems unlikely that *AmTGA27* and *AmGL11* are involved specifically in trichome formation—their expression was detected at all developmental stages and mainly in internal cells, especially the adaxial mesophyll. For them to function as substrates of Hairy needed for trichome repression their RNA or protein products would have to move to the epidermis, or *Hairy* would have move internally to modify them.

5.2 Evolution of the *Hairy* gene

Phylogenetic reconstruction of the Hairy-like GRXs combined expression analysis and VIGS in *Misopates* suggested that Hairy's trichome-repressing role evolved relatively late in the history of angiosperm, within the Lamiales after divergence of the lineages leading to *Mimulus* and the tribe Antirrhineae. This suggests that the bald phenotype in the Antirrhineae is a derived character. If the broader expression pattern of its paralogue *AmGRX2* was the ancestral, one possibility is that the new function of Hairy resulted from a change in its domain of expression to the epidermis. Here the Hairy GRX might have been able to modify transcription factors, such as

TGA and HD-Zip IV family members.

Within *Antirrhinum*, phylogentic reconstruction places alleles into two main clades—one comprising inactive alleles mainly from hairy species in subsection *Kickxiella*, the other mainly functional alleles from subsection *Antirrhinum*. Using *M. orontium* (which is bald) as outgroup suggested that baldness is the ancestral state in *Antirrhinum* and that a single mutation at the base of the Kickxiella clade could have given rise to the hariy phenotype. However, this interpretation might depend on choice of outgroup, because other members of the tribe Antirrhineae have a hairy phenotype. In previous research, *Antirrhinum* was placed in the *Antirrhinum* group of the tribe Antirrhineae, which includes New World genera (*Sairocarpus*, *Mohavea*, *Neogaerrhinum*) and Old World genera (*Acanthorrhinum*, *Antirrhinum* and *Misopates*) and is sister to the *Chaenohinum* group, which includes genera *Albraunia*, *Chaenorhinum* and *Holzeria* (Ogutcen & Vamosi, 2016). Within the *Antirrhinum* group, the geneus *Antirrhinum* was sister to New World genera, and genera *Acanthorrhinum* and *Misopates* were at the base of this lineage based on phylogenetic analysis of morphological data and nuclear and plastid DNA sequences (Vargas et al., 2004, Guzmán et al., 2015, Ogutcen & Vamosi, 2016), suggesting that *Antirrhinum*, New World genera, *Acanthorrhinum* and *Misopates* are a monophyletic group. *Acanthorrhinum* and *Misopates* species are recorded as glabous except for hairs in the inflorescence or stem bases (Sutton, 1988), suggesting these species have a bald phenotype. Therefore, the simplest explanation is that baldness is the ancestral trait in *Antirrhinum* group, which is consistent with phylogenetic reconstruction of *Hairy*-like sequences. Multiple loss-of-function mutations in some lineages would then have given rise to taxa with hairy phenotypes, possibly as an adaption to the Mediterranean climate.

The New World genera in the *Antirrhinum* group appear to have undergone whole-genome duplication and are likely the result of long-distance dispersals of an Old World ancestor (Thompson, 1988, Ogutcen & Vamosi, 2016). New World species differ in their distribution phenotypes, as do *Antirrhinum* species (*Sairocarpus* can be bald or hairy; *Mohavea* is hairy; *Neogaerrhinum* is bald) (Sutton,

1988). It suggests that New World species may have both active and inactive *Hairy* alleles as the result of independent loss-of-function mutations. Sampling these species would give a better understanding of trichome distribution and of the evolution of *Hairy*.

Different from trichomes of upper nodes and inflorescence, the trichome morphology of lower nodes is consistent in every sample we have tested. Very dense mixed glandular and eglandular trichomes (type III and V) occur on the basal part of the stems and lower leaves (from the base to the second node) suggesting that trichome morphology and density of lower nodes are not affected by the *Hairy* gene. These trichomes are formed during seedling stage or even earlier. In most case, young plants have higher trichome density to mature plants (Manetas et al., 1998, Pérez-Estrada et al., 2000). The presence of trichomes on early tissues is probably an ancient characteristic, protecting juvenile plants from UV radiation, drought, and herbivore. Therefore, trichome growth in early tissue possibly could be explained by the same mechanism in different families. Very dense trichomes are distributed on the inflorescence of all *Antirrhinum* species, with the exception of *A. siculum*. Inflorescence trichomes may act as physical barriers to protect flowers and developing fruits from biotic or abiotic stress and secrete some products like essential oil to attract pollinators. *A. siculum* is mainly distributed in Sicily, and is geographically isolated from other species (Rothmaler, 1956, Wilson & Hudson, 2011). There is a possibility that an independent mutation inactivated *A. siculum bald* gene, resulting in the loss of hairs in the higher vegetative parts and inflorescence, to adapt the environment of Sicily. Due to the geographical isolaton to other species, other species did not gain this mutation by hybridization.

Within the genus, neither bald species nor hairy species is monophyletic group in any published phylogeny. This raised the question that whether the variation in trichome distribution could be adaptive in *Antirrhinum*. All the *Kickxiella* species have hairy phenotype, and they are small plants growing on dry rock-faces and walls. Therefore, it could be explained as an ancestral character that has been retained without selection. However, hairy plants in subsection *Antirrhinum* are tall.

Species tend to evolve similar characters independently as adaptations to a particular environment (Wilson & Hudson, 2011). There is a possibility that hairy species from two subsections have evolved the hairy phenotype independently under certain conditions that hairiness can be advantageous. The recombinant alleles also suggest that some subsection *Antirrhinum* species gained hairy phenotype after hybridization with *subsection* Kickxiella.

References

Abascal F, Zardoya R, Posada D. 2005. ProtTest: selection of best-fit models of protein evolution. *Bioinformatics* 21: 2104-2105.

Abe M, Katsumata H, Komeda Y, Takahashi T. 2003. Regulation of shoot epidermal cell differentiation by a pair of homeodomain proteins in *Arabidopsis*. *Development* 130: 635-643.

Abe M, Takahashi T, Komeda Y. 2001. Identification of a cis-regulatory element for L1 layer-specific gene expression, which is targeted by an L1-specific homeodomain protein. *The Plant Journal* 26: 487-494.

Ariel FD, Manavella PA, Dezar CA, Chan RL. 2007. The true story of the HD-Zip family. *Trends in Plant Science* 12: 419-426.

Bedon F, Ziolkowski L, Walford SA, Dennis ES, Llewellyn DJ. 2014. Members of the MYBMIXTA-like transcription factors may orchestrate the initiation of fiber development in cotton seeds. *Frontiers in Plant Science* 5:

Beilstein MA, Al-Shehbaz IA, Kellogg EA. 2006. Brassicaceae phylogeny and trichome evolution. *American Journal of Botany* 93: 607-619.

Buchmann SL. 1987. The ecology of oil flowers and their bees. *Annual Review of Ecology and Systematics* 343-369.

Bushweller JH, Aaslund F, Wuethrich K, Holmgren A. 1992. Structural and functional characterization of the mutant *Escherichia coli* glutaredoxin (C14. fwdarw. S) and its mixed disulfide with glutathione. *Biochemistry* 31: 9288-9293.

Chen C, Yin S, Liu X, Liu B, Yang S, Xue S, Cai Y, Black K, Liu H, Dong M, Zhang Y, Zhao B, Ren H. 2016. The WD-Repeat Protein CsTTG1 Regulates Fruit Wart Formation through Interaction with the Homeodomain-Leucine Zipper I Protein Mict. *Plant physiology* 171: 1156-1168.

Costa MMR, Yang S, Critchley J, Feng X, Wilson Y, Langlade N, Copsey L, Hudson A. 2012. The genetic basis for natural variation in heteroblasty in *Antirrhinum*. *New Phytologist* 196: 1251-1259.

Dalin P, Ågren J, Björkman C, Huttunen P, Kärkkäinen K. 2008. Leaf trichome formation and plant resistance to herbivory. In: ed. *Induced plant resistance to herbivory* 89-105. Springer.

Darriba D, Taboada GL, Doallo R, Posada D. 2012. jModelTest 2: more models, new heuristics and parallel computing. *Nat Meth* 9: 772-772.

Ding M, Ye W, Lin L, He S, Du X, Chen A, Cao Y, Qin Y, Yang F, Jiang Y. 2015. The hairless stem phenotype of cotton (*Gossypium barbadense*) is linked to a copia-like retrotransposon insertion in a homeodomain-leucine zipper gene (HD1). *Genetics* 201: 143-154.

Doaigey A, Harkiss K. 1991. Application of epidermal characters to the taxonomy of european species of *Antirrhinum* (Schrophulariaceae). *Nordic journal of botany* 11: 513-524.

Estelle MA, Somerville C. 1987. Auxin-resistant mutants of *Arabidopsis thaliana* with an altered morphology. *Molecular and General Genetics MGG* 206: 200-206.

Ezgi O, Jolan T, B. KD, C. VJ. 2017. Diversifiication rates in Antirrhineae (Plantaginaceae): the contribution of range shifts and pollination modes. *Perspectives in Plant Ecology, Evolution and Systematics* 26: 39-52.

Fahn A. 2002. Functions and location of secretory tissues in plants and their possible evolutionary trends. *Israel Journal of Plant Sciences* 50: 59-64.

Güemes J, Mota JF. 2017. *Gadoria* (Antirrhineae, Plantaginaceae): A new genus, endemic from Sierra de Gádor, Almería, Spain. *Phytotaxa* 298: 201-221.

Gabriel SJ, Isabel M. 2001. Taxonomic study of *Linaria depauperata* and *L. supina* complexes in eastern Spain. *Annals of Botany* 87: 157-177.

Gan L, Xia K, Chen J-G, Wang S. 2011. Functional characterization of TRICHOMELESS2, a new single-repeat R3 MYB transcription factor in the regulation of trichome patterning in *Arabidopsis*. *BMC Plant Biology* 11: 176-176.

Garg R, Jhanwar S, Tyagi AK, Jain M. 2010. Genome-wide survey and expression analysis suggest diverse roles of glutaredoxin gene family members during development and response to various stimuli in rice. *DNA research* 17: 353-367.

Gersbach P. 2002. The essential oil secretory structures of *Prostanthera ovalifolia* (Lamiaceae). *Annals of botany* 89: 255-260.

Glover BJ, Perez-Rodriguez M, Martin C. 1998. Development of several epidermal cell types can be specified by the same MYB-related plant transcription factor. *Development* 125: 3497-3508.

Goujon M, McWilliam H, Li W, Valentin F, Squizzato S, Paern J, Lopez R. 2010. A new

bioinformatics analysis tools framework at EMBL-EBI. *Nucleic Acids Research* 38: W695-9.
Grünewald K, Eckert M, Hirschberg J, Hagen C. 2000. Phytoene Desaturase Is Localized Exclusively in the Chloroplast and Up-Regulated at the mRNA Level during Accumulation of Secondary Carotenoids in *Haematococcus pluvialis* (Volvocales, Chlorophyceae). *Plant physiology* 122: 1261-1268.
Gutsche N, Holtmannspötter M, Maß L, O'Donoghue M, Busch A, Lauri A, Schubert V, Zachgo S. 2017. Conserved redox-dependent DNA binding of ROXY glutaredoxins with TGA transcription factors. *Plant Direct* 1: 1-16.
Guzmán B, Gómez JM, Vargas P. 2015. Bees and evolution of occluded corollas in snapdragons and relatives (Antirrhineae). *Perspectives in Plant Ecology, Evolution and Systematics* 17: 467-475.
Hülskamp M, Miséra S, Jürgens G. 1994. Genetic dissection of trichome cell development in *Arabidopsis*. *Cell* 76: 555-566.
Handley R, Ekbom B, Ågren J. 2005. Variation in trichome density and resistance against a specialist insect herbivore in natural populations of *Arabidopsis thaliana*. *Ecological Entomology* 30: 284-292.
Holmgren A. 1989. Thioredoxin and glutaredoxin systems. *Journal of Biological Chemistry* 264: 13963-13966.
Hu G-X, Balangcod TD, Xiang C-L. 2012. Trichome micromorphology of the Chinese-Himalayan genus *Colquhounia* (Lamiaceae), with emphasis on taxonomic implications. *Biologia* 67: 867-874.
Hudson A, Critchley J, Erasmus Y. 2008. Propagating *Antirrhinum*. *Cold Spring Harbor Protocols* 2008: pdb. prot5052.
Huelsenbeck JP, Ronquist F. 2001. MRBAYES: Bayesian inference of phylogenetic trees. *Bioinformatics* 17: 754-755.
Huijser P, Schmid M. 2011. The control of developmental phase transitions in plants. *Development* 138: 4117-4129.
Humphries JA, Walker AR, Timmis JN, Orford SJ. 2005. Two WD-repeat genes from cotton are functional homologues of the *Arabidopsis thaliana TRANSPARENT TESTA GLABRA1* (*TTG1*) gene. *Plant Molecular Biology* 57: 67-81.
Inouye S, Takizawa T, Yamaguchi H. 2001. Antibacterial activity of essential oils and their major constituents against respiratory tract pathogens by gaseous contact. *Journal of Antimicrobial Chemotherapy* 47: 565-573.
Ishida T, Kurata T, Okada K, Wada T. 2008. A genetic regulatory network in the development of trichomes and root hairs. *Annual Review of Plant Biology* 59: 365-386.
Iwamoto M, Horikawa C, Shikata M, Wasaka N, Kato T, Sato H. 2014. Stinging hairs on the Japanese nettle *Urtica thunbergiana* have a defensive function against mammalian but not insect herbivores. *Ecological Research* 29: 455-462.
Juan R, Pastor J, Fernández I. 1996. Estudio de microcaracteres en frutos y semillas de *Antirrhinum* L.(Scrophulariaceae). *Acta botanica gallica* 143: 181-190.
Kang J-H, Campos ML, Zemelis-Durfee S, Al-Haddad JM, Jones AD, Telewski FW, Brandizzi F, Howe GA. 2016. Molecular cloning of the tomato Hairless gene implicates actin dynamics in trichome-mediated defense and mechanical properties of stem tissue. *Journal of experimental botany*
Kang J-H, Shi F, Jones AD, Marks MD, Howe GA. 2010. Distortion of trichome morphology by the hairless mutation of tomato affects leaf surface chemistry. *Journal of experimental botany* 61: 1053-1064.
Kirik V, Schnittger A, Radchuk V, Adler K, Hülskamp M, Bäumlein H. 2001. Ectopic Expression of the *Arabidopsis AtMYB23* Gene Induces Differentiation of Trichome Cells. *Developmental biology* 235: 366-377.
Kirik V, Simon M, Huelskamp M, Schiefelbein J. 2004a. The ENHANCER OF TRY AND CPC1 gene acts redundantly with TRIPTYCHON and CAPRICE in trichome and root hair cell patterning in *Arabidopsis*. *Developmental Biology* 268: 506-513.
Kirik V, Simon M, Wester K, Schiefelbein J, Hulskamp M. 2004b. ENHANCER of TRYand CPC 2(ETC2) reveals redundancy in the region-specific control of trichome development of *Arabidopsis*. *Plant Molecular Biology* 55: 389-398.
Koncz C, Schell J. 1986. The promoter of T L-DNA gene 5 controls the tissue-specific expression of chimaeric genes carried by a novel type of *Agrobacterium* binary vector. *Molecular and General Genetics MGG* 204: 383-396.
Levin DA. 1973. The Role of Trichomes in Plant Defense. *The Quarterly Review of Biology* 48: 3-15.
Li S, Gutsche N, Zachgo S. 2011. The ROXY1 C-terminal L** LL motif is essential for the interaction with TGA transcription factors. *Plant physiology* 157: 2056-2068.

Li S, Lauri A, Ziemann M, Busch A, Bhave M, Zachgo S. 2009. Nuclear activity of ROXY1, a glutaredoxin interacting with TGA factors, is required for petal development in *Arabidopsis thaliana*. *The Plant Cell* 21: 429-441.
Liang G, He H, Li Y, Ai Q, Yu D. 2014. MYB82 functions in regulation of trichome development in *Arabidopsis*. *Journal of experimental botany*
Linden H, Lucas MM, de Felipe MR, Sandmann G. 1993. Immunogold localization of phytoene desaturase in higher plant chloroplasts. *Physiologia Plantarum* 88: 229-236.
Luckwill LC. 1943. *The genus Lycopersicon: an historical, biological, and taxonomic survey of the wild and cultivated tomatoes*. Aberdeen: Aberdeen university press.
Ma D, Hu Y, Yang C, Liu B, Fang L, Wan Q, Liang W, Mei G, Wang L, Wang H. 2016. Genetic basis for glandular trichome formation in cotton. *Nature communications* 7: 10456.
Machado A, Wu Y, Yang Y, Llewellyn DJ, Dennis ES. 2009. The MYB transcription factor GhMYB25 regulates early fibre and trichome development. *The Plant Journal* 59: 52-62.
Manchado-Rojo M, Delgado-Benarroch L, Roca MJ, Weiss J, Egea-Cortines M. 2012. Quantitative levels of *Deficiens* and *Globosa* during late petal development show a complex transcriptional network topology of B function. *The Plant Journal* 72: 294-307.
Manetas Y, Grammatikopoulos G, Kyparissis A. 1998. The use of the portable, non-destructive, spad-502 (minolta) chlorophyll meter with leaves of varying trichome density and anthocyanin content. *Journal of Plant Physiology* 153: 513-516.
McWilliam H, Li w, Uludag M, Squizzato S, Park YM, Buso N, Cowley AP, Lopez R. 2013. Analysis tool we b services from the EMBL-EBI. *Nucleic Acids Research* 41: W597-W600.
Morohashi K, Zhao M, Yang M, Read B, Lloyd A, Lamb R, Grotewold E. 2007. Participation of the *Arabidopsis* bHLH factor GL3 in trichome initiation regulatory events. *Plant physiology* 145: 736-746.
Murmu J, Bush MJ, DeLong C, Li S, Xu M, Khan M, Malcolmson C, Fobert PR, Zachgo S, Hepworth SR. 2010. *Arabidopsis* Basic Leucine-Zipper Transcription Factors TGA9 and TGA10 Interact with Floral Glutaredoxins ROXY1 and ROXY2 and Are Redundantly Required for Anther Development. *Plant physiology* 154: 1492-1504.
Nakamura M, Katsumata H, Abe M, Yabe N, Komeda Y, Yamamoto KT, Takahashi T. 2006. Characterization of the Class IV Homeodomain-Leucine Zipper Gene Family in *Arabidopsis*. *Plant physiology* 141: 1363-1375.
Nogueira A, El Ottra JHL, Guimarães E, Machado SR, Lohmann LG. 2013. Trichome structure and evolution in Neotropical lianas. *Annals of botany* mct201.
Ogutcen E, Vamosi JC. 2016. A phylogenetic study of the tribe Antirrhineae: Genome duplications and long-distance dispersals from the Old World to the New World. *American Journal of Botany* 103: 1071-1081.
Olmstead RG, Reeves PA. 1995. Evidence for the Polyphyly of the Scrophulariaceae Based on Chloroplast *rbcL* and *ndhF* Sequences. *Annals of the Missouri Botanical Garden* 82: 176-193.
Pérez-Estrada LB, Cano-Santana Z, Oyama K. 2000. Variation in leaf trichomes of Wigandia urens: environmental factors and physiological consequences. *Tree Physiology* 20: 629-632.
Payne CT, Zhang F, Lloyd AM. 2000. GL3 encodes a bHLH protein that regulates trichome development in *Arabidopsis* through interaction with GL1 and TTG1. *Genetics* 156: 1349-1362.
Payne T, Clement J, Arnold D, Lloyd A. 1999. Heterologous myb genes distinct from GL1 enhance trichome production when overexpressed in *Nicotiana tabacum*. *Development* 126: 671-682.
Pinto E, Pina-Vaz C, Salgueiro L, Gonçalves MJ, Costa-de-Oliveira S, Cavaleiro C, Palmeira A, Rodrigues A, Martinez-de-Oliveira J. 2006. Antifungal activity of the essential oil of *Thymus pulegioides* on Candida, Aspergillus and dermatophyte species. *Journal of Medical Microbiology* 55: 1367-1373.
Preston JC, Hileman LC. 2010. SQUAMOSA-PROMOTER BINDING PROTEIN 1 initiates flowering in *Antirrhinum majus* through the activation of meristem identity genes. *The Plant Journal* 62: 704-712.
Prinz WA, Åslund F, Holmgren A, Beckwith J. 1997. The Role of the Thioredoxin and Glutaredoxin Pathways in Reducing Protein Disulfide Bonds in the *Escherichia coli* Cytoplasm. *Journal of Biological Chemistry* 272: 15661-15667.
Poethig RS. 1990. Phase change and the regulation of shoot morphogenesis in plants. *Science* 250: 923-930.
Puentes A, Ågren J. 2013. Trichome production and variation in young plant resistance to the specialist insect herbivore *Plutella xylostella* among natural populations of *Arabidopsis lyrata*.

Entomologia Experimentalis et Applicata 149: 166-176.
Qiao H, Wang H, Zhao L, Zhou J, Huang J, Zhang Y, Xue Y. 2004. The F-box protein AhSLF-S2 physically interacts with S-RNases that may be inhibited by the ubiquitin/26S proteasome pathway of protein degradation during compatible pollination in *Antirrhinum*. *The Plant Cell* 16: 582-595.
Qin G, Gu H, Ma L, Peng Y, Deng XW, Chen Z, Qu L-J. 2007. Disruption of phytoene desaturase gene results in albino and dwarf phenotypes in *Arabidopsis* by impairing chlorophyll, carotenoid, and gibberellin biosynthesis. *Cell Research* 17: 471-482.
Rebocho AB, Southam P, Kennaway JR, Bangham JA, Coen E. 2017. Generation of shape complexity through tissue conflict resolution. *eLife* 6: e20156.
Robinson JT, Thorvaldsdóttir H, Winckler W, Guttman M, Lander ES, Getz G, Mesirov JP. 2011. Intergrative Genomics Viewer. *Nature Biotechnology* 29: 24-26.
Ronquist F, Huelsenbeck JP. 2003. MrBayes 3: Bayesian phylogenetic inference under mixed models. *Bioinformatics* 19: 1572-1574.
Rothmaler W. 1956. *Taxonomische monographie der gattung Antirrhinum*. Akademie.
Rouhier N, Villarejo A, Srivastava M, Gelhaye E, Keech O, Droux M, Finkemeier I, Samuelsson G, Dietz KJ, Jacquot J-P. 2005. Identification of plant glutaredoxin targets. *Antioxidants & redox signaling* 7: 919-929.
Ruzin SE. 1999. *Plant microtechnique and microscopy*. 198. Oxford University Press New York.
Saez L, Crespo MB. 2005. A taxonomic revision of the *Linaria verticillata* group (Antirrhineae, Scrophulariaceae). *Botanical Journal of the Linnean Society* 148: 229-244.
Sandmann G, Schmidt A, Linden H, Böger P. 1991. Phytoene desaturase, the essential target for bleaching herbicides. *Weed Science* 39: 474-479.
Schiefelbein J. 2003. Cell-fate specification in the epidermis: a common patterning mechanism in the root and shoot. *Current opinion in plant biology* 6: 74-78.
Schilmiller AL, Last RL, Pichersky E. 2008. Harnessing plant trichome biochemistry for the production of useful compounds. *The Plant Journal* 54: 702-711.
Schnittger A, Folkers U, Schwab B, Jürgens G, Hülskamp M. 1999. Generation of a Spacing Pattern: The Role of TRIPTYCHON in Trichome Patterning in *Arabidopsis*. *The Plant Cell* 11: 1105-1116.
Schnittger A, Jurgens G, Hulskamp M. 1998. Tissue layer and organ specificity of trichome formation are regulated by GLABRA1 and TRIPTYCHON in *Arabidopsis*. *Development* 125: 2283-2289.
Schwarz S, Grande AV, Bujdoso N, Saedler H, Huijser P. 2008. The microRNA regulated SBP-box genes SPL9 and SPL15 control shoot maturation in *Arabidopsis*. *Plant Molecular Biology* 67: 183-195.
Senthil-Kumar M, Mysore KS. 2014. Tobacco rattle virus–based virus-induced gene silencing in *Nicotiana benthamiana*. *Nature Protocols* 9: 1549-1562.
Serrato-Valenti G, Bisio A, Cornara L, Ciarallo G. 1997. Structural and histochemical investigation of the glandular trichomes of *Salvia aurea* L. leaves, and chemical analysis of the essential oil. *Annals of botany* 79: 329-336.
Shikata M, Koyama T, Mitsuda N, Ohme-Takagi M. 2009. *Arabidopsis* SBP-Box Genes SPL10, SPL11 and SPL2 Control Morphological Change in Association with Shoot Maturation in the Reproductive Phase. *Plant and Cell Physiology* 50: 2133-2145.
Sievers F, Wilm A, Dineen D, Gibson TJ, Karplus K, Li W, Lopez R, McWilliam H, Remmert M, Söding J, Thompson JD, Higgins DG. 2011. Fast, scalable generation of high-quality protein multiple sequence alignments usgin Clustal omega. *Molecular Systems Biology* 7: 539.
Sutton DA. 1988. *A revision of the tribe Antirrhineae*. British Museum (Natural History).
Szymanski DB, Jilk RA, Pollock SM, Marks MD. 1998. Control of GL2 expression in *Arabidopsis* leaves and trichomes. *Development* 125: 1161-1171.
Telfer A, Bollman KM, Poethig RS. 1997. Phase change and the regulation of trichome distribution in *Arabidopsis thaliana*. *Development* 124: 645-654.
The Angiosperm Phylogeny G. 2009. An update of the Angiosperm Phylogeny Group classification for the orders and families of flowering plants: APG III. *Botanical Journal of the Linnean Society* 161: 105-121.
Thompson DM. 1988. Systematics of *Antirrhinum* (Scrophulariaceae) in the New World. *Systematic Botany Monographs* 22: 1-142.
Thorvaldsdóttir H, Robinson JT, Mesirov JP. 2013. Integrative Genomics Viewer (IGV): high-performance genomics data visualization and exploration *Briefings in Bioinformatics* 14: 178-192.
Tissier A. 2012. Glandular trichomes: what comes after expressed sequence tags? *The Plant Journal*

70: 51-68.
Treacy MF, Benedict JH, Segers JC, Morrison RK, Lopez JD. 1986. Role of Cotton Trichome Density in Bollworm (Lepidoptera: Noctuidae) Egg Parasitism. *Environmental Entomology* 15: 365-368.
Treacy MF, Zummo GR, Benedict JH. 1985. Interactions of host-plant resistance in cotton with predators and parasites. *Agriculture, Ecosystems & Environment* 13: 151-157.
Uphof JCT, Hummel K, Staesche K. 1962. *Plant hairs*. 4. Gebrüder Borntraeger Berlin-Nokolassee.
Vargas P, Carrió E, Guzmán B, Amat E, Güemes J. 2009. A geographical pattern of *Antirrhinum* (Scrophulariaceae) speciation since the Pliocene based on plastid and nuclear DNA polymorphisms. *Journal of Biogeography* 36: 1297-1312.
Vargas P, Rosselló JA, Oyama R, Güemes J. 2004. Molecular evidence for naturalness of genera in the tribe Antirrhineae (Scrophulariaceae) and three independent evolutionary lineages from the New World and the Old. *Plant Systematics and Evolution* 249: 151-172.
Vernoud V, Laigle G, Rozier F, Meeley RB, Perez P, Rogowsky PM. 2009. The HD-ZIP IV transcription factor OCL4 is necessary for trichome patterning and anther development in maize. *The Plant Journal* 59: 883-894.
Wada T, Tachibana T, Shimura Y, Okada K. 1997. Epidermal cell differentiation in *Arabidopsis* determined by a Myb homolog, CPC. *Science* 277: 1113-1116.
Walford S-A, Wu Y, Llewellyn DJ, Dennis ES. 2011. GhMYB25-like: a key factor in early cotton fibre development. *The Plant Journal* 65: 785-797.
Walford S-A, Wu Y, Llewellyn DJ, Dennis ES. 2012. Epidermal cell differentiation in cotton mediated by the homeodomain leucine zipper gene, GhHD-1. *The Plant Journal* 71: 464-478.

Wang J-W, Czech B, Weigel D. 2009. miR156-Regulated SPL Transcription Factors Define an Endogenous Flowering Pathway in *Arabidopsis thaliana*. *Cell* 138: 738-749.
Wang S, Kwak S-H, Zeng Q, Ellis BE, Chen X-Y, Schiefelbein J, Chen J-G. 2007. TRICHOMELESS1 regulates trichome patterning by suppressing GLABRA1 in *Arabidopsis*. *Development* 134: 3873-3882.
Wang S, Wang J-W, Yu N, Li C-H, Luo B, Gou J-Y, Wang L-J, Chen X-Y. 2004. Control of plant trichome development by a cotton fiber MYB gene. *The Plant Cell Online* 16: 2323-2334.
Webb DA. 1971. Taxonomic notes on *Antirrhinum* L. *Botanical Journal of the Linnean Society* 64: 271-275.
Wang Z, Xing S, Birkenbihl RP, Zachgo S. 2009. Conserved functions of *Arabidopsis* and rice CC-type glutaredoxins in flower development and pathogen response. *Molecular Plant* 2: 323-335.
Weir I, Lu J, Cook H, Causier B, Schwarz-Sommer Z, Davies B. 2004. *CUPULIFORMIS* establishes lateral organ boundaries in *Antirrhinum*. *Development* 131: 915-922.
Werker E. 2000. Trichome diversity and development. *Advances in botanical research* 31: 1-35.
Wilson Y. 2009. Evolutionary relationships and morphological variation between *Antirrhinum* species. PhD Thesis, Edinburgh: The University of Edinburgh.
Wilson Y, Hudson A. 2011. The evolutionary history of *Antirrhinum* suggests that ancestral phenotype combinations survived repeated hybridizations. *The Plant Journal* 66: 1032-1043.
Wu G, Park MY, Conway SR, Wang J-W, Weigel D, Poethig RS. 2009. The Sequential Action of miR156 and miR172 Regulates Developmental Timing in *Arabidopsis*. *Cell* 138: 750-759.
Xing S, Lauri A, Zachgo S. 2006. Redox regulation and flower development: a novel function for glutaredoxins. *Plant Biology* 8: 547-555.
Xing S, Zachgo S. 2008. ROXY1 and ROXY2, two *Arabidopsis* glutaredoxin genes, are required for anther development. *The Plant Journal* 53: 790-801.
Xue X-Y, Zhao B, Chao L-M, Chen D-Y, Cui W-R, Mao Y-B, Wang L-J, Chen X-Y. 2014. Interaction between Two Timing MicroRNAs Controls Trichome Distribution in *Arabidopsis*. *PLoS genetics* 10: e1004266.
Yan T, Chen M, Shen Q, Li L, Fu X, Pan Q, Tang Y, Shi P, Lv Z, Jiang W, Ma Y-n, Hao X, Sun X, Tang K. 2017. HOMEODOMAIN PROTEIN 1 is required for jasmonate-mediated glandular trichome initiation in *Artemisia annua*. *New Phytologist* 213: 1145-1155.
Yan T, Li L, Xie L, Chen M, Shen Q, Pan Q, Fu X, Shi P, Tang Y, Huang H, Huang Y, Huang Y, Tang K. 2018. A novel HD-ZIP IV/MIXTA complex promotes glandular trichome initiation and cuticle development in *Artemisia annua*. *New Phytologist* n/a-n/a.
Yang C, Li H, Zhang J, Luo Z, Gong P, Zhang C, Li J, Wang T, Zhang Y, Lu Ye, Ye Z. 2011. A regulatory gene induces trichome formation and embryo lethality in tomato. *Proceedings of the National Academy of Sciences* 108: 11836-11841.

Yousefi N, Zarre S, Heubl G. 2016. Molecular phylogeny of the mainly Mediterranean genera *Chaenorhinum*, *Kickxia* and *Nanorrhinum* (Plantaginaceae, tribe Antirrhineae), with focus on taxa in the Flora Iranica region. *Nordic journal of botany* 34: 455-463.
Yu N, Cai W-J, Wang S, Shan C-M, Wang L-J, Chen X-Y. 2010. Temporal control of trichome distribution by microRNA156-targeted SPL genes in *Arabidopsis thaliana*. *The Plant Cell Online* 22: 2322-2335.
Zachgo S, Perbal MC, Saedler H, Schwarz-Sommer Z. 2000. In situ analysis of RNA and protein expression in whole mounts facilitates detection of floral gene expression dynamics. *The Plant Journal* 23: 697-702.
Ziemann M, Bhave M, Zachgo S. 2009. Origin and diversification of land plant CC-type glutaredoxins. *Genome Biology and Evolution* 1: 265-277.
Zhao J-L, Pan J-S, Guan Y, Zhang W-W, Bie B-B, Wang Y-L, He H-L, Lian H-L, Cai R. 2015. Micro-trichome as a class I homeodomain-leucine zipper gene regulates multicellular trichome development in *Cucumis sativus*. *Journal of Integrative Plant Biology* 57: 925-935.
Zhu X, Dinesh-Kumar S, Doran T, Helliwell C. 2008. Virus-induced gene silencing (VIGS) to study gene function in plants. *RNA interference: methods for plants and animals* 26-49.

Appendices

Appendix 1: Foliar trichome morphology

Subsection *Antirrhinum*

1.1 *A. australe*

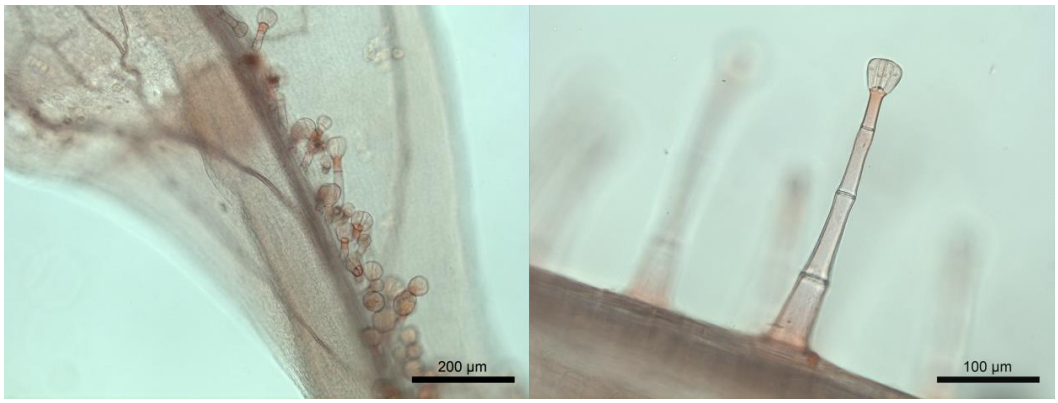

adaxial stem

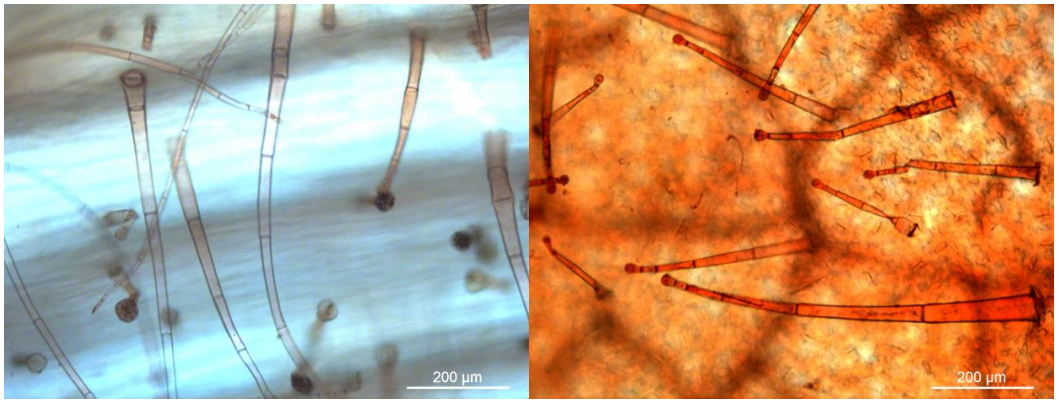

lower leaf adaxial lower leaf abaxial

1.2 *A. graniticum*

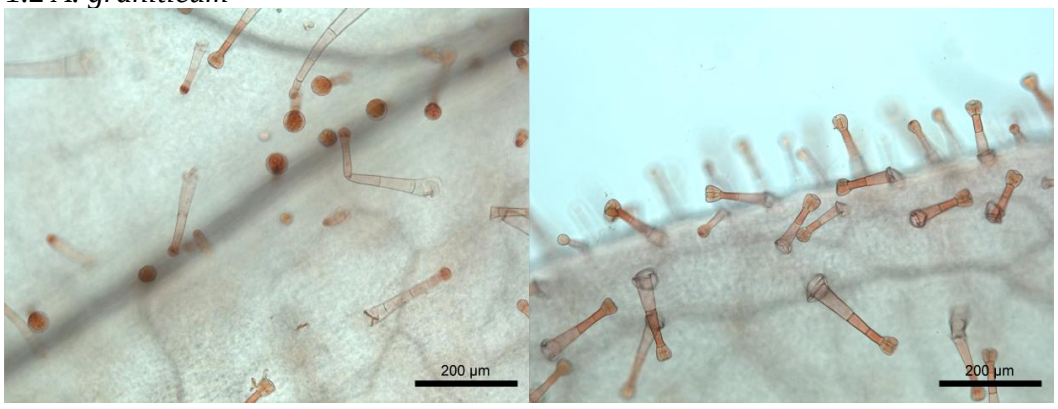

adaxial

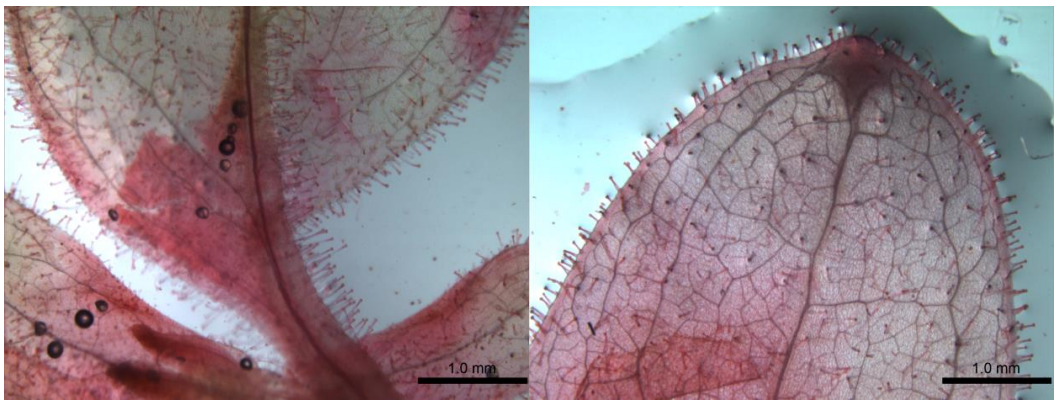

abaxial

1.3 *A. latifolium*

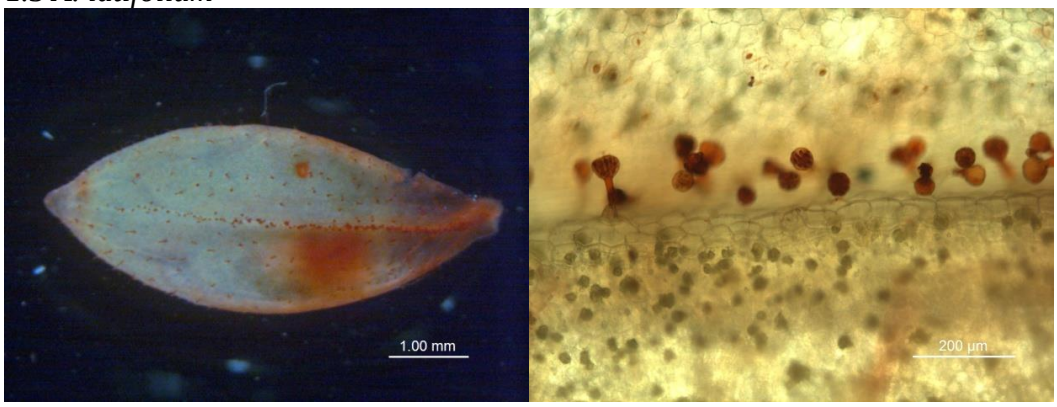

adaxial

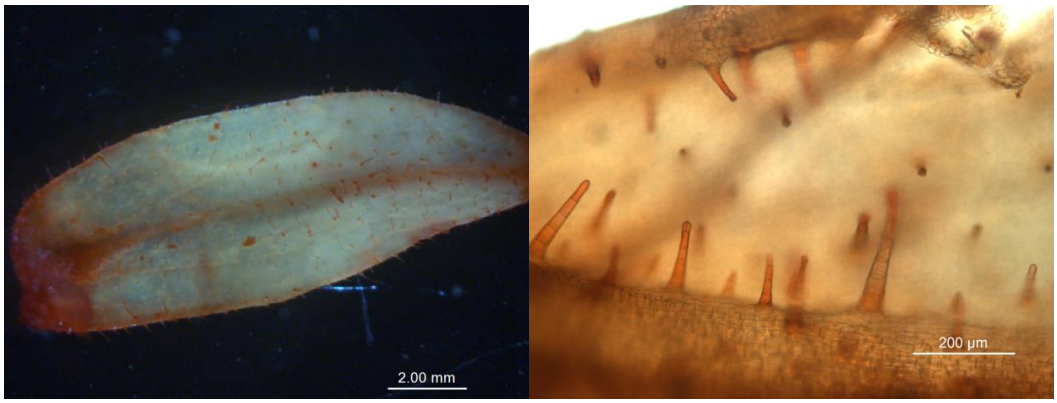

abaxial

1.4 *A. majus* subsp. *cirrhigerum*

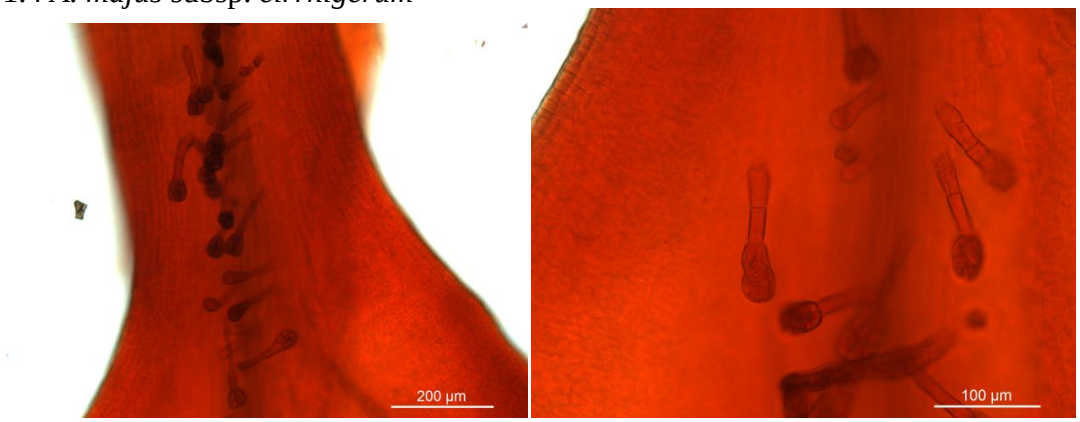

adaxial

1.5 *A. majus* subsp. *linkianum*

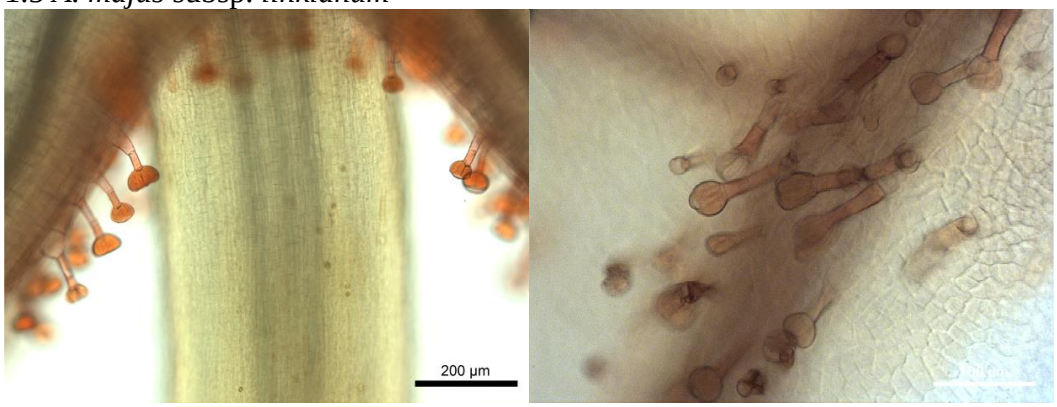

adaxial

1.6 *A. majus* subsp. *majus*

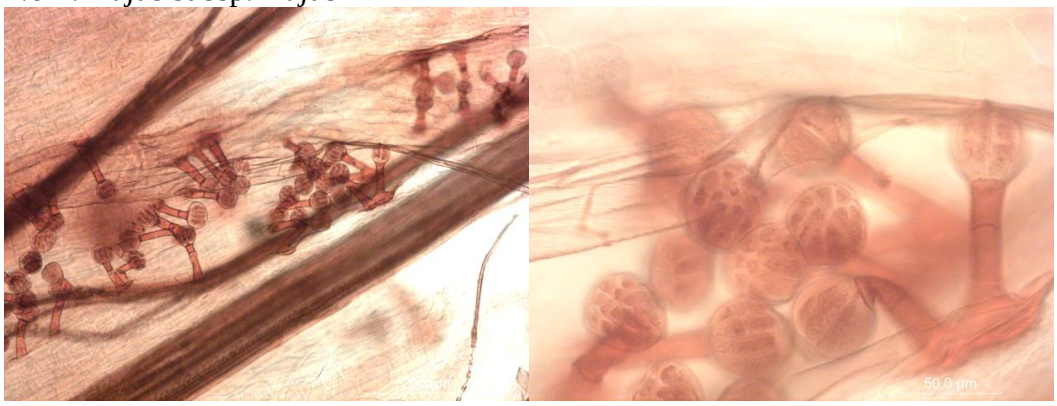

adaxial

1.7 *A. majus* subsp. *pseduomajus*

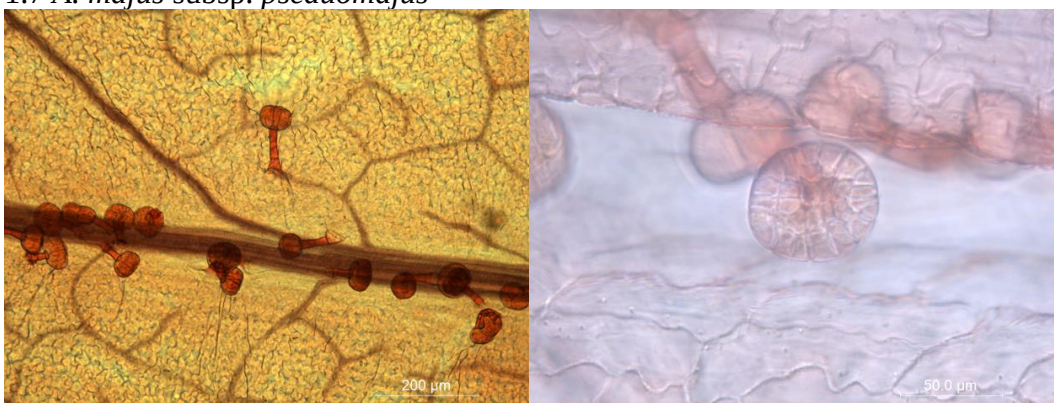

adaxial

1.8 *A. majus* subsp. *striatum*

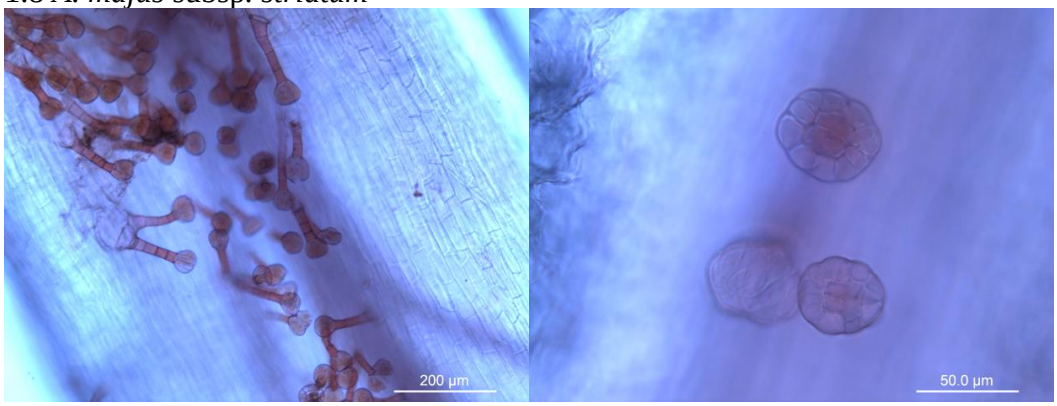

adaxial

1.9 *A. majus* subsp. *tortuosum*

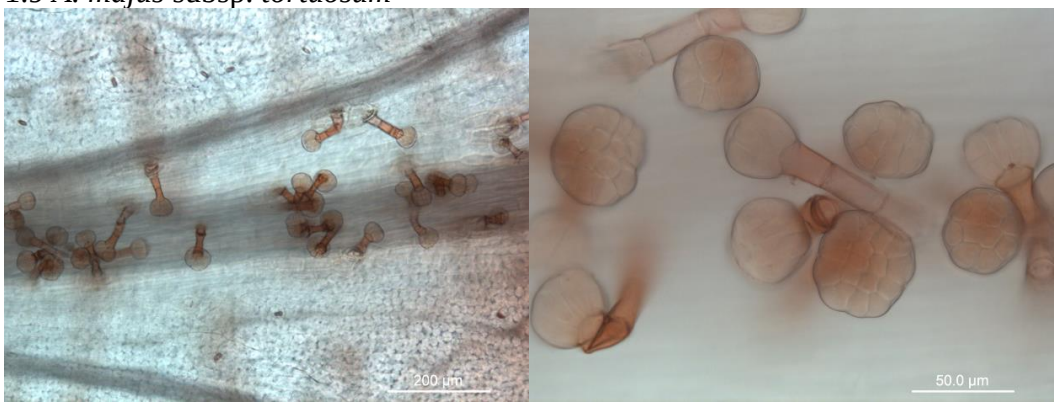

adaxial

1.10 *A. siculum*

adaxial

Subsection *Kickxiella*

1.11 *A. boissieri*

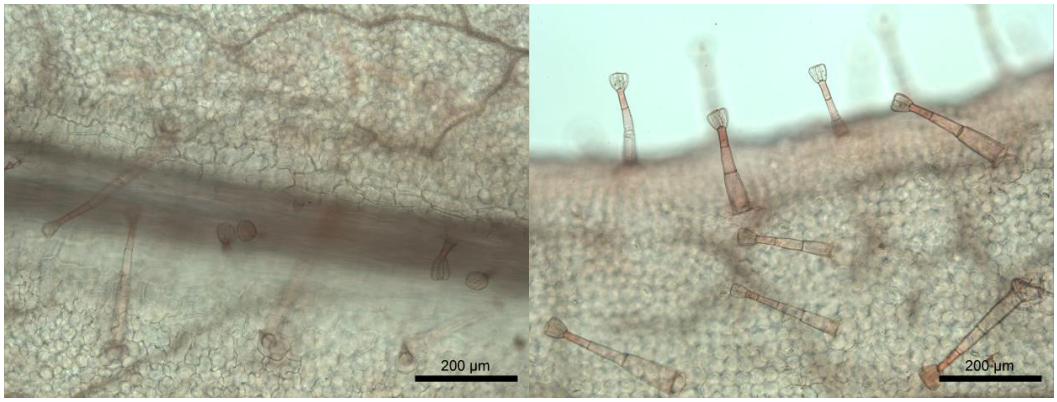

adaxial

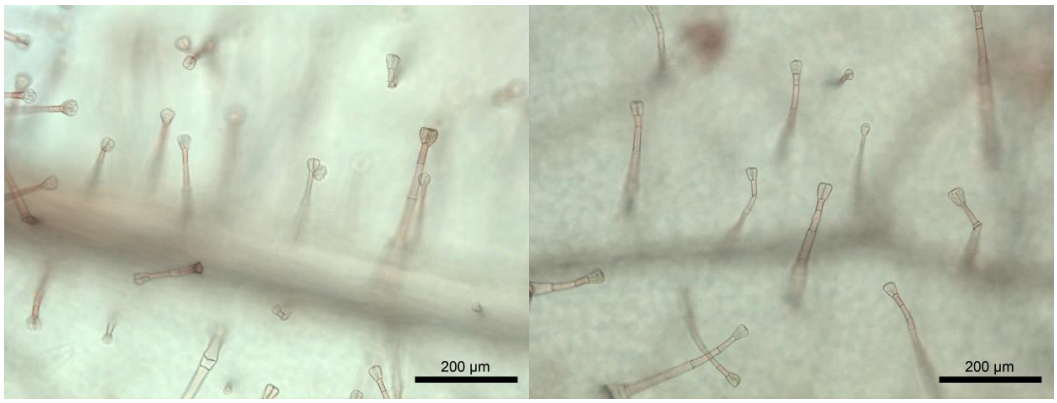

abaxial

1.12 *A. charidemi*

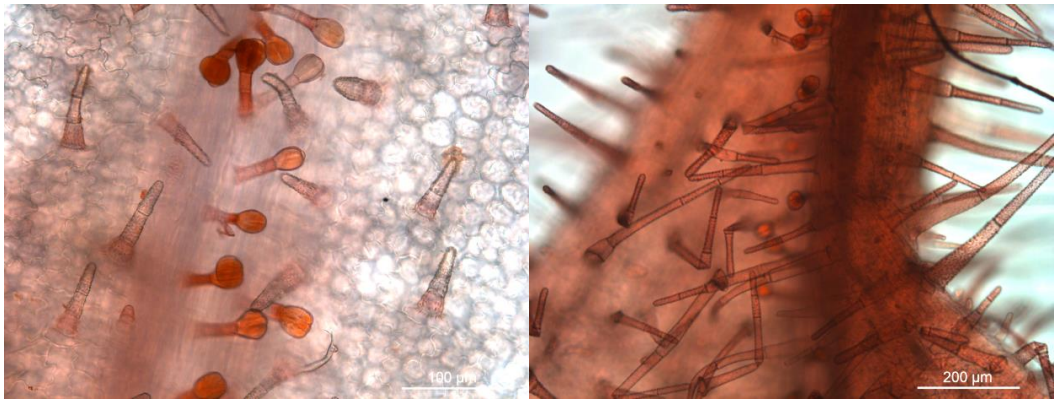

adaxial

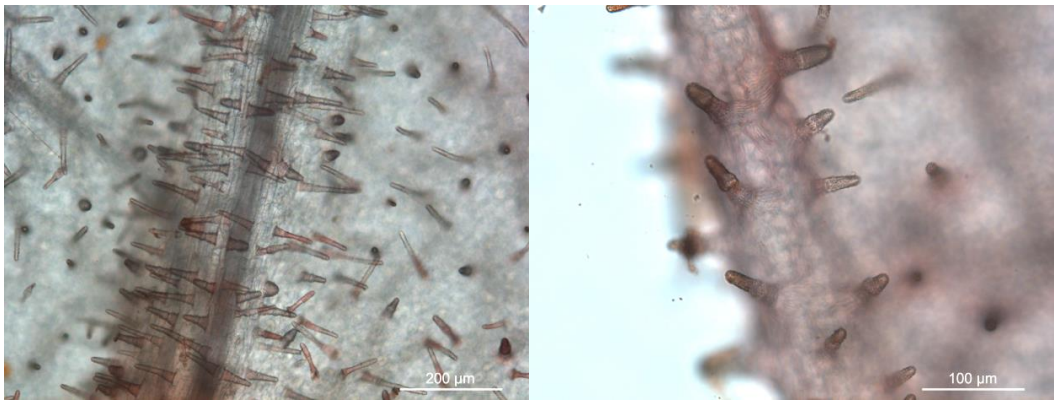

abaxial

1.13 *A. hispanicum*

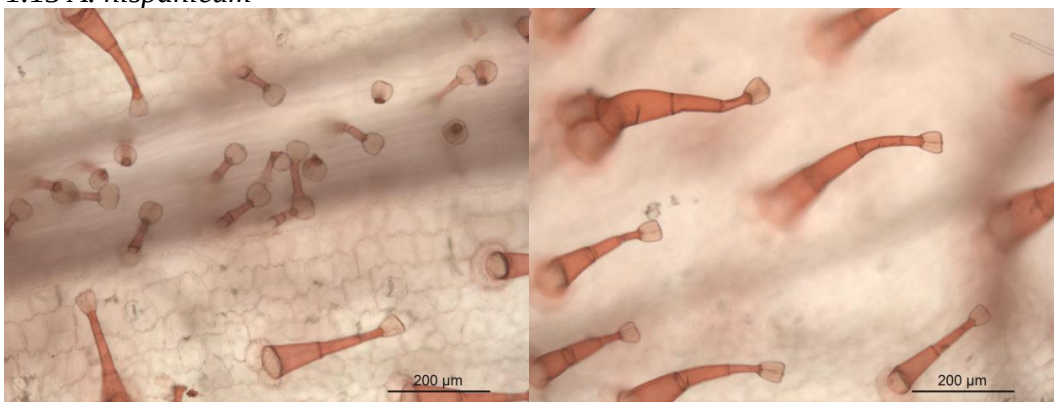

adaxial

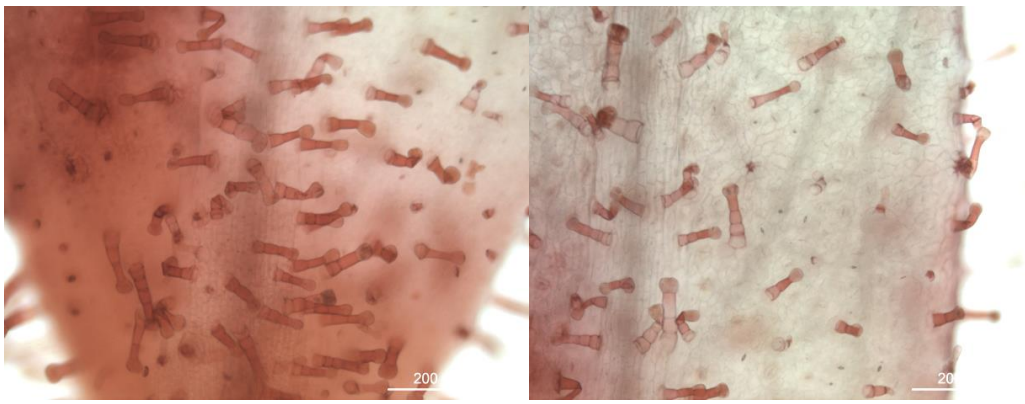

abaxial

1.14 *A. lopesianum*

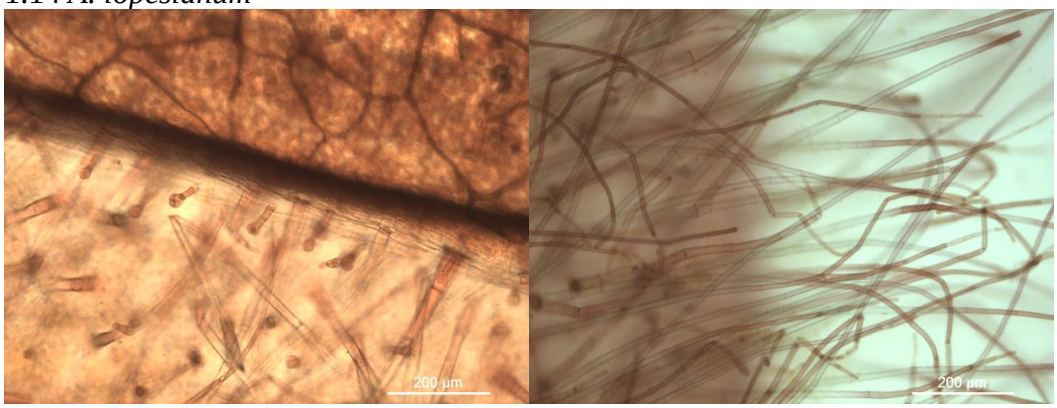

adaxial

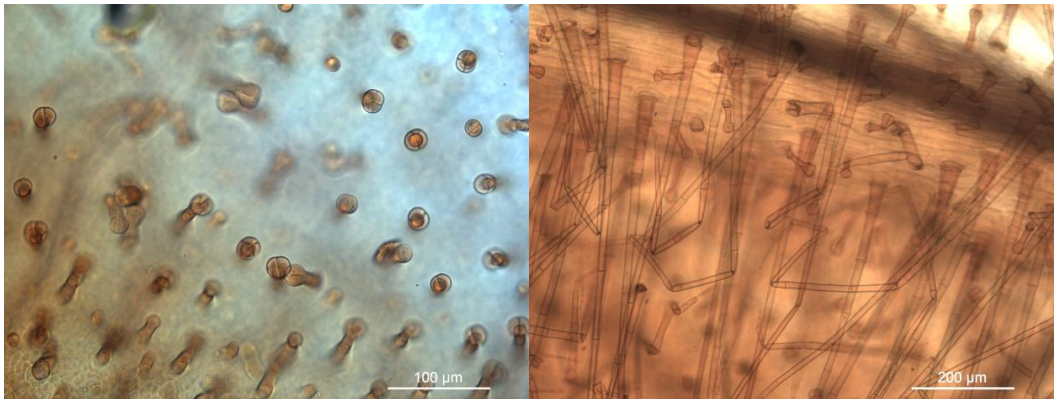

abaxial side of young leaf

abaxial side of mature leaf

1.15 *A. microphyllum*

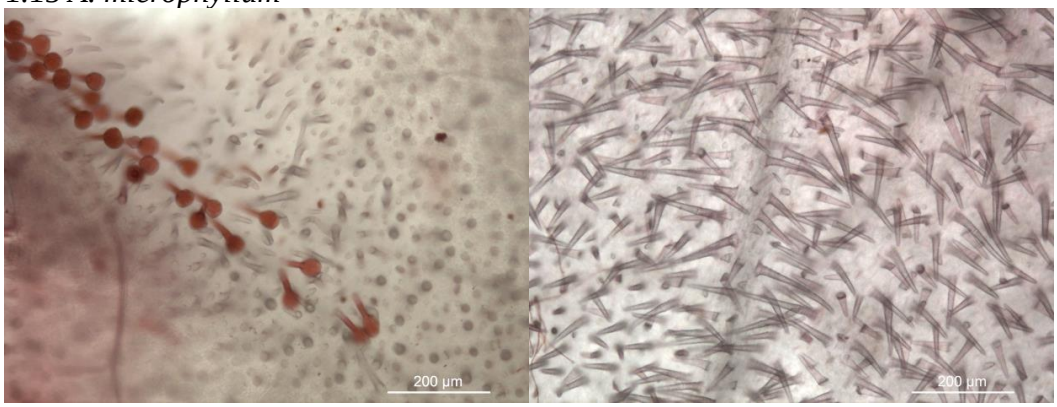

adaxial abaxial

1.16*A. molle*

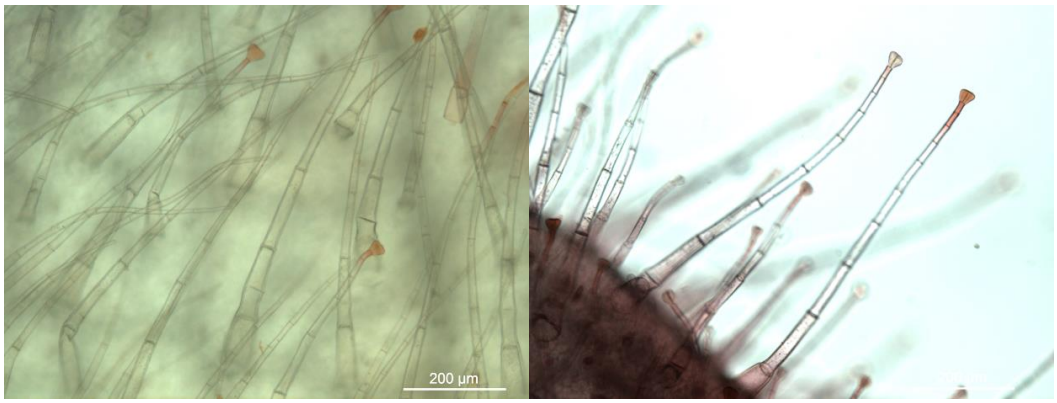

adaxial abaxial

1.17 *A. mollisimum*

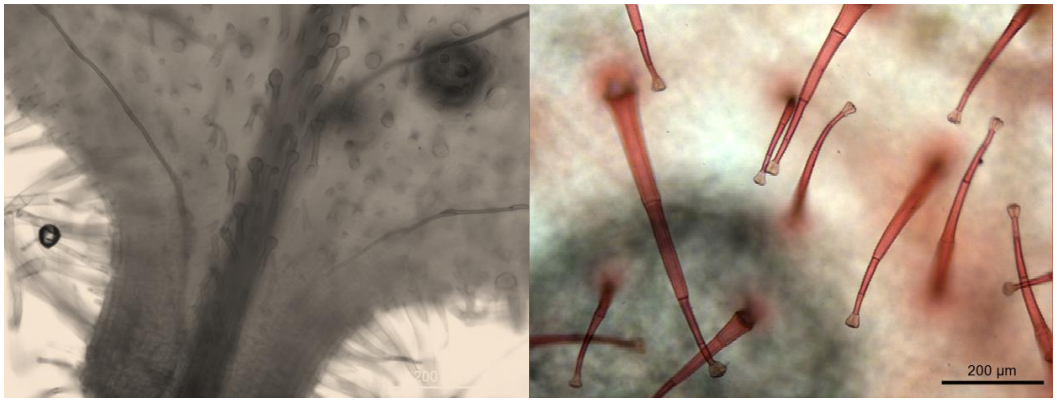

adaxial abaxial

1.18 *A. pertegasii*

adaxial

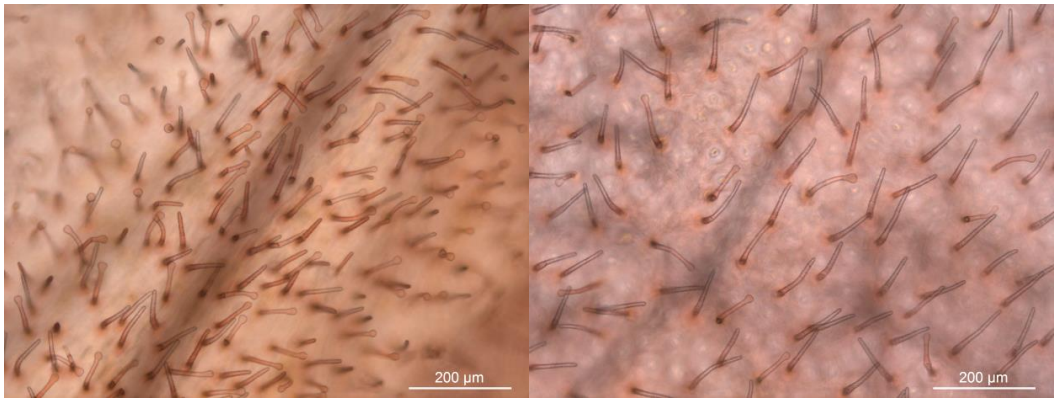

abaxial

1.19 *A. pulverulentum*

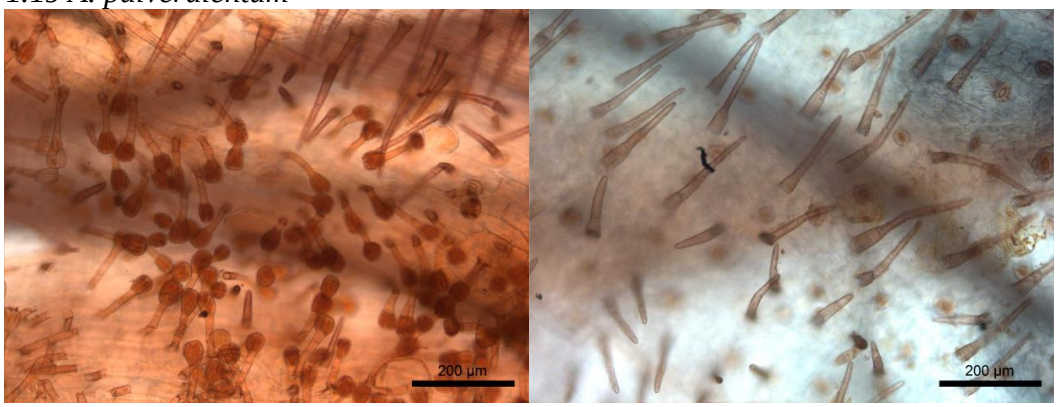

adaxial

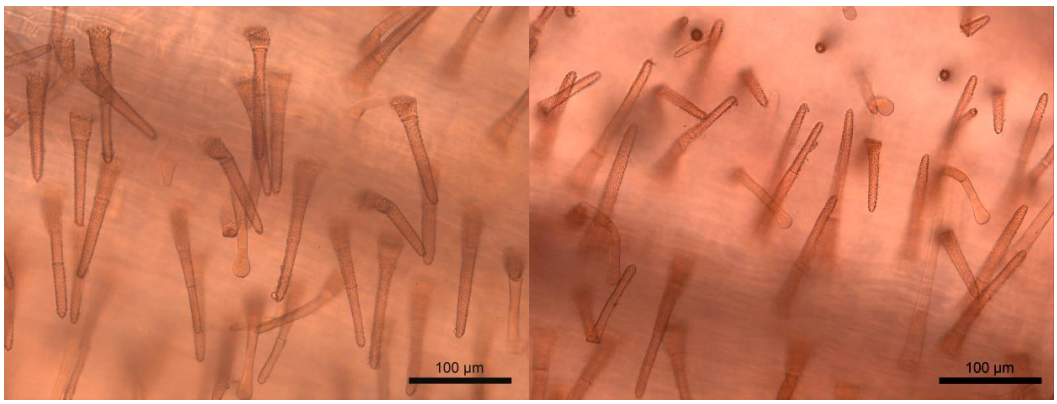

abaxial

1.20 *A. rupestre*

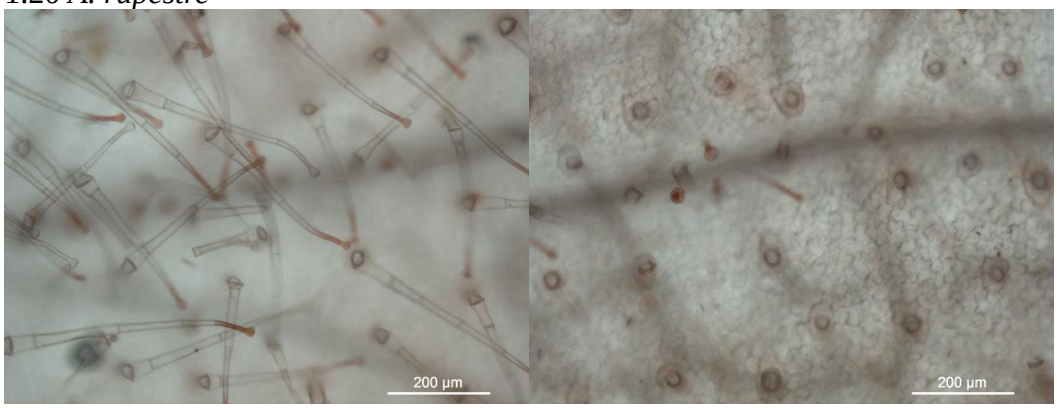

adaxial

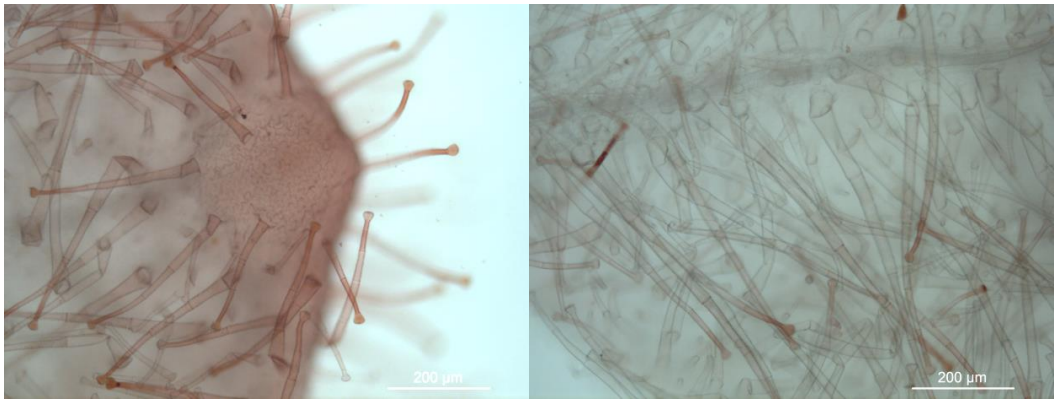

abaxial

1.21 *A. sempervirens*

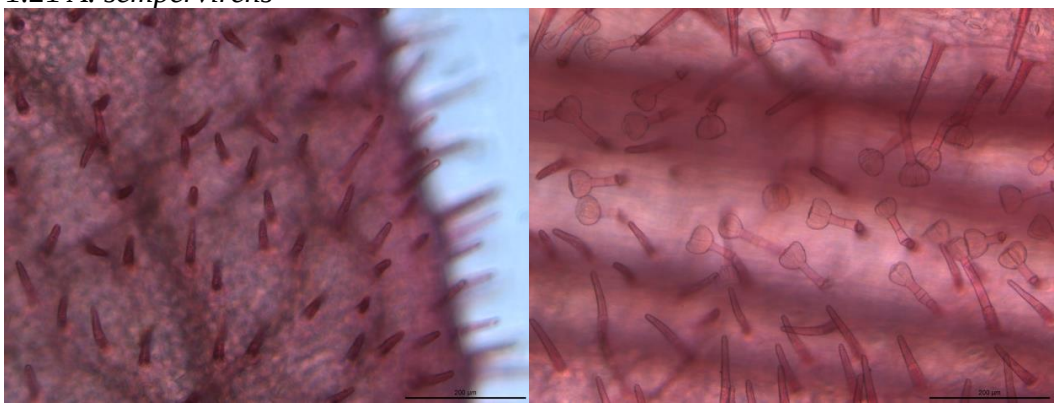

adaxial

1.22 *A. subbaeticum*

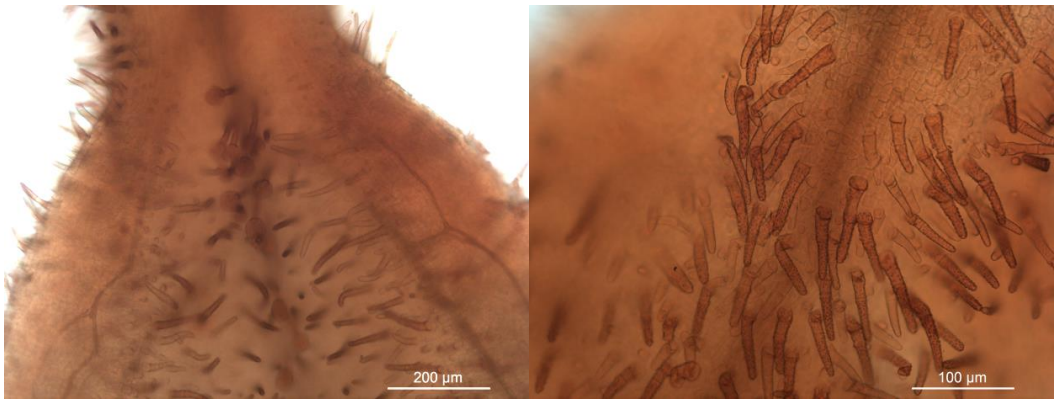

adaxial abaxial

1.23 *A. valentinum*

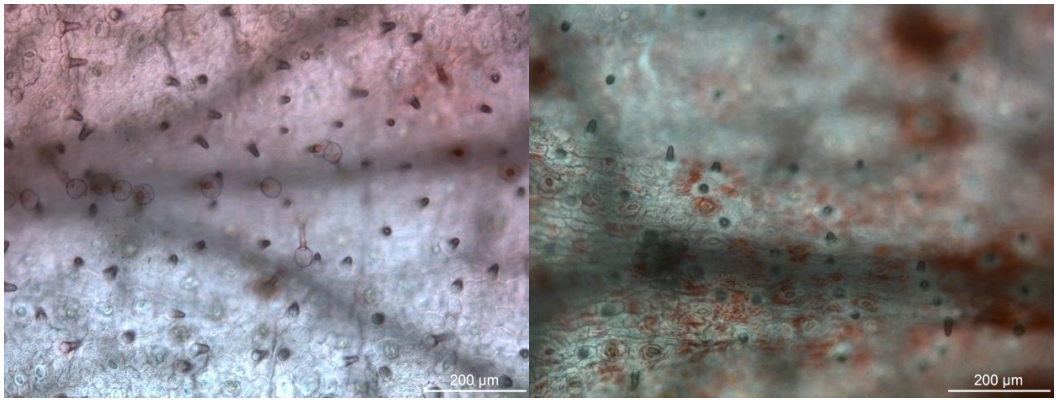

adaxial abaxial

Subsection *Streptosepalum*

1.23 *A. braun-blanquetii*

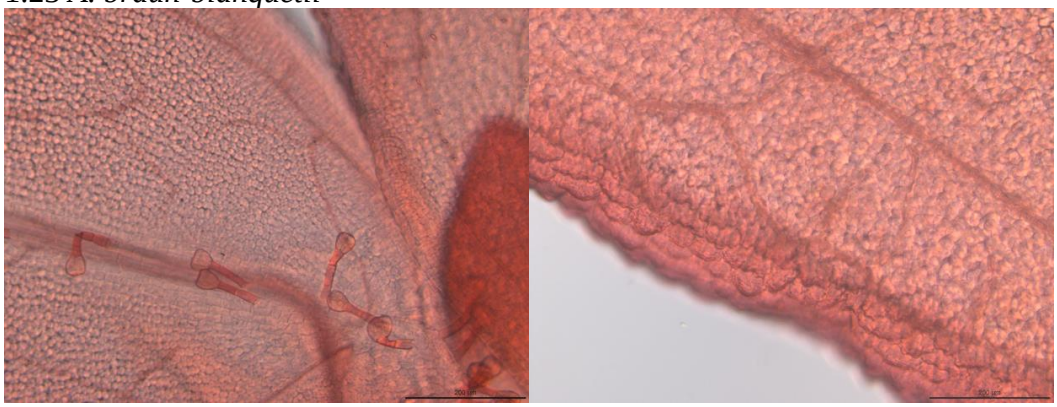

adaxial

1.24 *A. meonanthum*

Bald individuals

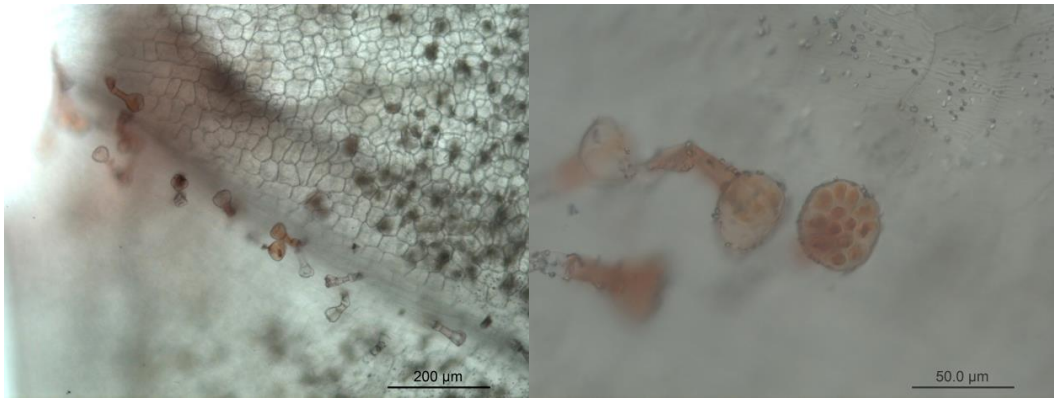

adaxial

Hairy individual

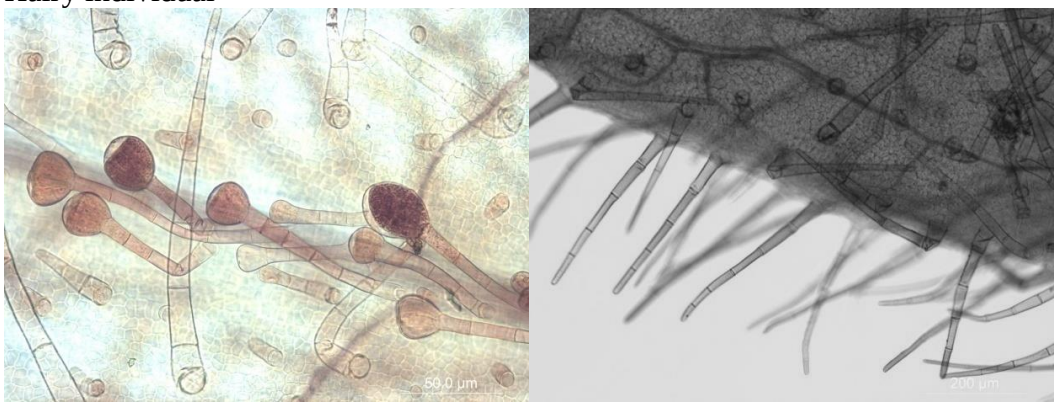

adaxial

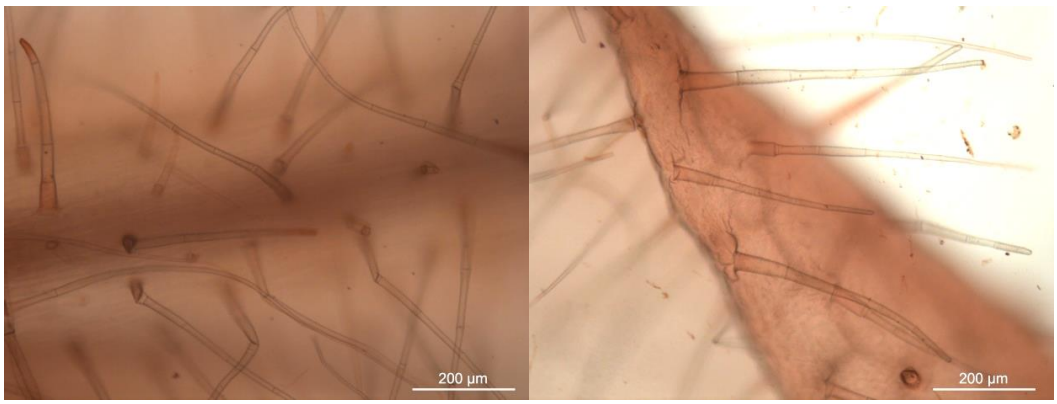

abaxial

Related species

1.25. *Maurandya scandens*

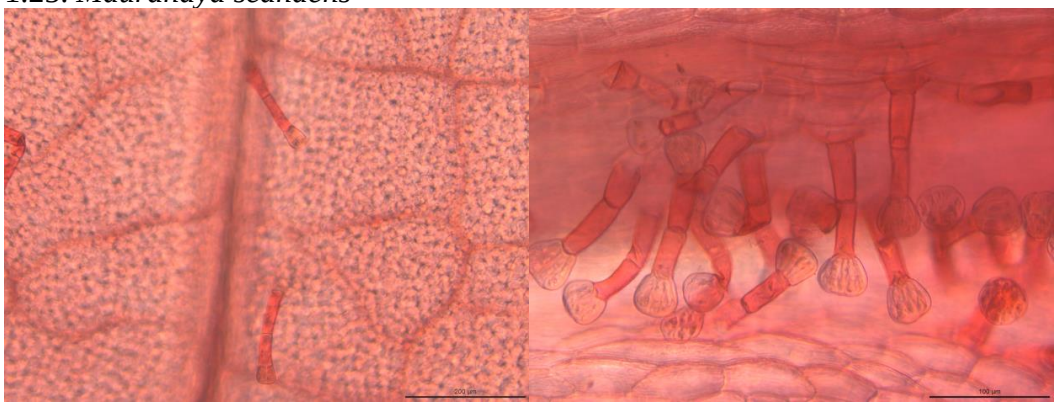
adaxial

1.26 *Maurandya antirrhiniflora*

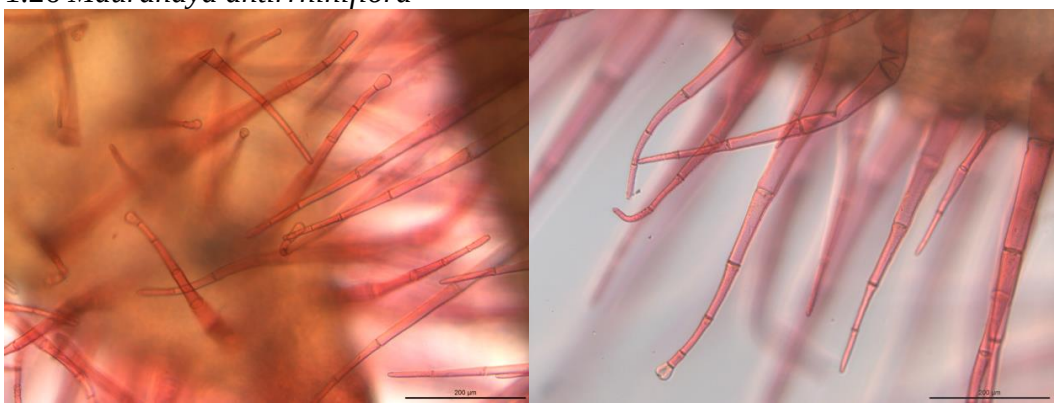
adaxial

1.27 *Gadoria falukei*

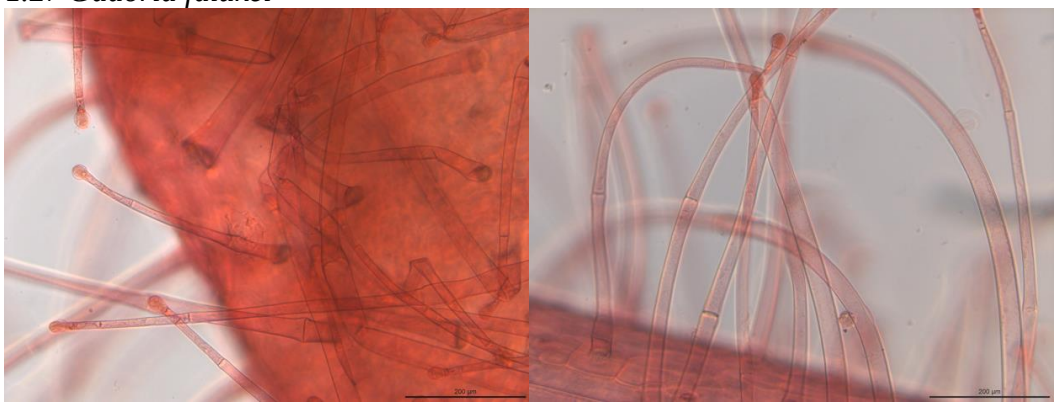

adaxial

After leaf clearing, samples were stained with Safranin O. Samples were collected from the higer vegetative nodes, except for those specifically indicated.

Appendix 2: Sepal trichome morphology

Subsection *Antirrhinum*

2.1 *A. australe*

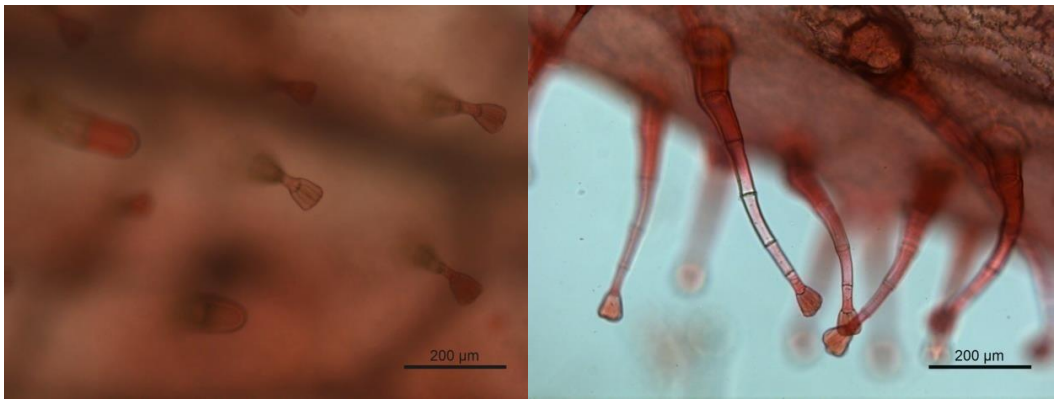

adaxial abaxial

2.2 *A. graniticum*

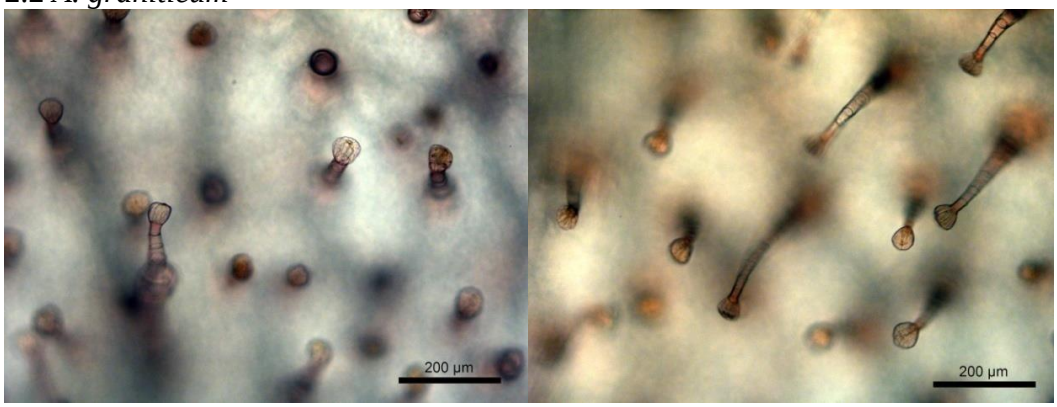

adaxial abaxial

2.3 *A. majus* subsp. *linkianum*

adaxial abaxial

2.4 *A. majus* subsp. *majus*

adaxial abaxial

2.5 *A. majus* subsp. *striatum*

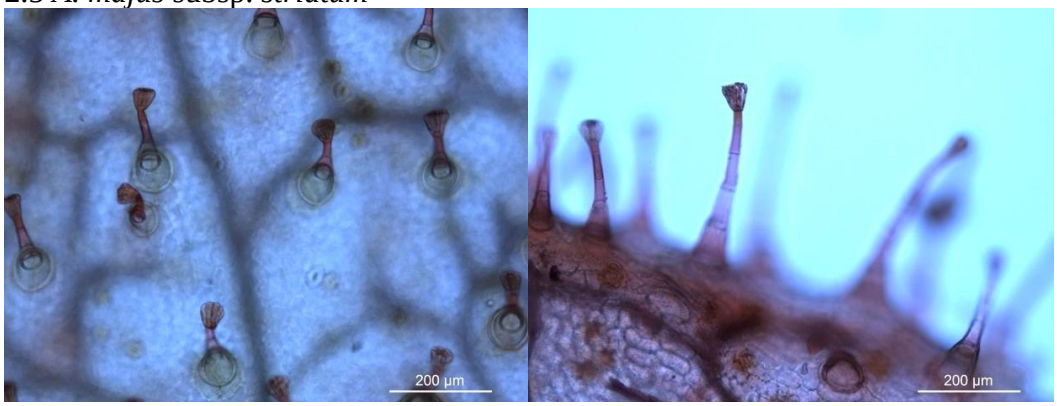

adaxial abaxial

2.6 *A. siculum*

adaxial abaxial

Subsection *Kickxiella*

2.7 *A. boissieri*

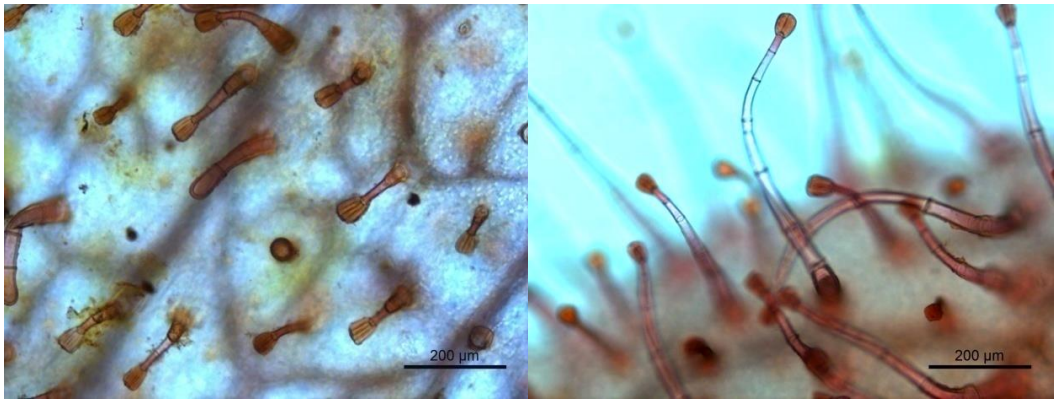

adaxial abaxial

2.8 *A. hispanicum*

adaxial abaxial

2.9 *A. molle*

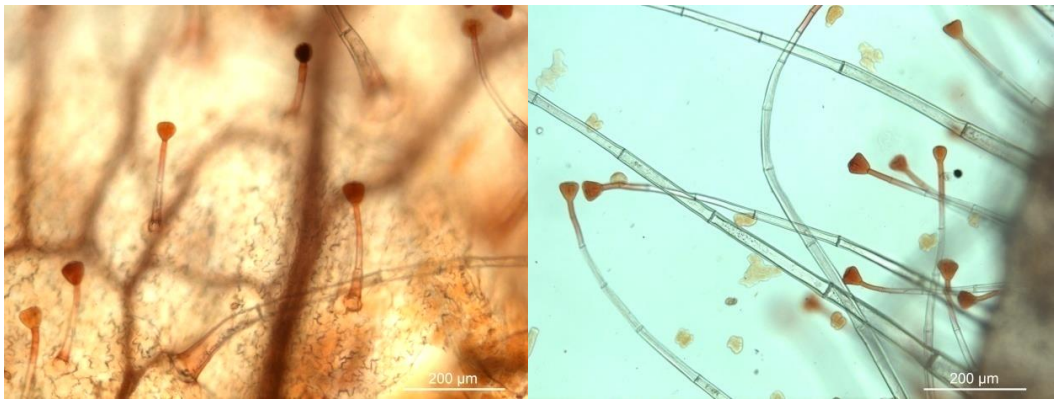

adaxial abaxial

2.10 *A. pertegasii*

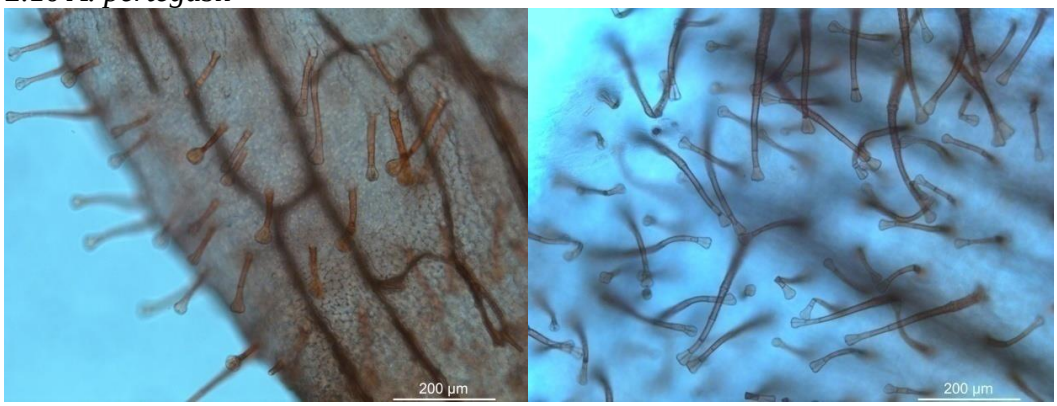

adaxial abaxial

2.11 *A. pulverulentum*

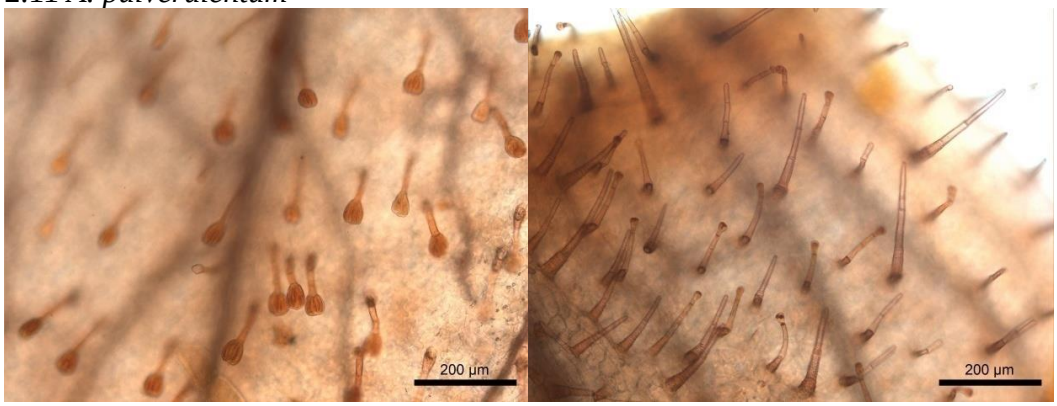

adaxia abaxial

2.12 *A. rupestre*

adaxial abaxial

2.13 *A. subbaeticum*

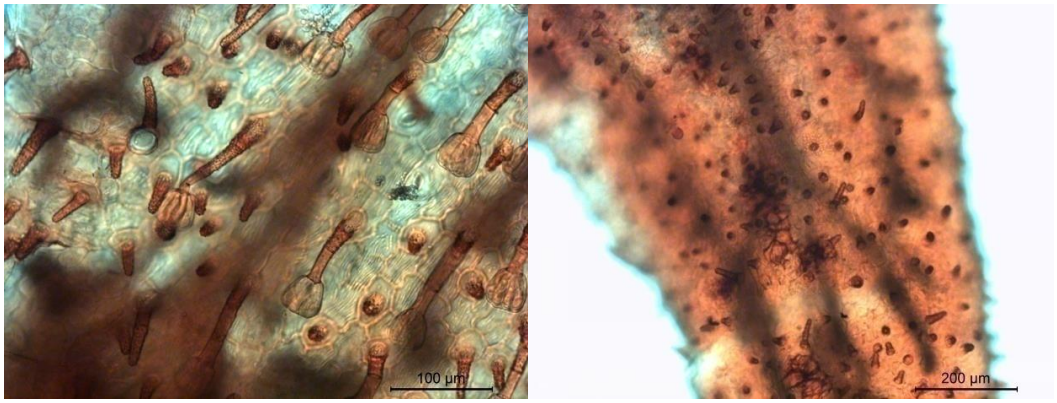

adaxial abaxial

2.14 *A. valentinum*

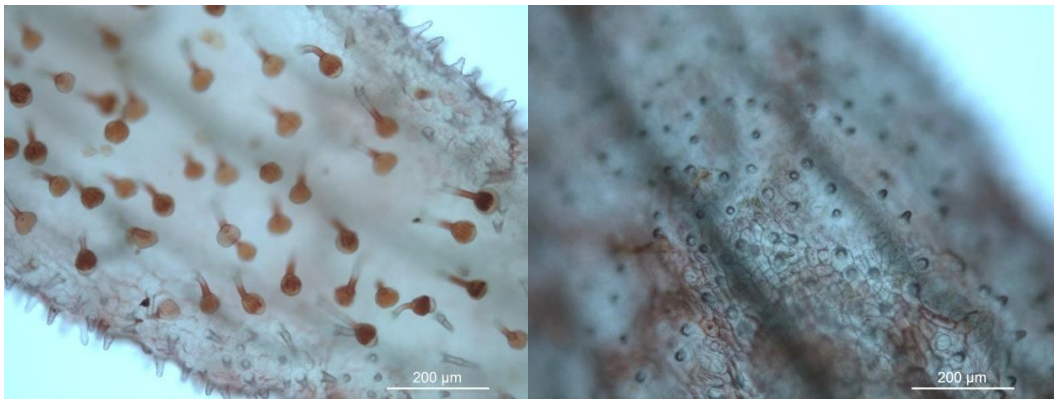

adaxial abaxial

Subsection *Streptosepalum*

2.15 *A. meonanthum*

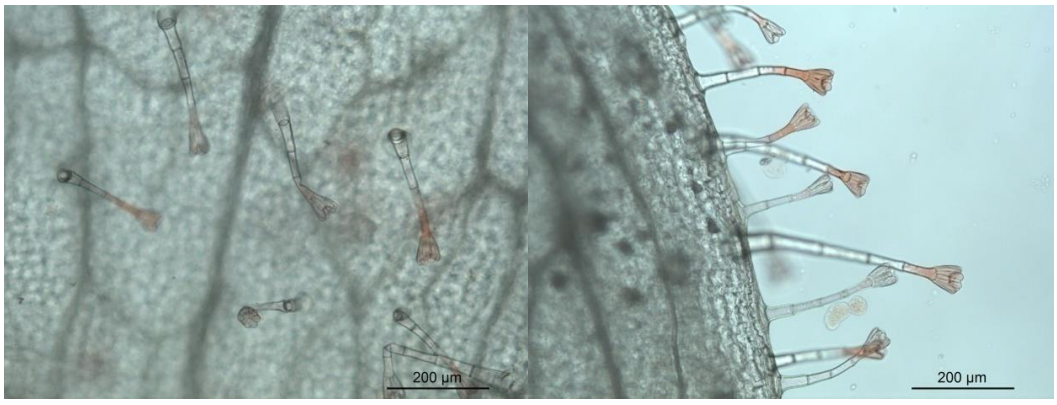

adaxial abaxial

Appendix 3: Expression of *GRX*40

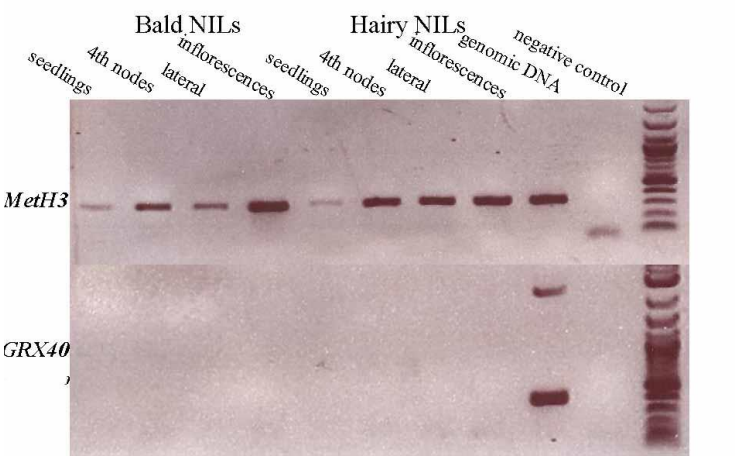

RNA samples were extracted from seedlings, shoot apices where the fourth leaves were 5 mm long (4th nodes), lateral meristems at the fourth node (lateral), and inflorescence meristem (inflorescence) of bald and hairy NILs. *Methionine synthase* (*MetH3*) in Scaffold 3 was used as an internal control for the presence of cDNA. A genomic DNA sample of a bald NIL plant was used a positive control for PCR and water was used as a negative control. The result suggested that the *GRX40* (in Scaffold 40) was not expressed in shoots and it is possible a pseudogene.

Appendix 4: Spatial localization of *AmGRX1* expression by *in situ* hybridization

4.1 Serial sections of a bald NIL individual

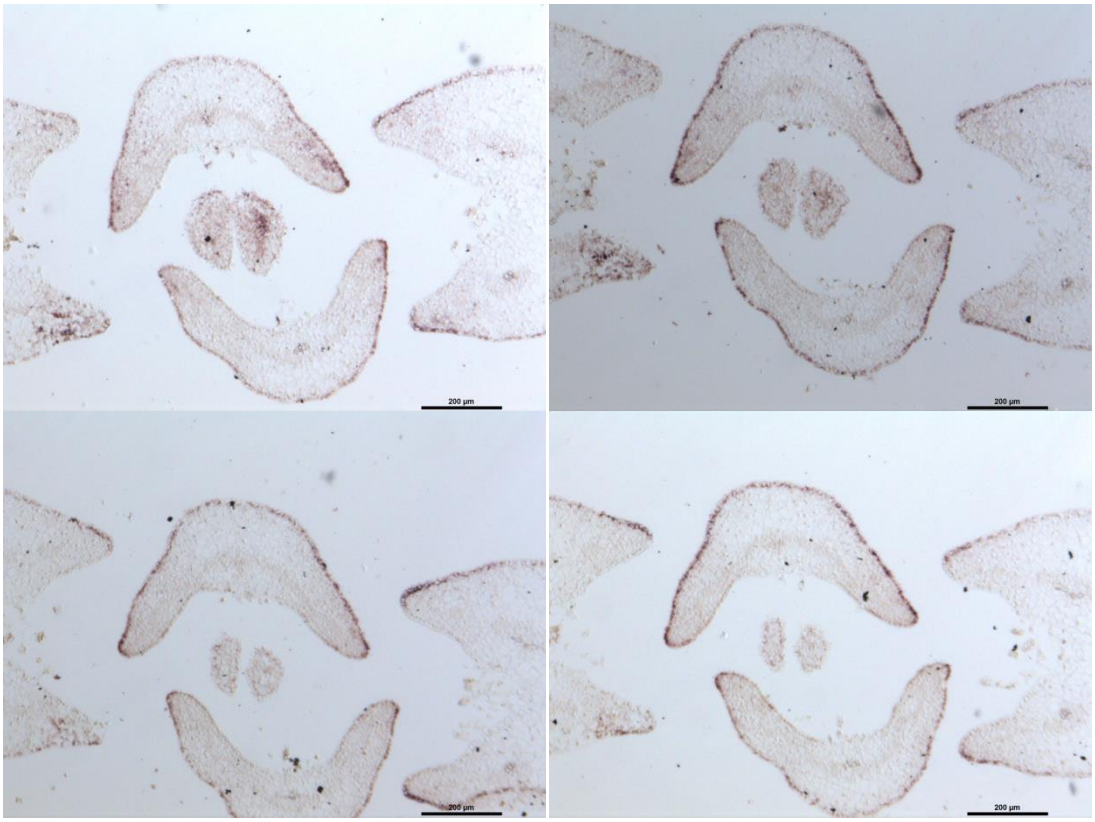

The spatial localization of *AmGRX1* mRNA in bald leaves of bald NILs was detected by *in situ* hybridization. The four serial sections above show the expression of *AmHairy* was limited to the epidermis of bald leaves. The expression is very low or undectectable in epidermal cells of the adaxial midrib. Purple staining in the vascular tissue of the midrib was also seen in the hairy NILs, so is assumed to be non-specific background. Here the fourth, fifth and sixth pairs of leaves are visible.

4.2 Signal in the stem (bald NIL and hairy NIL)

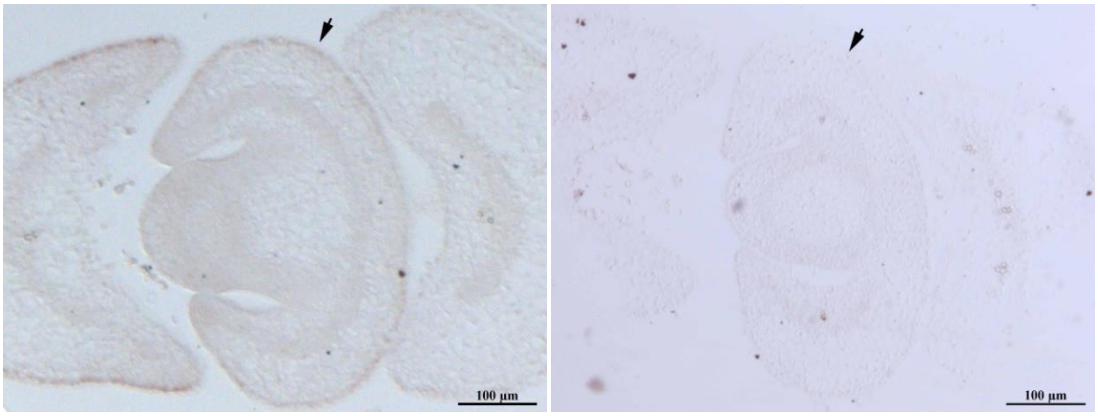

The expression of *AmGRX1* was also detected in the epidermis of bald stem (above node 2). Here the fifth leaves and stem (arrow) of bald NIL(left) and hairy NIL (right) are shown.

Appendix 5: Phenotypes of VIGS treated plants

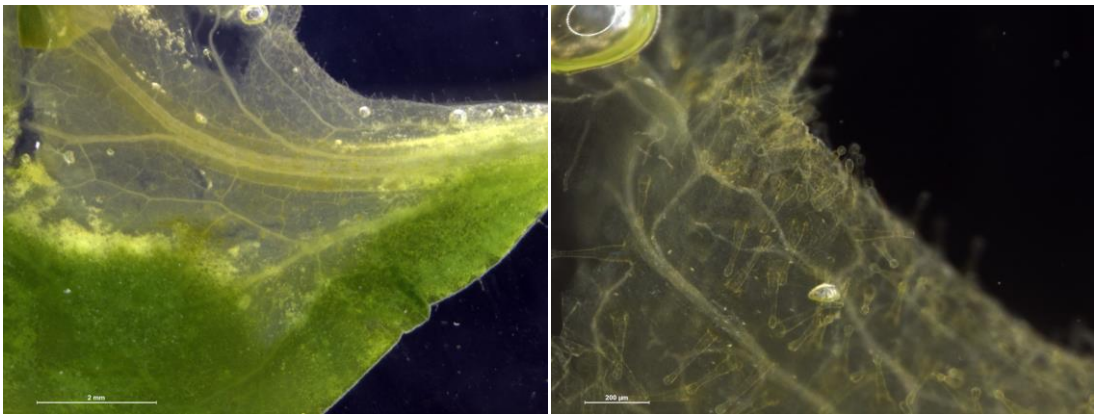

VIGS of *PDS* and *GRX1* allows type III trichomes to grow from the bleached area above node 2. The image on the left shows a bleached region of a leaf from the bald NIL at node 5, which had been partially cleared. The image on the right is a higer magnification of the same area, in which type III trichomes can be seen.

Appendix 6: Southern Blotting

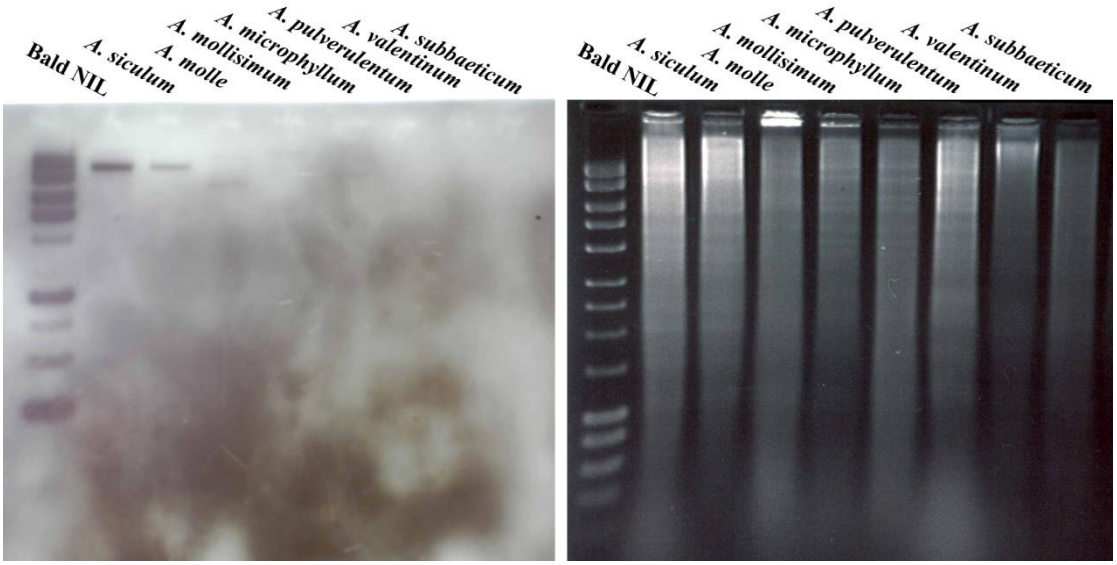

Left: Chemiluminescent detection of digoxigenin-labelled *AmHairy* probe on a Southern blot. Right: Ethidium bromide-stained DNA after electrophoresis before blotting. assay of hybiration. Right: Electrophoresis after digestion. Genomic DNA was extracted from the bald NIL, *A. siculum* AC1177, *A. molle* E51, *A. mollisimum* L21, *A. microphyllum* L74, *A. pulverulentum* L70, *A. valentinum* AC1173, *A. subbaeticum* E72. DNA was digested with *Eco*R I and *Xba* I and hybridized at moderate stringency with a probe of *AmHairy.*

Appendix 7: Sequence alignments

7.1 DNA sequence alignment of *Antirrhinum* and *Misopates Hairy* alleles

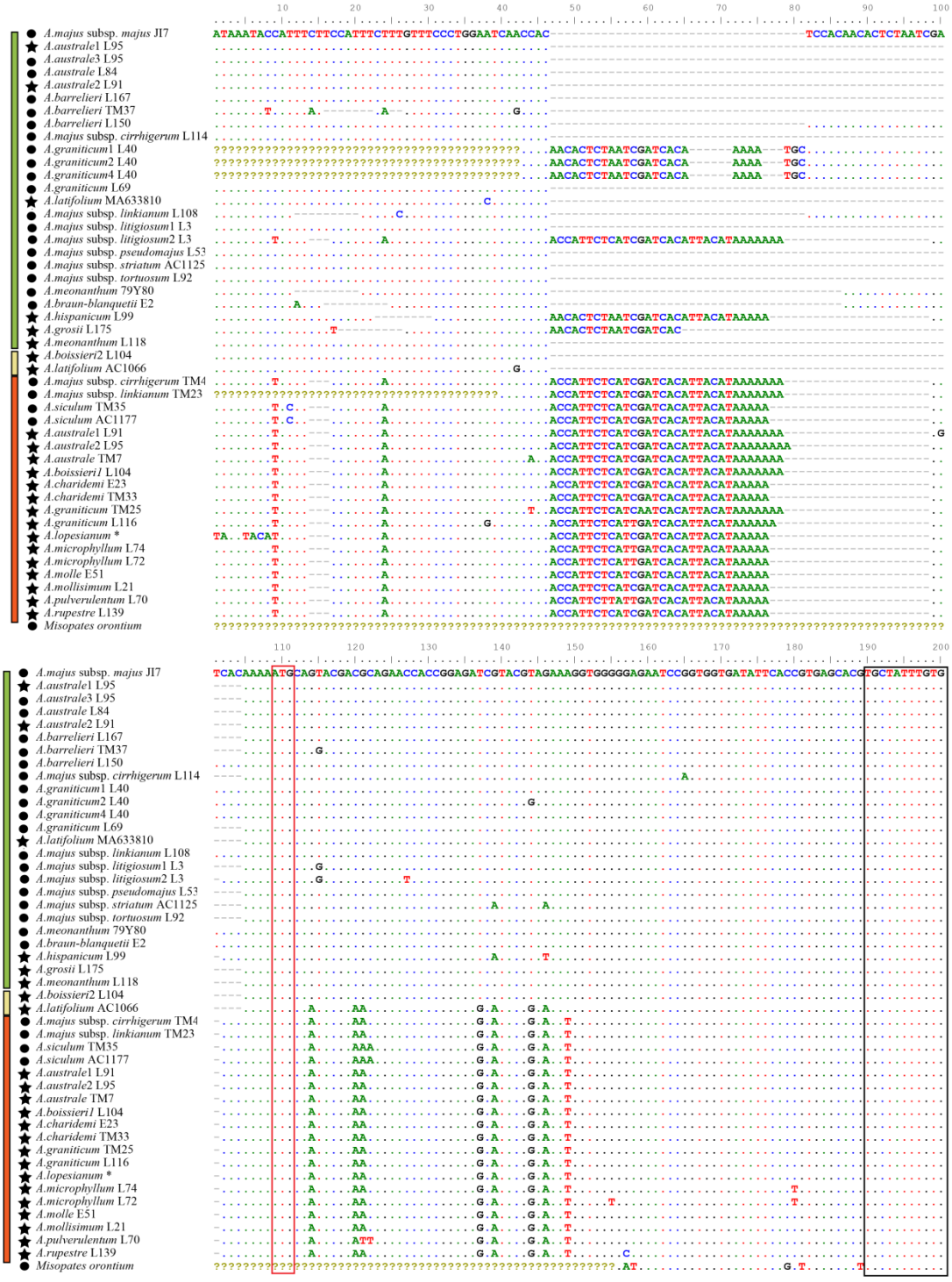

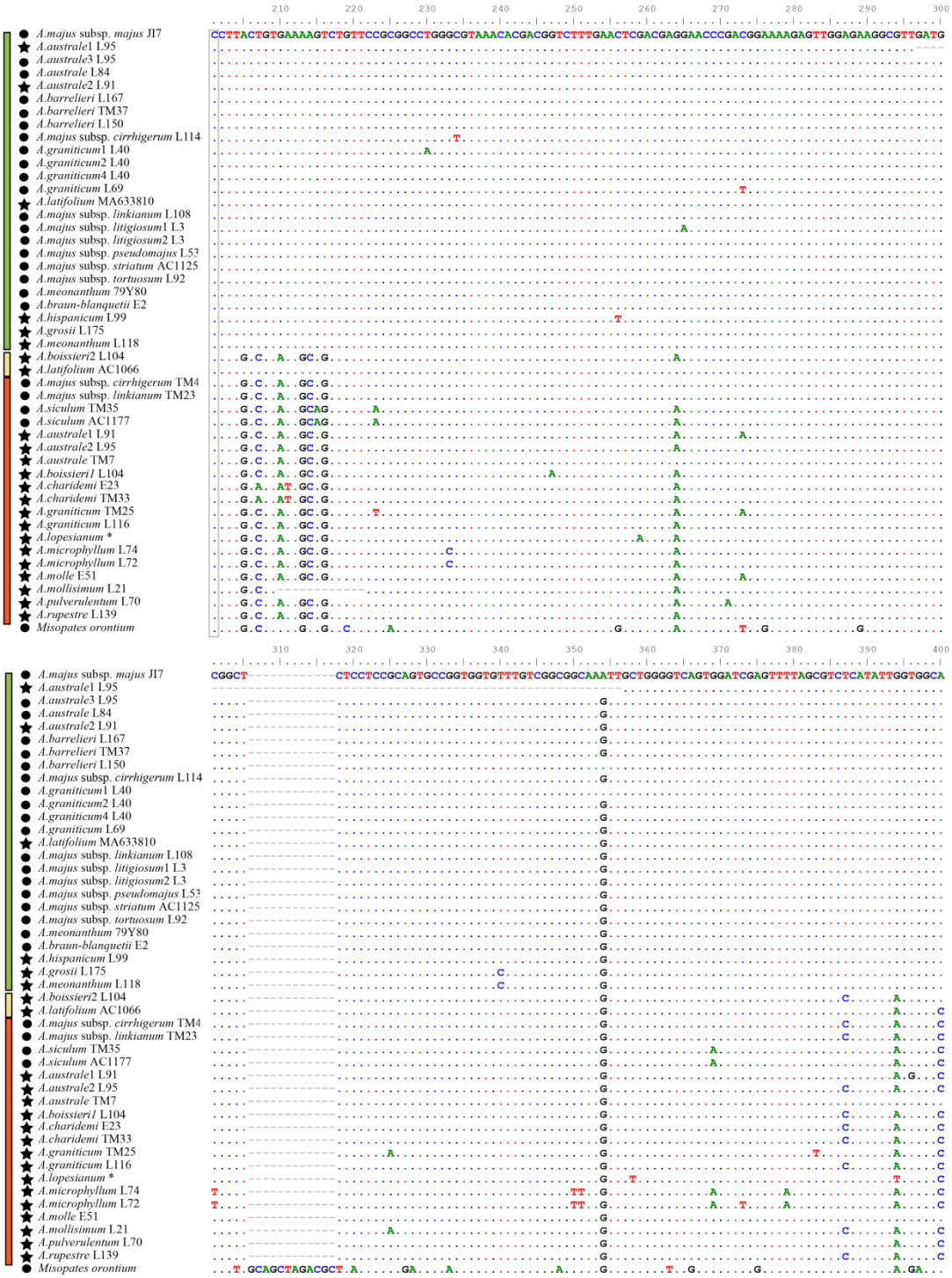
210 220 230 240 250 260 270 280 290 300
A.majus subsp. majus JI7
A.australe1 L95
A.australe3 L95
A.australe L84
A.australe2 L91
A.barrelieri L167
A.barrelieri TM37
A.barrelieri L150
A.majus subsp. cirrhigerum L114
A.graniticum1 L40
A.graniticum2 L40
A.graniticum4 L40
A.graniticum L69
A.latifolium MA633810
A.majus subsp. linkianum L108
A.majus subsp. litigiosum1 L3
A.majus subsp. litigiosum2 L3
A.majus subsp. pseudomajus L53
A.majus subsp. striatum AC1125
A.majus subsp. tortuosum L92
A.meonanthum 79Y80
A.braun-blanquetii E2
A.hispanicum L99
A.grosii L175
A.meonanthum L118
A.boissieri2 L104
A.latifolium AC1066
A.majus subsp. cirrhigerum TM4
A.majus subsp. linkianum TM23
A.siculum TM35
A.siculum AC1177
A.australe1 L91
A.australe2 L95
A.australe TM7
A.boissieri1 L104
A.charidemi E23
A.charidemi TM33
A.graniticum TM25
A.graniticum L116
A.lopesianum *
A.microphyllum L74
A.microphyllum L72
A.molle E51
A.mollisimum L21
A.pulverulentum L70
A.rupestre L139
Misopates orontium
310 320 330 340 350 360 370 380 390 400
A.majus subsp. majus JI7
A.australe1 L95
A.australe3 L95
A.australe L84
A.australe2 L91
A.barrelieri L167
A.barrelieri TM37
A.barrelieri L150
A.majus subsp. cirrhigerum L114
A.graniticum1 L40
A.graniticum2 L40
A.graniticum4 L40
A.graniticum L69
A.latifolium MA633810
A.majus subsp. linkianum L108
A.majus subsp. litigiosum1 L3
A.majus subsp. litigiosum2 L3
A.majus subsp. pseudomajus L53
A.majus subsp. striatum AC1125
A.majus subsp. tortuosum L92
A.meonanthum 79Y80
A.braun-blanquetii E2
A.hispanicum L99
A.grosii L175
A.meonanthum L118
A.boissieri2 L104
A.latifolium AC1066
A.majus subsp. cirrhigerum TM4
A.majus subsp. linkianum TM23
A.siculum TM35
A.siculum AC1177
A.australe1 L91
A.australe2 L95
A.australe TM7
A.boissieri1 L104
A.charidemi E23
A.charidemi TM33
A.graniticum TM25
A.graniticum L116
A.lopesianum *
A.microphyllum L74
A.microphyllum L72
A.molle E51
A.mollisimum L21
A.pulverulentum L70
A.rupestre L139
Misopates orontium

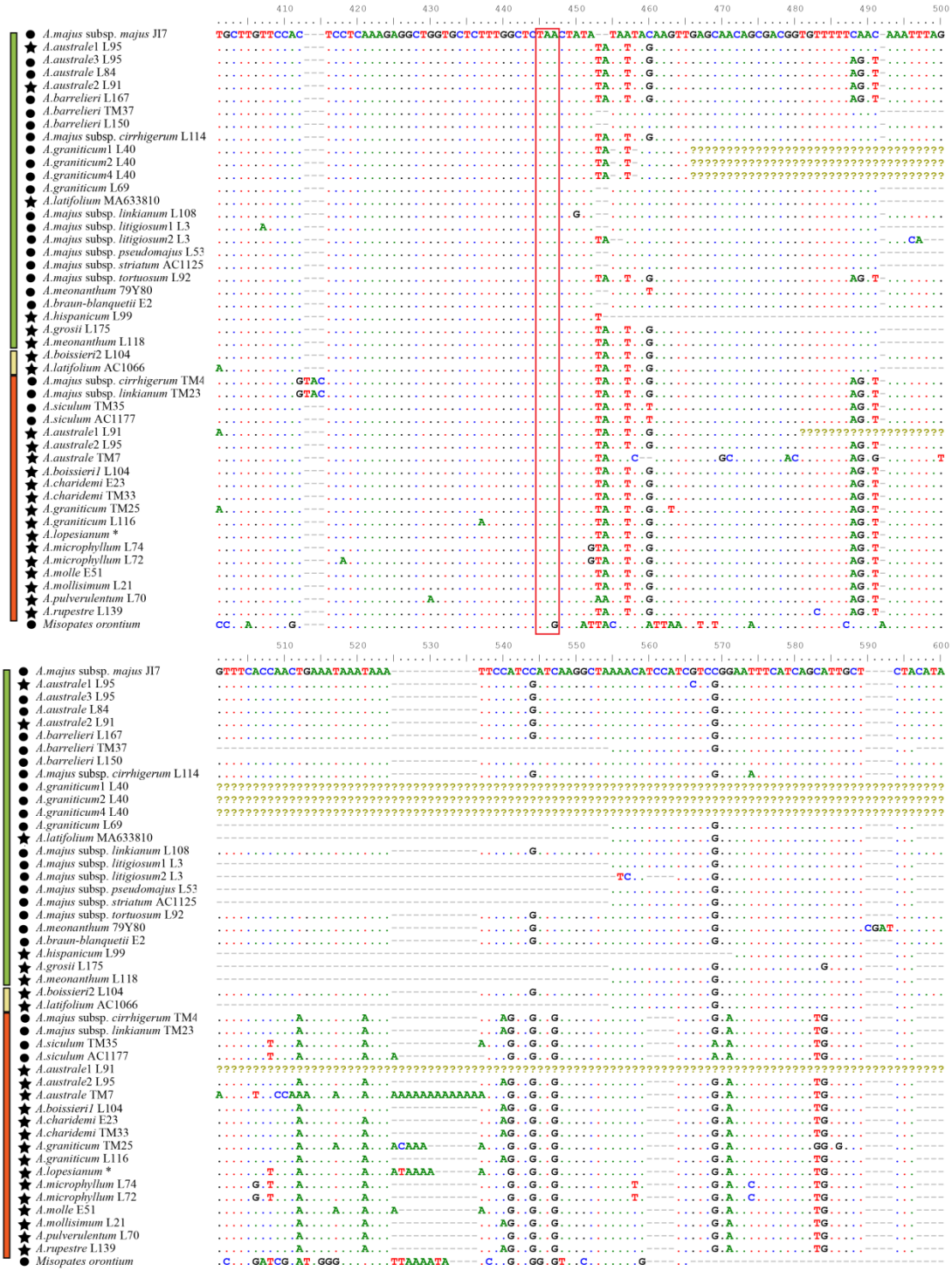
410 420 430 440 450 460 470 480 490 500
A.majus subsp. majus JI7
A.australe1 L95
A.australe3 L95
A.australe L84
A.australe2 L91
A.barrelieri L167
A.barrelieri TM37
A.barrelieri L150
A.majus subsp. cirrhigerum L114
A.graniticum1 L40
A.graniticum2 L40
A.graniticum4 L40
A.graniticum L69
A.latifolium MA633810
A.majus subsp. linkianum L108
A.majus subsp. litigiosum1 L3
A.majus subsp. litigiosum2 L3
A.majus subsp. pseudomajus L53
A.majus subsp. striatum AC1125
A.majus subsp. tortuosum L92
A.meonanthum 79Y80
A.braun-blanquetii E2
A.hispanicum L99
A.grosii L175
A.meonanthum L118
A.boissieri2 L104
A.latifolium AC1066
A.majus subsp. cirrhigerum TM4
A.majus subsp. linkianum TM23
A.siculum TM35
A.siculum AC1177
A.australe1 L91
A.australe2 L95
A.australe TM7
A.boissieri1 L104
A.charidemi E23
A.charidemi TM33
A.graniticum TM25
A.graniticum L116
A.lopesianum *
A.microphyllum L74
A.microphyllum L72
A.molle E51
A.mollisimum L21
A.pulverulentum L70
A.rupestre L139
Misopates orontium
510 520 530 540 550 560 570 580 590 600
A.majus subsp. majus JI7
A.australe1 L95
A.australe3 L95
A.australe L84
A.australe2 L91
A.barrelieri L167
A.barrelieri TM37
A.barrelieri L150
A.majus subsp. cirrhigerum L114
A.graniticum1 L40
A.graniticum2 L40
A.graniticum4 L40
A.graniticum L69
A.latifolium MA633810
A.majus subsp. linkianum L108
A.majus subsp. litigiosum1 L3
A.majus subsp. litigiosum2 L3
A.majus subsp. pseudomajus L53
A.majus subsp. striatum AC1125
A.majus subsp. tortuosum L92
A.meonanthum 79Y80
A.braun-blanquetii E2
A.hispanicum L99
A.grosii L175
A.meonanthum L118
A.boissieri2 L104
A.latifolium AC1066
A.majus subsp. cirrhigerum TM4
A.majus subsp. linkianum TM23
A.siculum TM35
A.siculum AC1177
A.australe1 L91
A.australe2 L95
A.australe TM7
A.boissieri1 L104
A.charidemi E23
A.charidemi TM33
A.graniticum TM25
A.graniticum L116
A.lopesianum *
A.microphyllum L74
A.microphyllum L72
A.molle E51
A.mollisimum L21
A.pulverulentum L70
A.rupestre L139
Misopates orontium

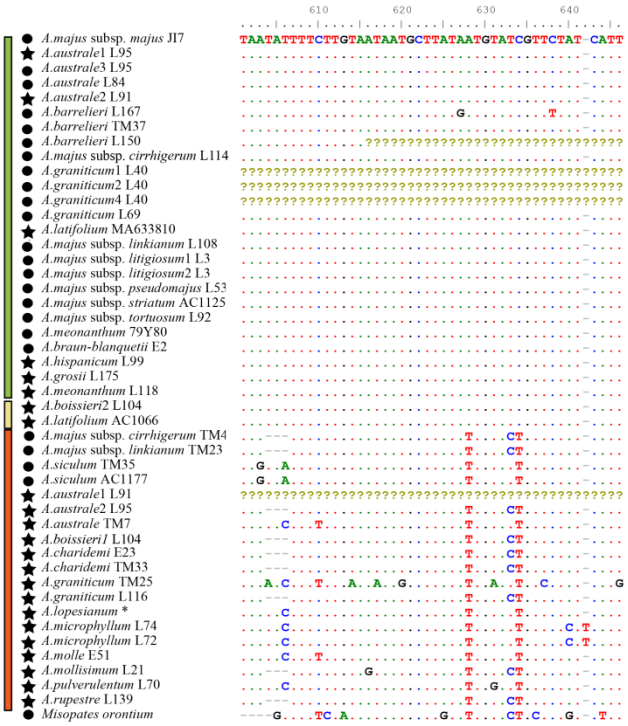

Alignment of *Antirrhinum Hairy* alleles and the sequence of *Misopates orontium*. The alignment was generated with the program Clustal Omega at the EMBL-EBI web server. The start codon and stop codon are indicated by red boxes. The residues encoding the active site motif of Cysteine-Tyrosine-Leucine-Cysteine (CYLC) are showed in a black box. Gaps are indicated by dashes, conserved nucleotides by dots, and missing data by question marks. On the left side, circles represent bald phenotypes and stars represent hairy phenotypes. Subsection *Antirrhinum*-like alleles (similar to *A. majus* subsp. *majus*) are marked with a green bar, *Kickxiella*-like alleles, which share SNPs that are not in *Antirrhinum*-like alleles, are marked with a red bar, while potential recombinant alleles, which have both *Antirrhinum*-like and *Kickxiella*-like regions are marked with a yellow bar.

7.2 Amino acid sequence alignment of *Antirrhinum* and *Misopates* Hairy proteins

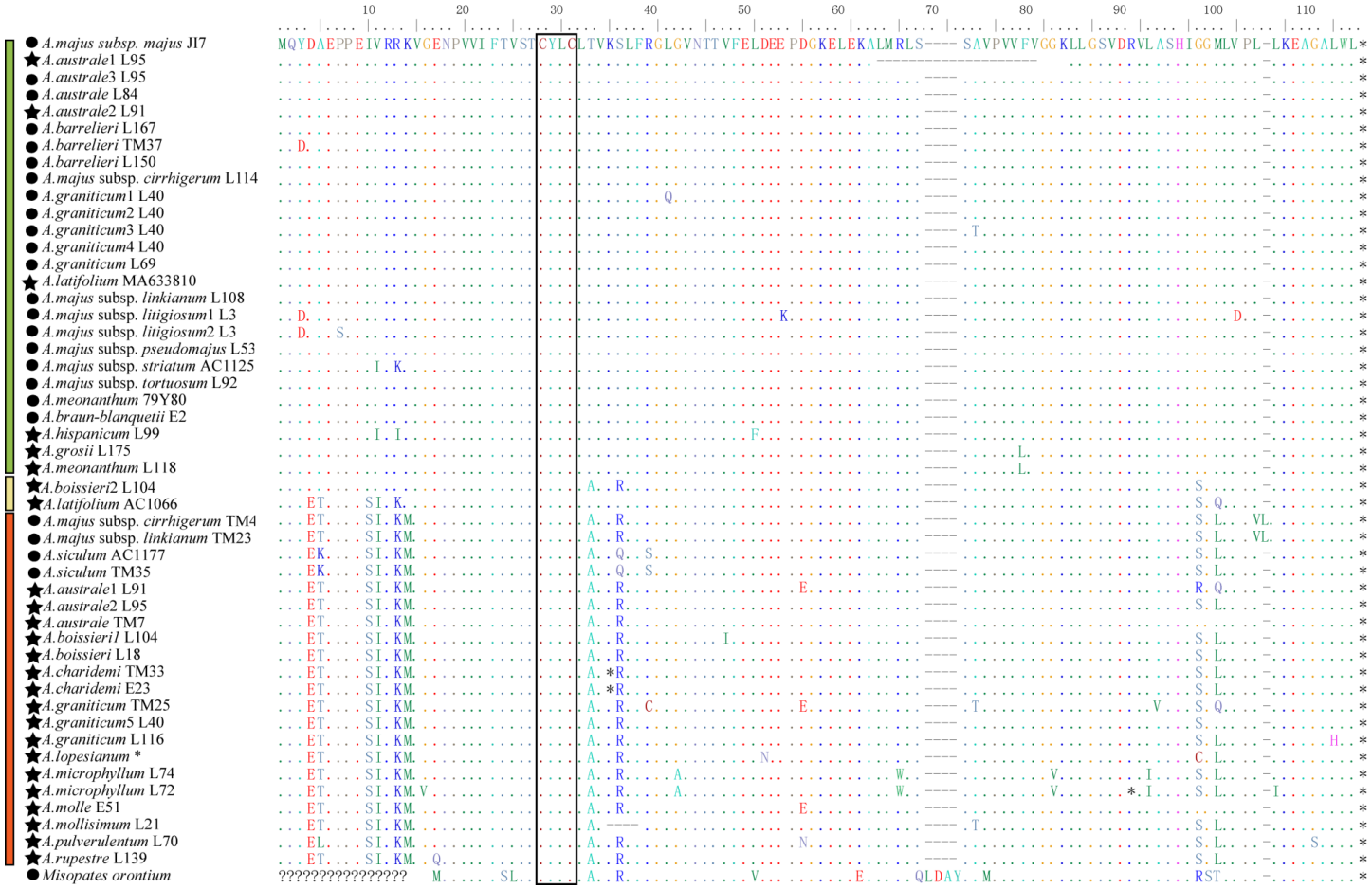

Alignment of *Antirrhinum* and *Misopates orontium* Hairy-like proteins (translated from DNA sequences). The alignment was generatedwith Clustal Omega at the EMBL-EBI web server.

7.3 Amino acid alignment of AmHairy, MoHairy and CoHairy with other GRXs

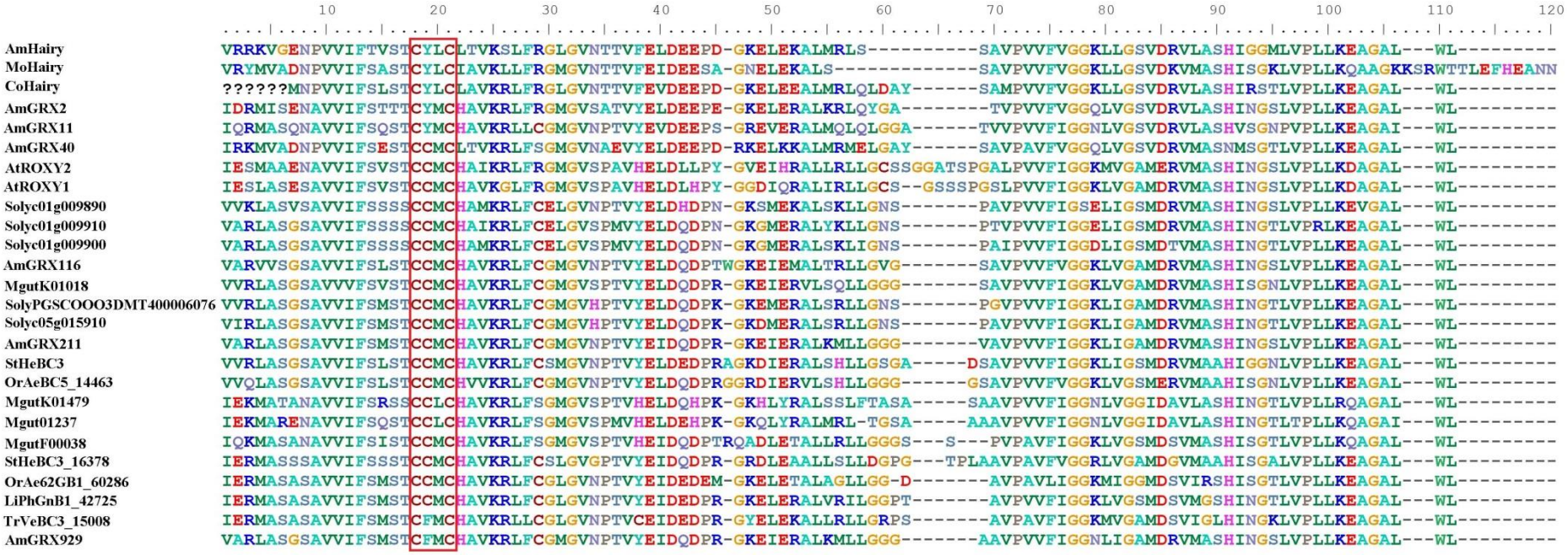

Alignment of inferred GRX proteins from *Antirrhinum majus subsp. majus* (Am), *Chaenorhinum origanifolium* (Co), *Misopates orontium* (Mo), *Mimulus guttatus* (Mgut), *Solanum lycopersicum* (Soly), *Arabidopsis thalianan* (At) and members of the Orobanchaceae (StHe, *Striga hermonthica*; OrAe, *Orobanche aegyptica*; LiPh, *Lindenbergia philippensis*; TeVe, *Triphysaria versicolor*).. The alignments were generated using Clustal Omega at EMBL-EBI. The active site Cysteine-X-X-Cysteine motif is indicted by a black box. Gaps are indicated by dashes, and missing data by question marks.

Appendix 8: *A. siculum* hybrids

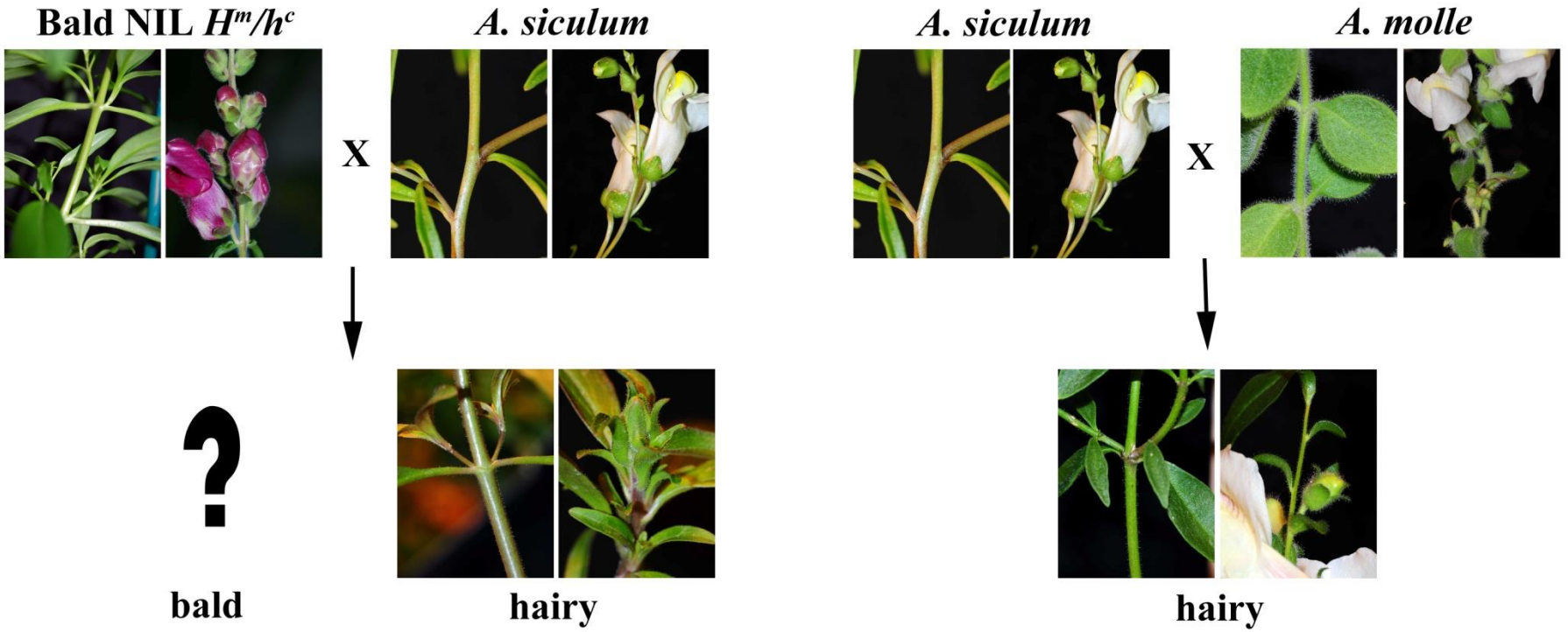

A. siculum (bald) was crossed with a heterozygous bald NIL to conduct allelism test. Due to the low fertilization rate and germination rate, only one progeny was generated, which was hairy. This suggests that *A. siculum* carries a recessive *hairy* allele and is bald because it lacks activity of a gene, or genes, needed for hair formation. *A. siculum* was crossed with *A. molle* (hairy, genotype *h*/*h*), and generated six hairy progeny, all hairy, consistent with involvement of a second locus. Here the middle vegetative parts and inflorescences of species and hybrids are shown. Unlike other species, *A. siculum* only has a few scattered trichomes distributed on its inflorescence, suggesting that the second locus or loci responsible for baldness of the later vegetative parts also promote trichome development in the inflorescence.